



NAVAL POSTGRADUATE SCHOOL

Monterey, California



THESIS

OPTIMAL DIGITAL CONTROL
OF
A BANK-TO-TURN MISSILE

by

Carlos A. L. Velloso

March 1984

Thesis Advisor:

Daniel J. Collins

Approved for public release; distribution unlimited

T215708

REPORT DOCUMENTATION PAGE

READ INSTRUCTIONS
BEFORE COMPLETING FORM

1. REPORT NUMBER		2. GOVT ACCESSION NO.	3. RECIPIENT'S CATALOG NUMBER
4. TITLE (and Subtitle) Optimal Digital Control of a Bank-to-Turn Missile		5. TYPE OF REPORT & PERIOD COVERED Master Thesis March 1984	
7. AUTHOR(s) Carlos Augusto Leal Velloso		6. PERFORMING ORG. REPORT NUMBER	
9. PERFORMING ORGANIZATION NAME AND ADDRESS Naval Postgraduate School Monterey, California 93940		8. CONTRACT OR GRANT NUMBER(s)	
11. CONTROLLING OFFICE NAME AND ADDRESS Naval Postgraduate School Monterey, California 93940		10. PROGRAM ELEMENT, PROJECT, TASK AREA & WORK UNIT NUMBERS	
14. MONITORING AGENCY NAME & ADDRESS (if different from Controlling Office)		12. REPORT DATE March 1984	
		13. NUMBER OF PAGES 154	
		15. SECURITY CLASS. (of this report) Unclassified	
16. DISTRIBUTION STATEMENT (of this Report) Approved for public release; distribution unlimited		15a. DECLASSIFICATION/DOWNGRADING SCHEDULE	
17. DISTRIBUTION STATEMENT (of the abstract entered in Block 20, if different from Report)			
18. SUPPLEMENTARY NOTES			
19. KEY WORDS (Continue on reverse side if necessary and identify by block number) Guidance and Control Optimal Digital Control Terminal Guidance Law Bank-to-Turn Missile			
20. ABSTRACT (Continue on reverse side if necessary and identify by block number) This work addresses the application of digital optimum control theory to a bank-to-turn missile. A optimal guidance law has been developed and tested in several scenarios using a 2-D model. Effects of sample rate, pitch angle, gravity and approximations for small and large roll excursions are discussed.			

Approved for public release; distribution unlimited.

Optimal Digital Control
of
a Bank-to-Turn Missile

by

Carlos A.L. Velloso
Major, Brazilian Air Force
B.S., Instituto Tecnológico de Aeronautica, Brasil, 1976

Submitted in partial fulfillment of the
requirements for the degree of

MASTER OF SCIENCE IN ENGINEERING SCIENCE

from the

NAVAL POSTGRADUATE SCHOOL
March 1984

ABSTRACT

This work addresses the application of digital optimum control theory to a bank-to-turn missile.

A optimal guidance law has been developed and tested in several scenarios, using a 2-D model. Effects of sample rate, pitch angle, gravity and approximations for small and large roll excursions are discussed.

TABLE OF CONTENTS

I.	INTRODUCTION	11
II.	MODEL OF THE SYSTEM	13
	A. INTRODUCTION	13
	B. ASSUMPTIONS	13
	C. THE CONTINUOUS MODEL	13
	D. THE DISCRETE MODEL	17
	1. Introduction	17
	2. Calculation of the Matrices $A(k)$, $B(k)$ and $E(k)$	19
III.	THE OPTIMAL CONTROLLER	29
	A. DERIVATION OF THE OPTIMAL CONTROLLER	29
	B. EXTENSION OF THE MODEL FOR LARGE ROLL ANGLES	36
	1. Effects on the Miss Distance of the Extension of the Model	42
	C. SIMULATION	44
	D. COMMENTS AND CONCLUSIONS	45
	1. Results	45
	2. Comments	47
IV.	ANALYSIS OF GAINS, SAMPLE RATE AND PITCH ANGLE	82
	A. ANALYSIS OF THE GAINS	82
	B. EFFECT OF THE SAMPLE RATE	84
	C. EFFECT OF THE INITIAL PITCH ANGLE	85
	D. EFFECT OF TIME TO INTERCEPT	88
V.	FINAL CONCLUSIONS AND COMMENTS	130

APPENDIX A: FORTRAN PROGRAM	132
LIST OF REFERENCES	153
INITIAL DISTRIBUTION LIST	154

LIST OF TABLES

I.	Results From Tests	81
II.	Results from Biased Control	96
III.	Results for Different Sample Periods	105
IV.	Results Using Pitch Angle	120
V.	Effect of Time to Intercept	129

LIST OF FIGURES

2.1	Reference Frames	27
2.2	Reference Frames	28
3.1	Representation of the System	51
3.2	Variation of Commands with Initial Roll Angle	52
3.3	Variation of Roll Angle - Small Angles	53
3.4	Variation of Roll Angle - Large Angles	54
3.5	Ideal Initial Roll Angles	55
3.6	Scenarios for Simulation	56
3.7	Commanded Acceleration- Case 0	57
3.8	Commanded Roll Rate- Case 0	58
3.9	Miss Distance in Z Direction- Case 0	59
3.10	Miss Distance in Y Direction- Case 0	60
3.11	Roll Angle- Case 0	61
3.12	Commanded Acceleration- Case 1	62
3.13	Commanded Roll Rate- Case 1	63
3.14	Miss Distance- Case 1	64
3.15	Roll Angle- Case 1	65
3.16	Commanded Acceleration- Case 2	66
3.17	Commanded Roll Rate- Case 2	67
3.18	Miss Distance- Case 2	68
3.19	Roll Angle- Case 2	69
3.20	Commanded Acceleration- Case 3	70
3.21	Commanded Roll Rate- Case 3	71
3.22	Miss Distance- Case 3	72
3.23	Roll Angle- Case 3	73
3.24	Commanded Acceleration- Case 4	74
3.25	Commanded Roll Rate- Case 4	75

3.26	Miss Distance- Case 4	76
3.27	Roll Angle- Case 4	77
3.28	Corrected Model	78
3.29	Boundary of the Commanded Acceleration	79
3.30	Corrections on the Roll Angle	80
4.1	Gains affecting the commanded acceleration	90
4.2	Gains Affecting the Commanded Roll Rate	91
4.3	Commanded Acceleration-Case 5	92
4.4	Commanded Roll Rate-Case 5	93
4.5	Miss Distance-Case 5	94
4.6	Roll Angle-Case 5	95
4.7	Commanded Acceleration-Case 6	97
4.8	Commanded Roll Rate-Case 6	98
4.9	Miss Distance-Case 6	99
4.10	Roll Angle-Case 6	100
4.11	Commanded Acceleration-Case 7	101
4.12	Commanded Roll Rate-Case 7	102
4.13	Miss distance-Case 7	103
4.14	Roll Angle-Case 7	104
4.15	Effect of Initial Pitch Angle	106
4.16	Scenarios With Pitch Angle	107
4.17	Commanded Acceleration-Case 8	108
4.18	Commanded Roll Rate-Case 8	109
4.19	Miss Distance-Case 8	110
4.20	Roll Angle-Case 8	111
4.21	Commanded Acceleration-Case 9	112
4.22	Commanded Roll Rate-Case 9	113
4.23	Miss Distance-Case 9	114
4.24	Roll Angle-Case 9	115
4.25	Commanded Acceleration-Case 10	116
4.26	Commanded Roll Rate-Case 10	117
4.27	Miss Distance-Case 10	118
4.28	Roll Angle-Case 10	119

4.29	Commanded Acceleration-Case 11	121
4.30	Commanded Roll Rate-Case 11	122
4.31	Miss Distance-Case 11	123
4.32	Roll Angle-Case 11	124
4.33	Commanded Acceleration-Case 12	125
4.34	Commanded Roll Rate-Case 12	126
4.35	Miss Distance-Case 12	127
4.36	Roll Angle-Case 12	128

ACKNOWLEDGEMENT

To my wife, Rosy, for her constant encouragment, support and love.

To my children, Ana, Antonio, Chica, Joao and Rita, for yours smiles and love.

Without you this work would be impossible.

I. INTRODUCTION

Because of threats from highly maneuverable high performance aircrafts and the need for increase standoff ranges, major improvements are needed in guidance and control capabilities of missiles.

The high maneuverability of targets, has led to defense missiles capable of develop higher lift accelerations and to more complex control laws, able to improve performance over well know laws as proportional navegation.

In order to accomplish these new requirements with large standoff ranges, propulsion systems using airbreathing engines has been studied and developed in recent years.

The advent of airbreathing engines leads natural to a consideration of bank-to-turn missiles in order to minimize the angle of attack of the inlets.

The necessity of more complex control laws, leads in a general way, to the application of modern control and estimation theory, since more complete informations of the states of missile and target are necessary than those states informed by sensors commonly in use in missiles today. This leads to the use of a airborne computer.

The present work adresses the design and evaluation of a optimal digital control for application to terminal guidance in a bank-to-turn missiles.

One continuous two dimensional model was adopted, in the following form:

$$\dot{X}(t) = A(t) x(t) + B(t) u(t) + E g \quad (1.1)$$

where the effect of gravity appears explicitly in the third term on the right hand side of expression 1.1.

After the development of a equivalent discrete model, the optimal control problem has been solved, using a modified Ricatti equation due to the existence of the third term representing to the gravity effect.

Next, several analysis has been made in order to check the effects of small and large roll excursions, the effect of the sample rate on the system, and the effect of the initial pitch angle, in order to check the validity of such two dimensional model, when applied in some scenarios of interest.

II. MODEL OF THE SYSTEM

A. INTRODUCTION

In the present work the problem of terminal guidance for long range, bank-to-turn missiles with ramjet engines, using a digitalized system has been investigated.

The model developed in reference 1 is used as the base for this work. After the digitalization of that model, an optimal control law was developed.

B. ASSUMPTIONS

Keeping the same assumptions as in ref.1, one has:

The missile is limited to $-2g$'s and $+15g$'s of commanded acceleration in the pitch plane, with zero lag. Also its yaw auto pilot has zero lag, yaw regulator maintains zero sideslip.

Missile thrust exactly cancels drag.

The angle of attack is assumed to be very small, which leads to the commanded acceleration acting normal to the velocity vector.

The missile will not have to roll through a large angle. (Further considerations will give to this at the end of the derivation of the control law).

C. THE CONTINUOUS MODEL

Using the same reference frames as in ref.1, one assumes:

-Body frame with x_b axis parallel to the longitudinal missile axis, positive y_b axis out of the left wing, and positive z_b axis upward. (see fig.2.1)

-Flight path axis with x_f axis parallel to the velocity vector, positive z_f axis pointing upwards and y_f axis pointing to the left. (see fig. 2.2)

In fig 2.1 and 2.2, the angles ϕ and θ are the Eulerian roll and pitch angles.

The state vector is given as

$$\underline{\dot{x}} = \left[y_f \quad \dot{y}_f \quad Aty \quad z_f \quad \dot{z}_f \quad Atz \quad \Delta\phi \right]^T \quad (2.1)$$

where y_f and z_f are the components of the relative target position, \dot{y}_f and \dot{z}_f are the relative target velocity, Aty and Atz are the components of target acceleration, which is exponentially decaying with a time constant τ .

$$\Delta\phi = \phi - \phi_0 \quad (2.2)$$

where ϕ_0 is the initial roll angle (at $t=0$).

The control vector is given as:

$$\underline{u} = \left[Ac \quad Pc \right]^T \quad (2.3)$$

where Ac is the commanded acceleration and Pc is the commanded roll rate.

The nonlinear plant equation is

$$\underline{\dot{x}} = f(\underline{x}, \underline{u}) + \underline{G} \quad (2.4)$$

or

$$\dot{\underline{X}} = \begin{bmatrix} \dot{y}_F \\ Aty + Ac \sin \phi \\ -Aty / \bar{G} \\ \dot{z}_F \\ Atz - Ac \cos \phi \\ -Atz / \bar{G} \\ P_c \end{bmatrix} + \begin{bmatrix} 0 \\ 0 \\ 0 \\ 0 \\ -g \cos \theta \\ 0 \\ 0 \end{bmatrix} \quad (2.5)$$

where g is gravity's acceleration and θ is the pitch angle as seen in fig.2.2

Linearizing and setting

$$\underline{G} = \underline{E} \underline{g} \quad (2.6)$$

one has

$$\dot{\underline{X}} = \begin{bmatrix} \dot{y}_F \\ Aty + A'_c (\cos \phi_0) \Delta \phi \\ -Aty / \bar{G} \\ \dot{z}_F \\ Atz + A'_c (\cos \phi_0) \Delta \phi \\ -Atz / \bar{G} \\ 0 \end{bmatrix} + \begin{bmatrix} 0 & 0 \\ \sin \phi_0 & 0 \\ 0 & 0 \\ 0 & 0 \\ -\cos \phi_0 & 0 \\ 0 & 0 \\ 0 & 0 \end{bmatrix} \quad (2.7)$$

where

$$E = \begin{bmatrix} 0 & 0 & 0 & 0 & -\cos \theta & 0 & 0 \end{bmatrix}^T \quad (2.8)$$

in eqn. 2.7, we have set

$$\cos \phi = \cos(\phi_0 + \Delta\phi) = \cos \phi_0 \cos \Delta\phi - \sin \phi_0 \sin \Delta\phi$$

$$\sin \phi = \sin(\phi_0 + \Delta\phi) = \sin \phi_0 \cos \Delta\phi + \cos \phi_0 \sin \Delta\phi$$

and expanded in $\Delta\phi$ which is considered small.

Now assuming that $A'c$, which is actually the desired control Ac , can be expressed in the form of:

$$A'c = Aco \left[1 - \frac{t}{Ti} \right] \quad (2.9)$$

with $Aco = Ac$ at $t=0$, one has

$$\dot{\underline{x}} = \underline{A} \underline{x} + \underline{B} \underline{u} + \underline{E} \underline{g} \quad (2.10)$$

where

$$\underline{A} = \begin{bmatrix} 0 & 1 & 0 & 0 & 0 & 0 & 0 \\ 0 & 0 & 1 & 0 & 0 & 0 & Aco \left[1 - \frac{t}{Ti} \right] \cos \phi_0 \\ 0 & 0 & -1/\delta & 0 & 0 & 0 & 0 \\ 0 & 0 & 0 & 0 & 1 & 0 & 0 \\ 0 & 0 & 0 & 0 & 0 & 1 & Aco \left[1 - \frac{t}{Ti} \right] \sin \phi_0 \\ 0 & 0 & 0 & 0 & 0 & -1/\delta & 0 \\ 0 & 0 & 0 & 0 & 0 & 0 & 0 \end{bmatrix} \quad (2.11)$$

(2.12)

$$\underline{B} = \begin{bmatrix} 0 & 0 \\ \sin \phi_0 & 0 \\ 0 & 0 \\ 0 & 0 \\ -\cos \phi_0 & 0 \\ 0 & 0 \\ 0 & 1 \end{bmatrix}$$

$$\underline{E} = \begin{bmatrix} 0 & 0 & 0 & 0 & -\cos \theta & 0 & 0 \end{bmatrix}^T \quad (2.13)$$

$$\underline{g} = g \quad (2.14)$$

D. THE DISCRETE MODEL

1. Introduction

With the introduction of a digital computer to control the continuous-time system, one has to have some kind of interface in order to take care of the communication between the discrete and continuous-time systems. In this case it will be considered, A-to-D and D-to-A converters as samplers and zero-order holders as in reference 2.

In such case, considering the system:

$$\dot{\underline{x}}(t) = \underline{A}(t) \underline{x}(t) + \underline{B}(t) \underline{u}(t) + \underline{E}(t) \underline{g}(t) \quad (2.15)$$

one can write the state of the system at time $t(k+1)$ as :

$$x(t_{k+1}) = \phi(t_{k+1}, t_k) x(t_k) + \int_{t_k}^{t_{k+1}} \phi(t_{k+1}, \eta) B(\eta) d\eta u(t_k) \quad (2.16)$$

$$+ \int_{t_k}^{t_{k+1}} \phi(t_{k+1}, \eta) E(\eta) d\eta g(t_k)$$

where $\phi(t, t_0)$ is the transition matrix of the system represented by eqn. 2.13.

Furthermore, we will consider that the sampling instants are equally spaced, or:

$$t_{k+1} - t_k = T \quad (2.17)$$

$$t_{k+1} = kT + T \quad (2.18)$$

so one can replace

$$t_k = kT$$

thus,

$$x(kT+T) = \phi(kT+T) x(kT) \quad (2.19)$$

$$+ \int_{kT}^{kT+T} \phi(kT+T, \eta) B(\eta) d\eta u(kT)$$

$$+ \int_{kT}^{kT+T} \phi(kT+T, \eta) E(\eta) d\eta g(kT)$$

or in a simplified notation:

$$x(k+1) = A_d(k) x(k) + B_d(k) u(k) \quad (2.20)$$

$$+ E_d(k) g(k)$$

where,

$$A_d(k) = \phi(kT+T, kT) \quad (2.21)$$

$$B_d(k) = \int_{kT}^{kT+T} \phi(kT+T, \eta) B(\eta) d\eta \quad (2.22)$$

$$E_d(k) = \int_{kT}^{kT+T} \phi(kT+T, \eta) B(\eta) d\eta \quad (2.23)$$

2. Calculation of the Matrices A(k), B(k) and E(k)

It is straightforward to show, using the sparseness of the matrix A(t), that the transition matrix of equation 2-19 is :

$$\phi(kT+T) = \begin{bmatrix} 1 & T & Ad_{13} & 0 & 0 & 0 & Ad_{17} \\ 0 & 1 & Ad_{23} & 0 & 0 & 0 & Ad_{27} \\ 0 & 0 & e^{-T/6} & 0 & 0 & 0 & 0 \\ 0 & 0 & 0 & 1 & T & Ad_{46} & Ad_{47} \\ 0 & 0 & 0 & 0 & 1 & Ad_{56} & Ad_{57} \\ 0 & 0 & 0 & 0 & 0 & e^{-T/6} & 0 \\ 0 & 0 & 0 & 0 & 0 & 0 & 1 \end{bmatrix} \quad (2.24)$$

where:

$$A_{d_{1,3}} = A_{d_{4,6}} = \bar{\sigma} T - \bar{\sigma}^2 (1 - e^{-T/\bar{\sigma}})$$

$$A_{d_{2,3}} = A_{d_{5,6}} = (1 - e^{-T/\bar{\sigma}})$$

For the calculation of the others terms one may make use of the property of the transition matrix that:

$$\frac{d\phi(t_2, t_1)}{dt_2} = A(t_2) A_d(t_2, t_1)$$

so,

$$\frac{dA_d(kT+T, kT)}{d(kT+T)} = A(kT+T) A_d(kT+T, kT)$$

For A (2,7) :

$$\frac{dA_{d_{2,7}}(kT+T, kT)}{d(kT+T)} = A_{d_{2,7}}(kT+T) = A_{co} \left[1 - \frac{t}{T_i} \right] \cos \phi_0 \Big]_{kT+T}$$

$$\frac{dA_{d_{2,7}}(kT+T, kT)}{d(kT+T)} = A_{co} \left[1 - \frac{kT+T}{T_i} \right] \cos \phi_0$$

$$A_{d_{2,7}} = A_{co} \cos \phi_0 \int_{kT}^{kT+T} \left[1 - \frac{kT+T}{T_i} \right] d(kT+T)$$

$$A_{d_{2,7}} = A_{co} \cos \phi_0 \left[T - \left[\frac{2k+1}{2} \frac{T}{T_i} \right] T^2 \right]$$

For A (1,7) :

$$\frac{dA_{d_{1,7}}(kT+T, kT)}{d(kT+T)} = A_{d_{2,7}}(kT+T, kT)$$

$$A_{d_{1,7}}(kT+T, kT) = \int_{kT}^{kT+T} A_{d_{2,7}} d(kT+T)$$

$$Ad_{4,7} = \left[T^2 - \left[\frac{2k+1}{2T_i} \right] T^3 \right] A \cos \phi_0$$

Doing the same process for $Ad(5,7)$ and $Ad(4,7)$ one has:

$$Ad_{4,7} = A \cos \phi_0 \left[T^2 - \left[\frac{2k+1}{2T_i} \right] T^3 \right]$$

$$A = A \cos \phi_0 \left[T - \left[\frac{2k+1}{2T_i} \right] T^2 \right]$$

For the derivation of the matrix $B_d(k)$ one needs according to eqn. 2-22

$$\phi(kT+T) B(\eta) = A_d(kT+T, \eta) B(\eta)$$

where,

$$A_d(kT+T, \eta) = \begin{bmatrix} 1 & A\eta_{1,2} & A\eta_{1,3} & 0 & 0 & 0 & A\eta_{1,7} \\ 0 & 1 & A\eta_{2,3} & 0 & 0 & 0 & A\eta_{2,7} \\ 0 & 0 & A\eta_{3,3} & 0 & 0 & 0 & 0 \\ 0 & 0 & 0 & 1 & A\eta_{4,5} & A\eta_{4,6} & A\eta_{4,7} \\ 0 & 0 & 0 & 0 & 1 & A\eta_{5,6} & A\eta_{5,7} \\ 0 & 0 & 0 & 0 & 0 & A\eta_{6,6} & 0 \\ 0 & 0 & 0 & 0 & 0 & 0 & 1 \end{bmatrix}$$

where $A\eta$ represents $A_d(kT+T, \eta)$, and

$$B(\eta) = \begin{bmatrix} 0 & 0 \\ \sin \phi_0 & 0 \\ 0 & 0 \\ 0 & 0 \\ -\cos \phi_0 & 0 \\ 0 & 0 \\ 0 & 0 \end{bmatrix}$$

thus

$$A_d(kT+T, \eta) B(\eta) = \begin{bmatrix} A\eta_{1,2} \sin \phi_0 & A\eta_{1,7} \\ \sin \phi_0 & A\eta_{2,7} \\ 0 & 0 \\ -A\eta_{4,6} \cos \phi_0 & A\eta_{4,7} \\ -\cos \phi_0 & A\eta_{5,7} \\ 0 & 0 \\ 0 & 0 \end{bmatrix}$$

where

$$A\eta_{1,2} = kT+T - \eta = A\eta_{4,5}$$

$$A\eta_{2,7} = \left[kT+T - \frac{(kT+T)^2}{2Ti} - \eta + \frac{\eta^2}{2Ti} \right] A\cos \phi_0$$

$$A\eta_{1,7} = \left[T(kT+T) - \left[\frac{2k+1}{2Ti} \right] (kT+T) T^2 - \right. \\ \left. - T\eta + \left[\frac{2k+1}{2Ti} \right] T^2 \eta \right] A\cos \phi_0$$

$$A\eta_{4,7} = \left[T(kT+T) - \left[\frac{2k+1}{2Ti} \right] (kT+T) T^2 - \right. \\ \left. - T\eta + \left[\frac{2k+1}{2Ti} \right] T^2 \eta \right] A\sin \phi_0$$

$$A\eta_{5,7} = \left[kT+T - \frac{(kT+T)^2}{2Ti} - \eta + \frac{\eta^2}{2Ti} \right] A\sin \phi_0$$

and for $B_d(k)$:

$$B_d = \begin{bmatrix} B_{d_{1,1}} & B_{d_{1,2}} \\ \sin \phi_0 & B_{d_{2,2}} \\ 0 & 0 \\ B_{d_{4,1}} & B_{d_{4,2}} \\ -\cos \phi_0 & B_{d_{5,2}} \\ 0 & 0 \\ 0 & T \end{bmatrix}$$

where

$$B_{d_{1,1}} = \int_{kT}^{kT+T} (kT+T-\eta) d\eta \sin \phi_0 = -\frac{T^2}{2} \sin \phi_0$$

$$B_{d_{4,1}} = -\frac{T^2}{2} \cos \phi_0$$

$$B_{d_{2,2}} = \int_{kT}^{kT+T} A \eta_{2,7} d\eta$$

which after some algebraic work has been found

$$B(k) = \left[\frac{T^2}{2} - \frac{(kT+T)^3}{3Ti} - \frac{(kT+T)^2 kT}{2Ti} - \frac{(kT)^2}{6Ti} \right] A \cos \phi_0$$

and

$$B_{d_{1,2}}(k) = \int_{kT}^{kT+T} A \eta_{1,7} d\eta$$

which can be found to be:

$$B_{d_{1,2}}(k) = \left[\frac{T^3}{2} - \frac{1}{2} - \left[\frac{2k+1}{2Ti} \right] T^4 \right] A \cos \phi_0$$

thus

$$B_{d_{4,2}}(k) = \left[\frac{T^3}{2} - \frac{1}{2} - \left[\frac{2k+1}{2Ti} \right] T^4 \right] A \cos \sin \phi_0$$

$$B_{d_{5,2}}(k) = \left[\frac{T^2}{2} - \frac{(kT+T)^3}{3Ti} + \frac{(kT+T)^2}{2Ti} kT - \frac{(kT)^3}{6Ti} \right] A \cos \sin \phi_0$$

In the same way:

$$\phi(kT+T, \eta) E(\eta) = \begin{bmatrix} 0 \\ 0 \\ 0 \\ -T \cos \theta \\ -\cos \theta \\ 0 \\ 0 \end{bmatrix}$$

thus $\underline{E}(k)$ is equal to

$$\underline{E} = \begin{bmatrix} 0 & 0 & 0 & 0 & -\frac{T^2}{2} \cos \theta & -T \cos \theta & 0 & 0 \end{bmatrix}$$

where we have considered θ as a constant angle. (Further comments on this after development of the control law).

Notice that throughout this work, the commanded acceleration has been considered an unknown and the assumption has been made that it will be in the form of eqn.2.9. One will need in further developments to consider the control A_c as a known $A_c(k)$, which will be a constant between kT and $kT+T$. With such assumptions, the discrete representation of the system is easily found to be :

$$\underline{x}(k+1) = \underline{A}(k) \underline{x}(k) + \underline{B}(k) \underline{u}(k) + \underline{E} g \quad (2.26)$$

where

$$A_d = \begin{bmatrix} 1 & T & A_{d_{1,3}} & 0 & 0 & 0 & A_{d_{1,7}} \\ 0 & 1 & A_{d_{2,3}} & 0 & 0 & 0 & A_{d_{2,7}} \\ 0 & 0 & e^{-T/\tau} & 0 & 0 & 0 & 0 \\ 0 & 0 & 0 & 1 & T & A_{d_{4,6}} & A_{d_{4,7}} \\ 0 & 0 & 0 & 0 & 1 & A_{d_{5,6}} & A_{d_{5,7}} \\ 0 & 0 & 0 & 0 & 0 & e^{-T/\tau} & 0 \\ 0 & 0 & 0 & 0 & 0 & 0 & 1 \end{bmatrix} \quad (2.27)$$

with

$$A_{d_{1,3}} = \tau T - \tau^2 (1 - e^{-T/\tau}) = A_{d_{4,6}}$$

$$A_{d_{2,3}} = \tau (1 - e^{-T/\tau}) = A_{d_{5,6}}$$

$$A_{d_{1,7}} = -\frac{T^2}{2} A_c \cos \phi_0$$

$$A_{d_{2,7}} = T A_c \cos \phi_0$$

$$A_{d_{4,7}} = -\frac{T^2}{2} A_c \sin \phi_0$$

$$A_{d_{5,7}} = T A_c \sin \phi_0$$

and

$$B_d(k) = \begin{bmatrix} \frac{T^2}{2} \sin \phi_0 & \frac{T^3}{6} A_c \cos \phi_0 \\ T \sin \phi_0 & \frac{T^2}{2} A_c \cos \phi_0 \\ 0 & 0 \\ -\frac{T^2}{2} \cos \phi_0 & \frac{T^3}{6} A_c \sin \phi_0 \\ -T \cos \phi_0 & \frac{T^2}{2} A_c \sin \phi_0 \\ 0 & 0 \\ 0 & T \end{bmatrix}$$

and

$$E_d(k) = \begin{bmatrix} 0 \\ 0 \\ 0 \\ -\frac{T^2}{2} \cos \theta \\ -T \cos \theta \\ 0 \\ 0 \end{bmatrix}$$

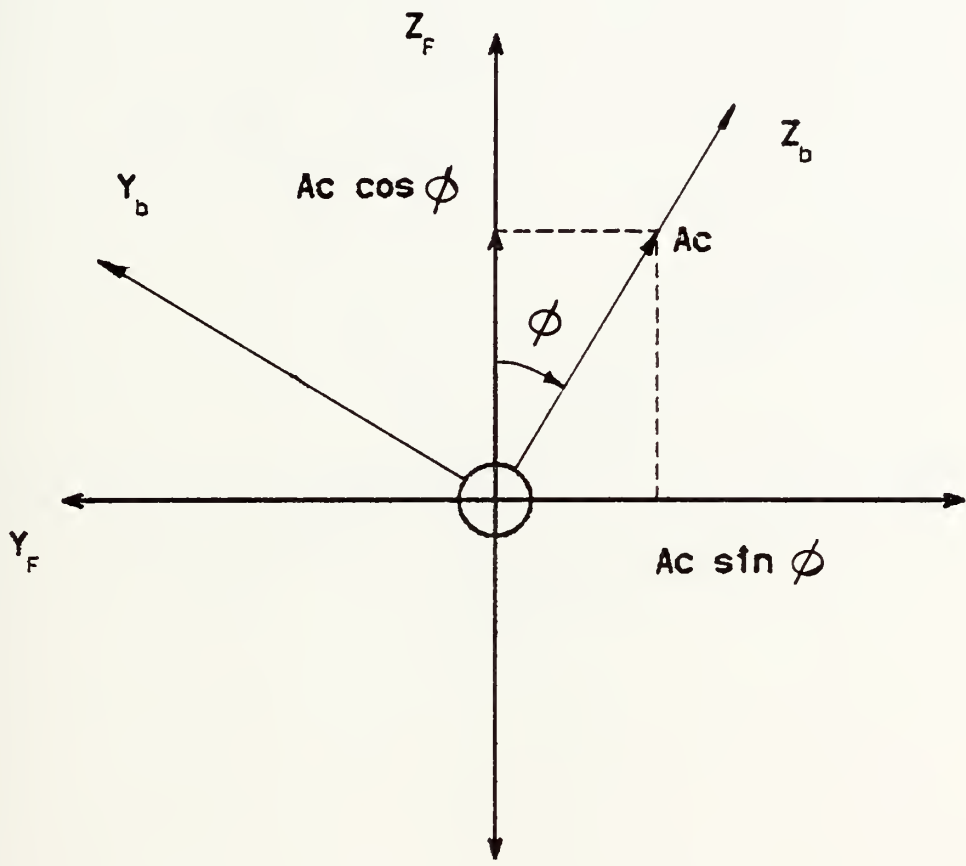


Figure 2.1 Reference Frames.

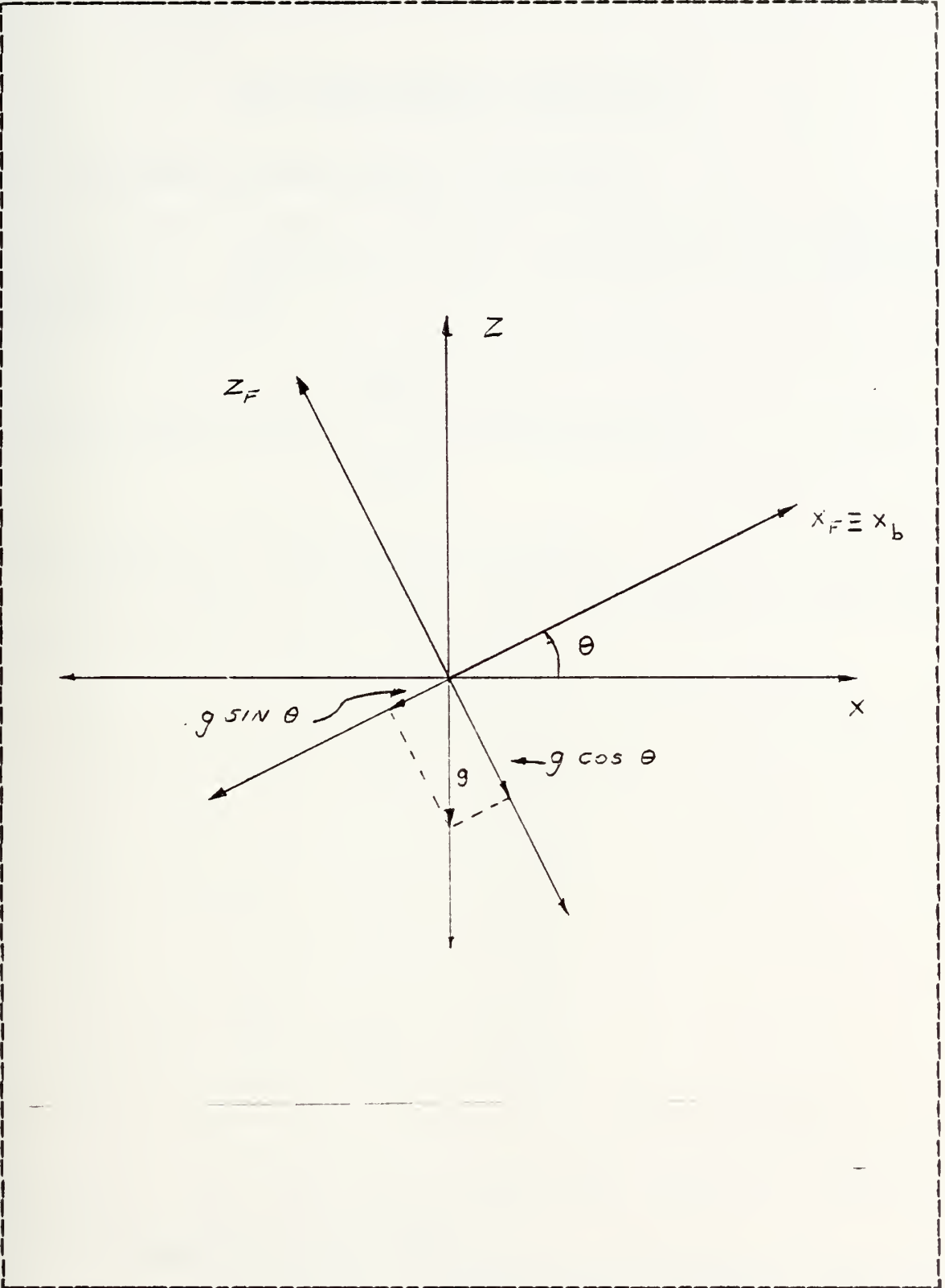


Figure 2.2 Reference Frames.

III. THE OPTIMAL CONTROLLER

A. DERIVATION OF THE OPTIMAL CONTROLLER

In order to have a suitable guidance law to implement the control commands, we will minimize the following performance index:

$$J = \frac{1}{2} x^T(N) W(N) x(N) + \sum_{k=0}^{N-1} \frac{1}{2} u^T(k) Q(k) u(k) \quad (3.1)$$

where $x(N)$ is the final state at $t=T$

As we want to minimize the final miss distance, the weighting matrix $W(N)$ is taken as

$$\begin{bmatrix} 1 & 0 & 0 & 0 & 0 & 0 & 0 \\ 0 & 0 & 0 & 0 & 0 & 0 & 0 \\ 0 & 0 & 0 & 0 & 0 & 0 & 0 \\ 0 & 0 & 0 & 1 & 0 & 0 & 0 \\ 0 & 0 & 0 & 0 & 0 & 0 & 0 \\ 0 & 0 & 0 & 0 & 0 & 0 & 0 \\ 0 & 0 & 0 & 0 & 0 & 0 & 0 \end{bmatrix} \quad (3.2)$$

and $Q(k)$ is a two by two positive definite symmetric weighting matrix to be chosen.

In the derivation of the solution, reference 3 has been followed keeping in mind that the state equation has the form:

$$\underline{x}(k+1) = \underline{A}(k) \underline{x}(k) + \underline{B}(k) \underline{u}(k) + \underline{E} g \quad (3.3)$$

or

$$\underline{x}(k+1) = f(\underline{x}(k), \underline{u}(k), g) \quad (3.4)$$

where the third term, which represents the effect of the gravity has been considered constant.

Considering that the performance index is in the form:

$$J = \phi[x(N)] + \sum_{k=0}^{N-1} L(k) [x(k), u(k), g(k)] \quad (3.5)$$

we need to find a sequence of $u(k)$ that minimizes J .

Adjoin the system equation to J with a multiplier $\lambda(n)$

$$J = \phi[x(N)] + \sum_{k=0}^{N-1} \left\{ L(k) [x(k), u(k), g] + \lambda^T(k+1) \left\{ f_k[x(k), u(k), g] - x(k+1) \right\} \right\} \quad (3.6)$$

and defining a scalar sequence $H(k)$

$$H(k) = L(k) [x(k), u(k), g] + \lambda^T(k+1) f_k [x(k), u(k), g] \quad (3.7)$$

$k=0, 1, 2, \dots, n-1$

one has:

$$J = \phi [x(N)] - \lambda^T(N) x(N) + \quad (3.8)$$

$$+ \sum_{k=1}^{N-1} [H(k) - \lambda^T(k) x(k)] + H(0)$$

Considering differential changes in J:

$$dJ = \left[\frac{\partial \phi}{\partial x(N)} - \lambda^T(N) \right] dx(N) + \quad (3.9)$$

$$+ \sum_{k=1}^{N-1} \left\{ \left[\frac{\partial H(k)}{\partial x(k)} - \lambda^T(k) \right] dx(k) + \right.$$

$$\left. + \frac{\partial H(k)}{\partial u(k)} du(k) \right\} + \frac{\partial H(0)}{\partial x(0)} dx(0) +$$

$$+ \frac{\partial H(0)}{\partial u(0)} du(0)$$

choosing the multiplier $\lambda(k)$ so that

$$\lambda^T(k) - \frac{\partial H(k)}{\partial x(k)} = 0 \quad (3.10)$$

thus

$$\frac{\partial L(k)}{\partial x(k)} + \lambda^T(k+1) \frac{\partial f_k}{\partial x(k)} = \lambda^T(k)$$

and

$$\frac{\partial H(k)}{\partial u(k)} = 0 \quad (3.11)$$

with boundary condition

$$\lambda^T(N) = \frac{\partial \phi}{\partial x(N)} \quad (3.12)$$

we obtain the minimization of the performance index.

In the present case we have:

$$J = \frac{1}{2} x^T(N) W(N) x(N) + \sum_{k=0}^{N-1} u^T(k) Q(k) u(k) + \lambda^T(k+1) \left[A(k) x(k) + B(k) u(k) + E g - x(k+1) \right] \quad (3.13)$$

and $H(k)$:

$$H(k) = \frac{1}{2} u^T(k) Q(k) u(k) + \lambda^T(k+1) \left[A(k) x(k) + B(k) u(k) + E g \right] \quad (3.14)$$

then in order to minimize J :

$$\frac{\partial H(k)}{\partial u(k)} = u^T(k) Q(k) + \lambda^T(k+1) B(k) = 0 \quad (3.15)$$

or considering that $Q(k) = Q(k)$

$$Q(k) u(k) = - B^T(k) \lambda(k+1)$$

and

$$\lambda^T(k) = \frac{\partial H(k)}{\partial x(k)} \quad (3.16)$$

$$\lambda^T(k) = \lambda^T(k+1) A(k)$$

and

$$\lambda^T(N) = x^T(N) W(N) \quad (3.17)$$

Notice that we are not weighting the states in the performance index, except the last state. A more general form could be obtained, with all states being weighting, if we change the eqn 3.16 to:

$$\lambda^T(k) = \lambda^T(k+1) A(k) + x^T(k) W1(k) \quad (3.18)$$

where $W1(k)$ is the weighting matrix of the states.

With equations 3.15, 3.16 and 3.17 one is able to find the sequence of $u(k)$ that will give the minima controls.

Such set of equations can be solved by the sweep method as in ref. 2 .

We will look for a solution of the form:

$$u(k) = -F(k)x(k) - FG(k)g(k) \quad (3.19)$$

what means that the commanded acceleration and roll rate, will have a correction due to the effect of gravity.

Placing:

$$\lambda(k) = S(k) x(k) + SG(k) g(k) \quad (3.20)$$

from eqn. 3.15

$$Q(k) u(k) = -B^T(k) \left[S(k+1) x(k+1) + SG(k+1) g(k+1) \right]$$

from eqn. 3.3

$$Q(k) u(k) = -B^T(k) S(k+1) \left[A(k) x(k) + \right. \quad (3.21) \\ \left. + B(k) u(k) + E g \right] - B^T(k) SG(k+1) g(k+1)$$

so

$$\left[Q(k) + B^T(k) S(k+1) B(k) \right] u(k) = \\ -B^T(k) S(k+1) A(k) x(k) - B^T(k) S(k+1) E g(k) - \\ -B^T(k) SG(k+1) g(k+1)$$

considering that g is a constant

$$u(k) = - \left[Q(k) + B^T(k) S(k+1) B(k) \right]^{-1} \quad (3.22)$$

$$\begin{bmatrix} B^T(k) & S(k+1) & A(k) & x(k) + \\ + \left[B^T(k) & S(k+1) & E + B^T(k) & Sg(k+1) \right] & g \end{bmatrix}$$

so:

$$u(k) = -F(k)x(k) - FG(k)g$$

where

$$F = \left[Q(k) + B^T(k) S(k+1) B(k) \right]^{-1}. \quad (3.23)$$

$$\cdot B^T(k) S(k+1) A(k)$$

$$FG = \left[Q(k) + B^T(k) S(k+1) B(k) \right]^{-1} \quad (3.24)$$

$$\left[B^T(k) S(k+1) E + B^T Sg(k+1) \right]$$

from eqn. 3.16 and 3.19

$$\begin{aligned} \lambda(k) &= A^T(k) \lambda(k+1) = A^T(k) \left[S(k+1)x(k+1) + SG(k+1)g(k+1) \right] = \\ &= A^T(k) S(k+1) A(k) x(k) + A^T(k) S(k+1) B(k) u(k) \\ &+ A^T(k) S(k+1) Eg + A^T(k) SG(k+1) g(k+1) \end{aligned}$$

from eqn. 3.19

$$\begin{aligned} \lambda(k) &= A^T(k) S(k+1) A(k) x(k) + A^T(k) S(k+1) B(k) \\ &\cdot \left[-F(k) x(k) - FG(k) g \right] + A^T(k) S(k+1) Eg + \\ &+ A^T(k) SG(k) g(k+1) \end{aligned}$$

so, as g is a constant:

$$S(k)x(k) + SG(k)g = \left[A^T(k) S(k+1) A(k) - A(k) S(k+1) B(k) F(k) \right] +$$

$$+ \left[A^T(k) S(k+1) E - A^T(k+1) B(k) FG(k) \right. \\ \left. + A(k) SG(k+1) \right] g$$

thus

$$S(k) = A^T(k) S(k+1) A(k) - A^T(k) S(k+1) B(k) F(k) \quad (3.25)$$

and

$$SG(k) = A^T(k) S(k+1) E - A^T(k) S(k+1) B(k) FG(k) + \\ + A^T(k) SG(k+1) \quad (3.26)$$

These equations, 3.25, 3.26, 3.23 and 3.24 can be solved backwards with the final condition:

$$S(N) = W(N)$$

$$SG(N) = 0$$

Notice that this satisfies our previous boundary condition in eqn. 3.17 where:

$$S(N) = W(N) \times (N)$$

$$S(N) \times (N) = W(N) \times (N)$$

so

$$S(N) = W(N)$$

B. EXTENTION OF THE MODEL FOR LARGE ROLL ANGLES

Up to this point, one has to take into account that throughout the development of this work, the angle has been considered small, it is necessary to relax this restriction.

In order to do that, the system has been broken in two blocks as in figure 3.1.

The first block is a representation of the algorithm which will calculate the optimal commands. The algorithm has contain with itself an exact model of the system or missile. The model of the missile is initialized from the information on the initial states, the initial input command A_{c0} and initial roll angle (at $t=0$); and computes the optimal gains and further the optimal commands which will be feed to the missile.

The method adopted in computing the optimal commands is more easily understood if one considers figure 3.2.

In figure 3.2, the lines numbered as 0 in the graph for A_c and for P_c are the optimal commands for a given initial roll angle (ϕ_0). Lines number 1 are the commands for a second initial roll angle (ϕ_1) larger than ϕ_0 , and so on. Thus in figure 3.2 one has a family of optimal commands for any initial roll angle.

Notice that the upper line of the graph of A_c represents the accelerations of a missile which had at $t=0$ a correct initial roll angle in order to hit the target with no comands in roll rate.

In the present method the computer performs the calculation of the commands only for the first step of time and then feeds these commands to the missile. The missile is then driven to the next state ($x(k+1)$) and feed-backs to the computer the information on the roll angle at that step. The roll angle feed-backs from the missile is considered by the algorithm as the initial roll angle at $t=0$ and the next commands are calculated. Notice that at this second step the algorithm will feed to the system the second command (at $t=\tau_1$). This process is them repeated until t is equal to the intercepted time.

It is important to realize that with this method of calculation, since the algorithm was developed with the assumption of small roll excursions some error is expected due to the fact that in computing the gains by solving a Ricatti equation backwards, as has been done, it is necessary to update the system from $t=0$ to $t=T_i$ at each step, and in this process the roll angle is not small. Notice however that we are applying the commands only in one step, and if one expects that the roll rate will decrease to zero, as we are increasing in time, the variation of the roll angle will tend to decrease, so, we can expect that the error will decrease as the time increases.

Another important point to be studied is how the missile itself (second block in fig. 3.2) has to be implemented in order to be valid for small and large roll excursions.

It is considered that one has the perfect knowledge of the commands, thus the missile is modeled as a state variable system as in eqn 2.26 with the initial roll angle being update at each step. In this way the system will take the initial roll angle as the summation of all previous initial roll angles. (see fig 3.4)

From the original variables one has for the state $\Delta\phi$, the following:

$$\Delta\phi(k+1) = \Delta\phi(k) + P_c(k) T \quad (3.27)$$

which is show in figg. 3.3, where the initial roll angle is kept constant and $\Delta\phi$ is update each step.

Notice however that considering large roll excursions (see fig. 3.4) and keeping in mind that the angle ϕ has been defined as

$$\phi = \phi_0 + \Delta\phi$$

the expression 3.27 is not valid, since in modeling the system it was assumed that $\Delta\phi$ would be small.

This leads to a change in the expression for the variation of $\Delta\phi$ as in fig. 3.4. In fig. 3.4, the angle $\Delta\phi$ is update at each step, so one has:

$$\Delta\phi(k+1) = P_c(k) T \quad (3.28)$$

By consideration of the equation 2.27 it can be seen that by setting the element $A(7,7)$ to zero, one can obtain equation 3.28.

Thus the missile model for large roll excursions will be represented by the following equation.

$$x(k+1) = A(k) x(k) + B(k) u(k) + E g$$

where

$$A(k) = \begin{bmatrix} 1 & T & A_{1,3} & 0 & 0 & 0 & A_{1,7} \\ 0 & 1 & A_{2,3} & 0 & 0 & 0 & A_{2,7} \\ 0 & 0 & e^{-T/\tau} & 0 & 0 & 0 & 0 \\ 0 & 0 & 0 & 1 & T & A_{4,6} & A_{4,7} \\ 0 & 0 & 0 & 0 & 1 & A_{5,6} & A_{5,7} \\ 0 & 0 & 0 & 0 & 0 & e^{-T/\tau} & 0 \\ 0 & 0 & 0 & 0 & 0 & 0 & A_{7,7} \end{bmatrix} \quad (3.29)$$

where $A(7,7)=0$,for large roll excursions

$A(7,7)=1$,for small roll excursions

$$B = \begin{bmatrix} \frac{T^2}{2} \sin \phi_0 & \frac{T^3}{6} A_c \cos \phi_0 \\ T \sin \phi_0 & \frac{T^2}{2} A_c \cos \phi_0 \\ 0 & 0 \\ -\frac{T^2}{2} \cos \phi_0 & \frac{T^3}{6} A_c \sin \phi_0 \\ -T \cos \phi_0 & \frac{T^2}{2} A_c \sin \phi_0 \\ 0 & 0 \\ 0 & T \end{bmatrix} \quad (3.30)$$

$$E = \begin{bmatrix} 0 \\ 0 \\ 0 \\ -\frac{T^2}{2} \cos \theta \\ -T \cos \theta \\ 0 \\ 0 \end{bmatrix} \quad (3.31)$$

We will redefine the states x_1 , as the relative position, x_2 as the relative velocity in the Y direction and x_3 as the target acceleration in Y direction. The states x_4 , x_5 and x_6 has the same meaning, but in the Z direction and

x_1 , is $\Delta\phi$. In this representation of the system, $x_1(k)$ is equal to the component of the miss distance along the Y direction and:

$$x_1(k+1) = y_p(k+1) = y_p(k) + \dot{y}_p(k) T + \quad (3.32)$$

$$+ \left[\zeta T - \zeta^2 (1 - e^{-T/\zeta}) \right] A_t y(k) + \frac{T^2}{2} A_c(k) \cos\phi_0 \Delta\phi(k) \\ + \frac{T^2}{2} \sin\phi_0 A_c(k) + \frac{T^3}{6} A_c(k) \cos\phi_0 P_c(k)$$

The first three terms in the RHS of eqn.3.32, are easily seen as the contribution to the miss distance of respectively the previous miss distance, relative velocity and target acceleration. The following two terms represents the contribution of the commanded acceleration and the last term represents the effect of coupled A_c and P_c , and tends to be small due to the cube of the sample period.

For the component of miss distance in the Z direction, one has:

$$x_4(k+1) = z_p(k+1) = z_p(k) + \dot{z}_p(k) T + \\ + \left[\zeta T - \zeta^2 (1 - e^{-T/\zeta}) \right] A_t z(k) + \frac{T^2}{2} A_c(k) \sin\phi_0 \Delta\phi(k) - \\ - \frac{T^2}{2} \cos\phi_0 A_c(k) + \frac{T^3}{6} A_c(k) \sin\phi_0 P_c(k) - \frac{T^2}{2} \cos\theta g$$

where its terms have the same physical meaning as in the expression for $x(k+1)$, with the effect of the gravity added to the expression.

Since one can notice that in the representation of the miss distance in Y direction appear two terms as a function of $\cos\phi_0$, and in the representation of the miss distance in Z direction appear two terms as function of $\sin\phi_0$, it is

interesting to verify that the fourth term in the RHS of both expressions acts like a correction for the fifth term. Referring to fig. 3.4b, one can see that at any step of time, the commanded acceleration is actually,

$$Ac \cos \phi_0 - \Delta Ac$$

and considering small angles:

$$\begin{aligned} \Delta Ac &= Ac \cos \phi_0 - Ac \cos(\phi_0 + \Delta \phi) = \\ &= Ac \cos \phi_0 - Ac [\cos \phi_0 \Delta \phi - \sin \phi_0 \sin \Delta \phi] = \\ &= Ac \sin \phi_0 \Delta \phi \end{aligned}$$

The same idea can be applied to the expression for $x(k+1)$.

The terms x_2 and x_5 , represent the relative velocity, and are:

$$\begin{aligned} x_2(k+1) &= \dot{y}_F(k) + \zeta (1 - e^{-T/\tau}) Aty(k) + Ac(k) \cos \phi_0 T \\ &+ Ac(k) \sin \phi_0 T + \frac{T^2}{2} Ac(k) \cos \phi_0 Pc(k) \end{aligned}$$

$$\begin{aligned} x_5(k+1) &= \dot{z}_F(k) + \zeta (1 - e^{-T/\tau}) Atz(k) + Ac(k) \sin \phi_0 T - \\ &- Ac(k) \cos \phi_0 T + \frac{T^2}{2} Ac(k) \sin \phi_0 Pc(k) - T \cos \theta g \end{aligned}$$

Where the two first terms in the RHS represents the effect of the velocity and acceleration at a previous step, and the other three terms has the same meaning as previously stated.

The terms x_3 and x_6 are the target accelerations, in this model being exponentially decaying.

1. Effects on the Miss Distance of the Extension of the Model

In previous subsection, a extension of the model for large roll excursions has been performed. Notice that there are two models of the system being used. The first one, used

in the algorithm is valid only for small roll excursions, and a second model, valid for small and large roll excursions used as a representation of the missile.

The algorithm with the first model, as explained before, is initialized at each step with the actual roll angle of the missile, and performs the calculation of the commands.

In order to check the effect of the extension of the model on the miss distance, one can define a ideal initial roll angle ($\phi_{o,ideal}$), as the roll angle at $t=0$ in order to have the commanded acceleration vector pointing to the projected final target's position. This means that the missile would not have to roll to hit the target (see fig 3.5), thus the commanded roll rate calculated by the algorithm will be equal to zero. This implies that from that point ahead, the roll angle is constant and equal to $\phi_{o,ideal}$, and that the time history of the control A_c will be a straight line.

The fact that the roll angle will tend to this limit deserves an investigation. Notice that, as show in fig. 3.2, at the moment the missile reaches its maximum roll angle, the control A_c will be the required acceleration to hit the target if the missile initial roll angle was $\phi_{o,ideal}$. This means that the control A_c computed would be correct only if the missile would have turned immediately to this angle.

For very small angles, the previous comment would be acceptable, but in a normal situation, as showed in figure 3.5, the missile will only reach the ideal initial roll angle after some time, and due to the vertical component of the acceleration, when this occurs the missile would be in a position above the ideal trajectory, which means that it would follow a course parallel to the ideal trajectory to intercept.

One can see that such problem will lead to a large miss distance, in the case that the target acceleration it is not small. Thus, some correction is necessary in order to improve the missile performance.

Figure 3.5b shows the missile at some point of its trajectory where it has reached its maximum roll angle, thus it is at a parallel course with its ideal trajectory to intercept. At this point, since all the states are known, it is possible to recompute a new ϕ_{ideal} . So, if at this point the computer is fed with the states at this point it will compute the commands in order to drive the missile to the new ϕ_{ideal} , which will introduce the desired correction. Notice that such correction can be made during all the flight, from $t=0$, to $t=T_i$.

In the present work this method has been accomplished by feeding-back to the computer the roll angle and all the states of the missile. With this information the computer is able to perform the calculation of the corrected commands at each step of time. However as the states are being updated, it is also necessary to update the time to intercept, which has been done using the time to go to intercept, or:

$$T_i(k) = T_i - k T$$

where T_i is the nominal time to intercept.

C. SIMULATION

In order to keep the same assumptions as reference 1, the matrix Q (weighting the control) has been put as suggested in such reference or:

$$\begin{bmatrix} b_1 & 0 \\ 0 & b_2 \end{bmatrix}$$

(3.33)

with

$$b_1 = 5.78 \cdot 10^3$$

$$b_2 = 5.0 \text{ meters}$$

Five different cases were run:

Case 0, tested with one simple model valid only for small roll angles begins with missile and target on parallel courses to the inertial x axis, the target 100 meters above the missile and with an evasive manoeuvre exponentially decaying with time constant of 20 seconds. The initial acceleration of target was -0.5 g's in y direction. (see fig. 3.6)

Case 1, with the same scenarios as case 0, but was run using the algorithm for large roll excursions.

Case 2, is the same scenario as in case 1, except that the initial acceleration of target was -1.0 g's in the y direction. (Same as case 1 in ref. 1).

Case 3, the same as case 2, with target acceleration of -4 g's. (Same as case 2 in the reference 1)

Case 4, same as case 3 but with target at initial position 600 meters below the missile. (Same as case 3 in reference 1.)

D. COMMENTS AND CONCLUSIONS

1. Results

In case 0, the missile begins its trajectory commanding 26.5 m/sec^2 and the time history of the control A_c follows exactly a straight line in the form suggested in

ref. 1, as seen in fig.3.7 The control P_c , beginning at .35 rad per second, is decaying and reaches zero at $k=80$ (see fig.3.8). Figures 3.9 and 3.10 show the miss distance, where one can see that the missile is crossing the target with a CG-to-CG distance of 1.5 meters.

Figure 3.11, shows the time history for the roll angle, which as expect, reaches a constant value, with the missile crossing target at $t=T_i$, with a bank of .44 radians.

In case 1, which was run with the model for large roll excursions, the missile kept the same A_{co} , but there is a very small increase in further commanded acceleration in order to correct the effect of the roll angle on the vertical component of the control A_c , as seen in fig.3.12, and table I.

Figure 3.13 shows that the roll rate decreases almost as before, and the final roll angle is .42 rds, as shown in fig.3.15 and table I. Referring to figure 3.14 there is a change in the final miss distance, which is better than case 0, due to a improvement in its Z component (see table I). This results in a final CG-to-CG miss distance of .65 meters.

In case 2, the missile has the same A_c at $t=0$, but with the correction for roll angle being increased due to the increase of target acceleration (see fig.3.16), the commanded A_c reaches a larger peak value.

The initial value of the commanded roll rate is .69 radians, which is larger than case 1, due to the increase in the target acceleration. In figure 3.18, there is no noticeable change in the shape of the curve for Z direction, and in the Y direction the final distance is about the same as in case 1. The CG-to-CG distance at $t=T_i$ is .73 meters. The larger roll rate leads to larger roll angles as seen in fig. 3.19, where the final roll angle is .72 radians.

The effect of target acceleration can be easily seen in case 3, where one can see that with the same A_{co} , the accelerations are largely increased from this point, and the missile begins its trajectory with very high roll rate (see figures 3.20 and 3.21). There is a change in the Z component of the miss distance, that decreases its final value to .05 meters, but now the miss distance in Y direction is made worse as shown in figure 3.22, which leads to a final CG-to-CG distance of 1.5 meters. In fig. 3.23 one can see that the missile crosses the target with a bank angle of 1.26 radians.

In case 4, due to the position of target 600 meters under the missile, the initial commanded acceleration is negative and reaches the limit of -2 g's. The initial roll rate begins at a smaller value than in case 3 but increases during the initial part of the flight reaching its peak value at 1.75 seconds when again as in the previous cases begins to decay. As the missile banks to roll angles larger than 90 degrees, the acceleration goes to positive values, as seen in figures 3.24 and 3.25. Figure 3.26, shows the worse case among these in respect to the miss distance, mainly in the Z direction, and in the final cg-to-cg distance, which is equal to 4.43 meters. Also the final roll angle of 3.0 radians is the largest among all these cases, as seen in fig. 3.27.

2. Comments

Defining the projected zero effort miss distance (ZEM) as the miss distance the missile cross the target with no commands. It can be calculated at $t=0$ as the initial distance between target and missile plus the miss distance due to the gravity or:

$$ZEM = z(0) + \frac{1}{2} g t^2 \quad (3.34)$$

which is equal in all the three first cases.

In the first three cases, the initial missile's commanded acceleration is the same as seen in table 3.1. Considering that the control A_c necessary to correct the initial miss distance can be calculated as:

$$A_{C_{ZEM_0}} = \left\{ \frac{ZEM_z}{\frac{T_i^2}{2} - \frac{T_i^2}{6}} \right\} = 26.7 \quad (3.35)$$

which is close to the initial control A_c .

This suggests that the initial A_c , would be that one necessary to correct the initial ZEM in Z direction, which agrees with reference 1. Notice however that in all cases the initial A_c is less than the calculated value of A_{C_0} , which agrees with the previous statement that some error was expected in the initial part of the computations.

Considering the ideal initial roll angle as defined before, one has:

$$\phi_{o,ideal} = \tan^{-1} \left[\frac{ZEM_y}{ZEM_z} \right] \quad (3.36)$$

From table I, and figures showing roll angles, it can be verified that the missile is banking to reach angles larger than $\phi_{o,ideal}$, in order to correct its trajectory to hit the target.

Therefore, in all cases, the missile begins its trajectory with an A_{C_0} (discussed before), and a roll rate

which is proportional to the target acceleration in the Y direction. As the missile rolls at decreasing roll rates, the commanded acceleration is changed in order for to compensate the effect of the roll angle on its Z direction component. At some time when the control Pc is zero or near zero, the control Ac begins to follow a linear law, as suggested in eqn. 2.7:

$$A_c = A_{c0} \left[1 - \frac{t}{T_i} \right]$$

Notice however that the term A_{c0} in this equation is no more the actual initial commanded acceleration, but that one the missile would have if its initial roll angle was equal to the final .

Such behavior defines a boundary in the control A_c which is clearly seen in 3.29, where the commanded acceleration is bounded by the curve of the control A_c the missile would have if its initial ϕ_0 was equal to $\phi_{0,ideal}$ (or, if no commanded roll was necessary to reach the target).

Althoug the missile commands roll angles larger than the ideal initial roll angle, it is possible to do a prediction- with no no computer work- of an aproximation for the maximum acceleration the missile would experience during its flighth, as following (see fig. 3.32):

$$A_c = \left[\frac{ZEM_z}{\frac{T_i^2}{2} + \frac{T_i^2}{6}} \right] \frac{1}{\cos \phi_{0,ideal}} \quad (3.37)$$

where $\phi_{0,ideal}$ comes from eqn.3.50, and A_c is a streight line as in fig 3.32.

Other interesting point is that the missile is commanding to reach roll angles about twice of $\phi_{0,ideal}$ when the target is at small accelerations, and when at large

accelerations, the missile is making a small correction on its roll angle, as shown in table I.

One can see from the figures showing miss distance, that the relative position of missile to target is about the same in all three initial cases. Thus, the new ϕ_{ideal} at each point is the same. As the $\phi_{o,ideal}$ computed at $t=0$ is smaller when the target is at small accelerations, the correction has to be larger in order to hit the target, as seen in figure 3.30.

In table I, one can see the final miss distances, the final miss distance cg to cg and the final roll angle. Such results show that with this digitalized model, good results has been obtained.

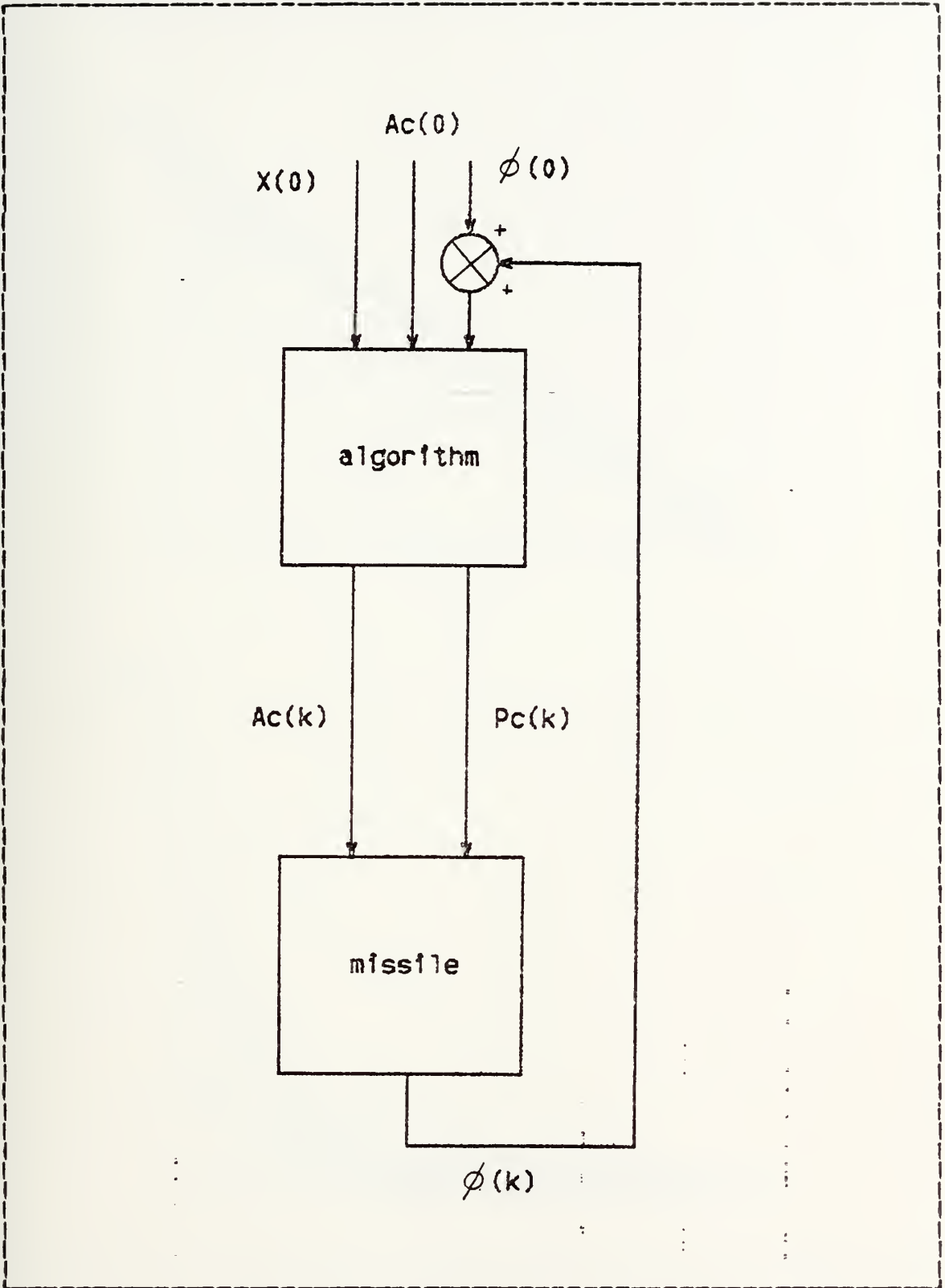


Figure 3.1 Representation of the System.

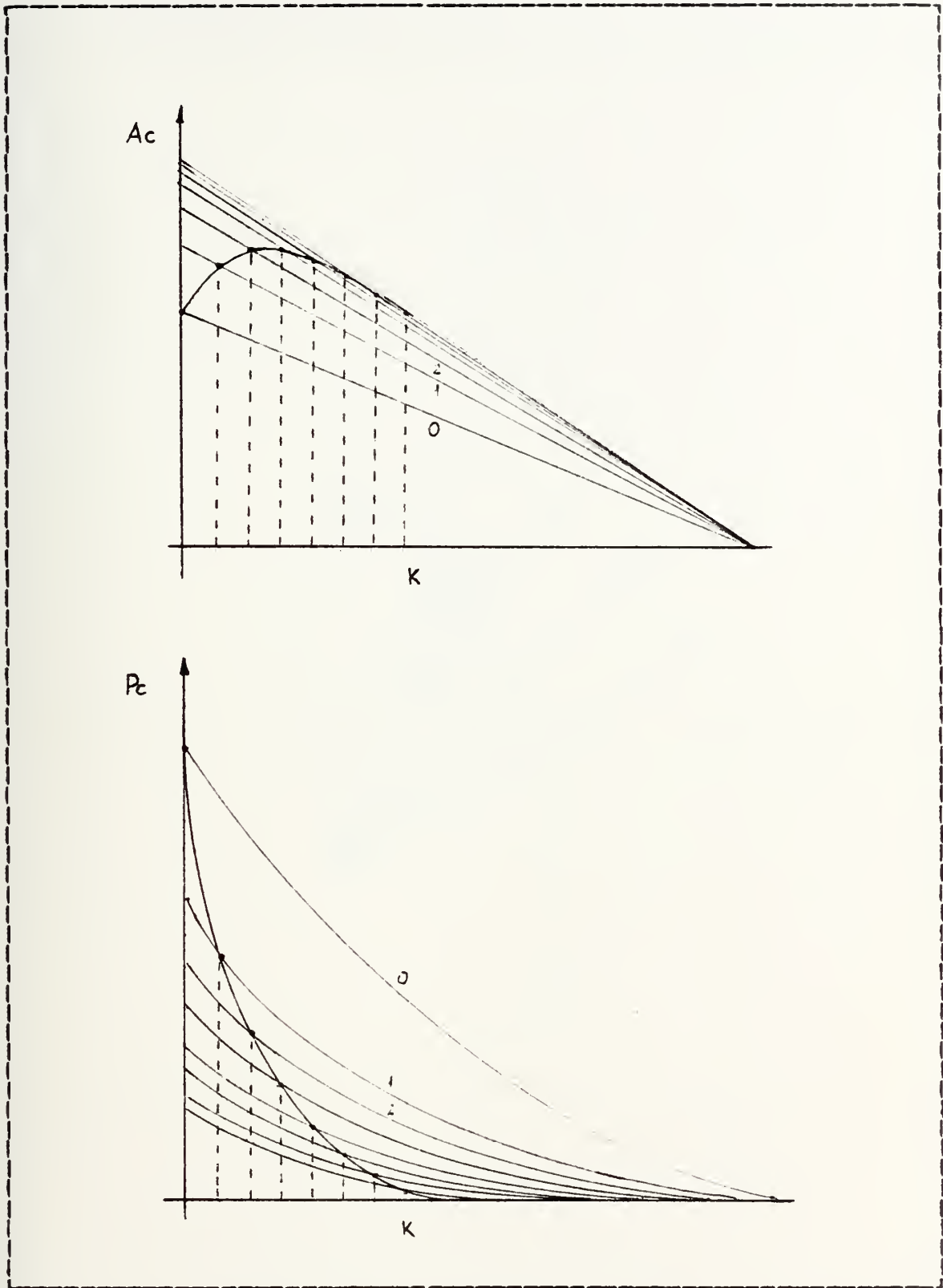


Figure 3.2 Variation of Commands with Initial Roll Angle.

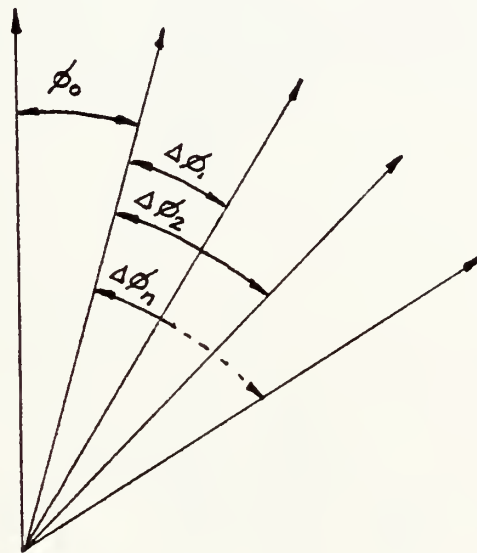


Figure 3.3 Variation of Roll Angle - Small Angles.

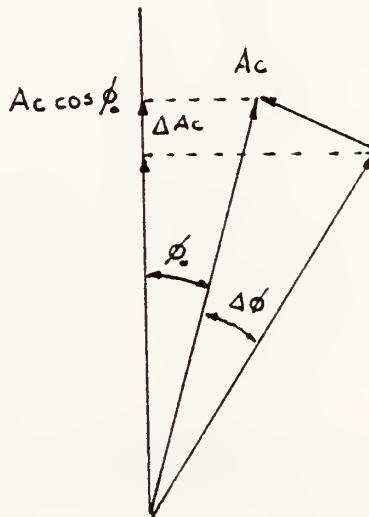
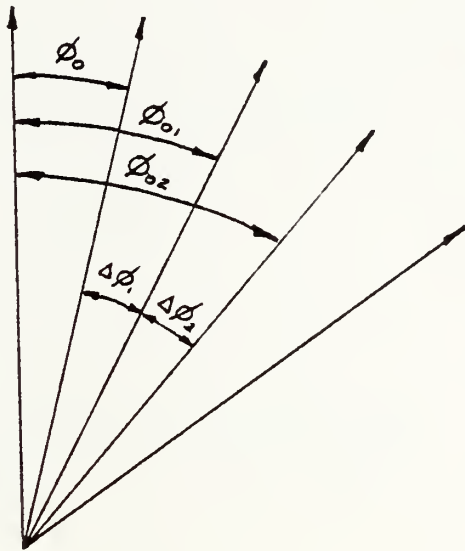


Figure 3.4 Variation of Roll Angle - Large Angles.

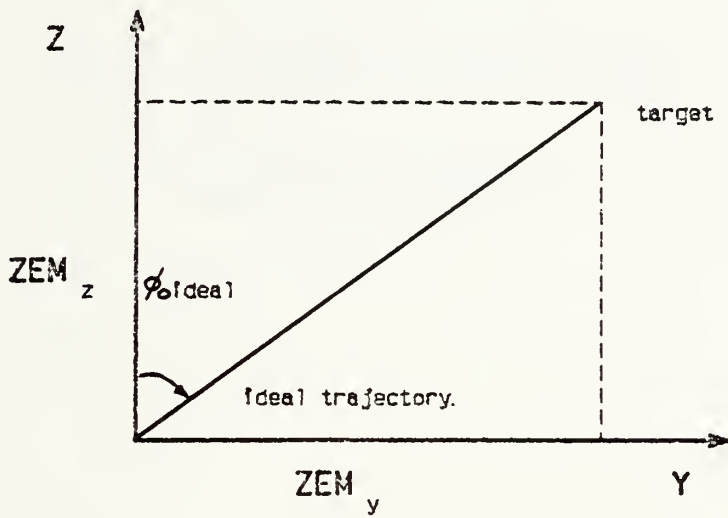


Figure 3.5a

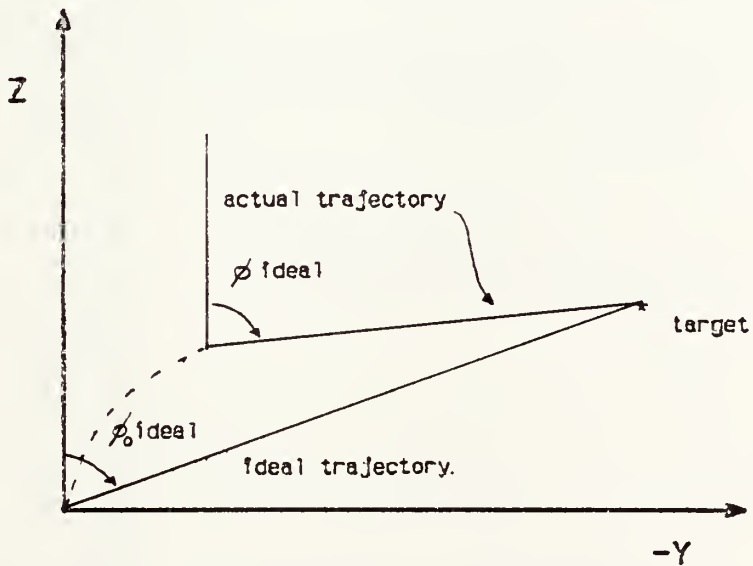


Figure 3.5b

Figure 3.5 Ideal Initial Roll Angles.

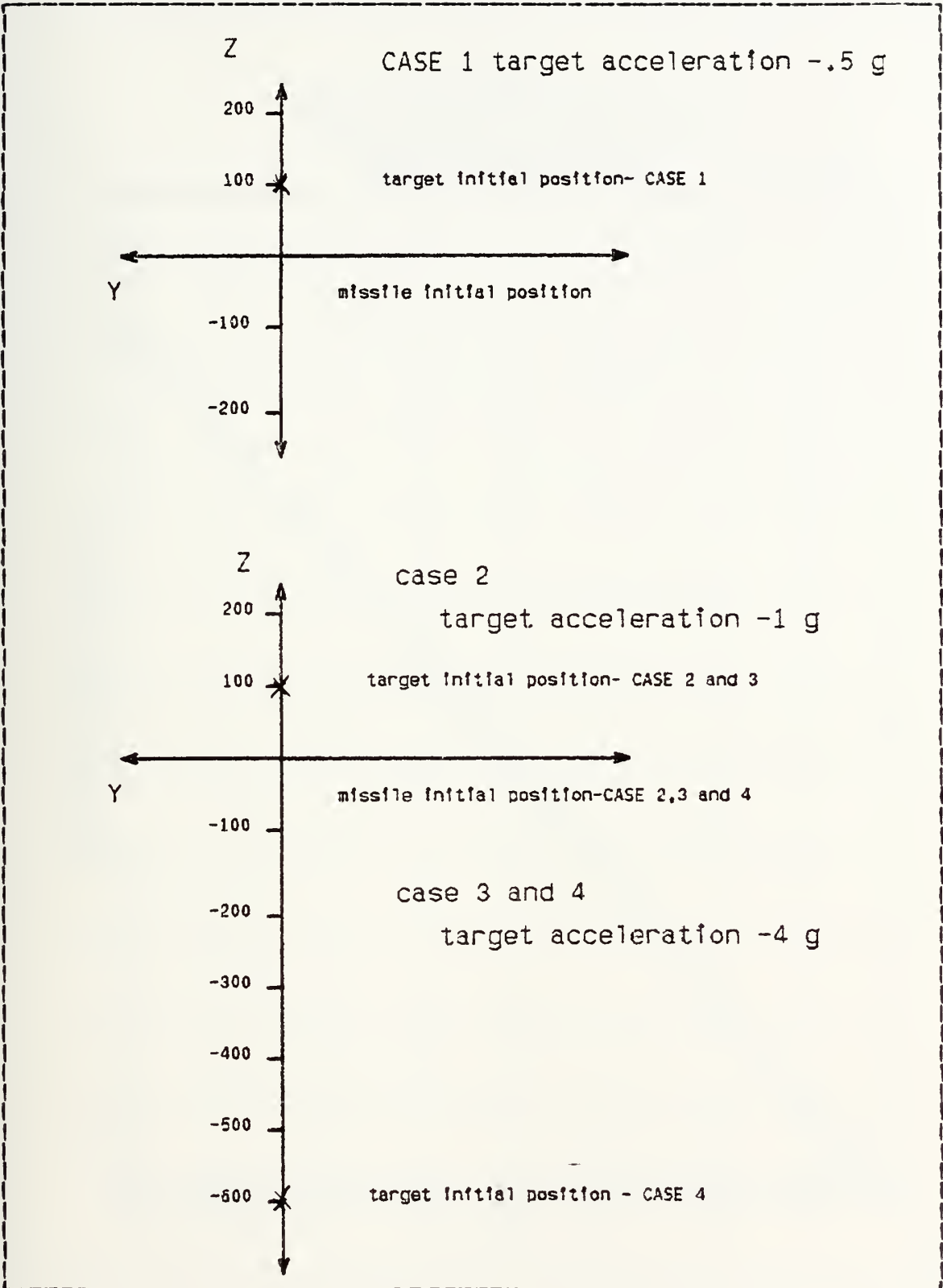


Figure 3.6 Scenarios for Simulation.

CASE 0
INITIAL TARGET ACCELERATION--.5 G
INITIAL TARGET POSITION- 100 M
SAMPLE PERIOD-0.05 SEC

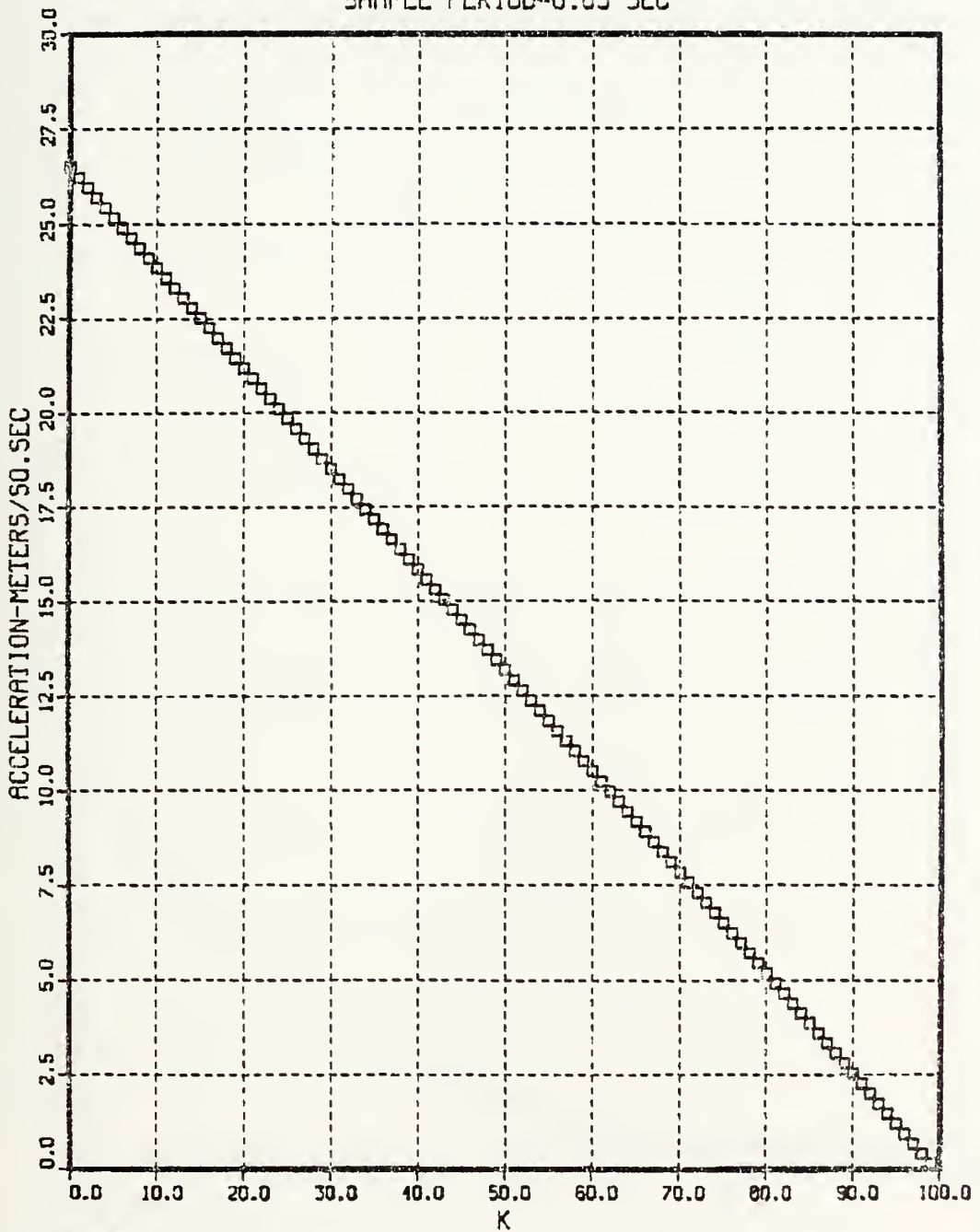


Figure 3.7 Commanded Acceleration- Case 0.

CASE 0
INITIAL TARGET ACCELERATION--.5 G
INITIAL TARGET POSITION- 100 M
SAMPLE PERIOD-0.05 SEC

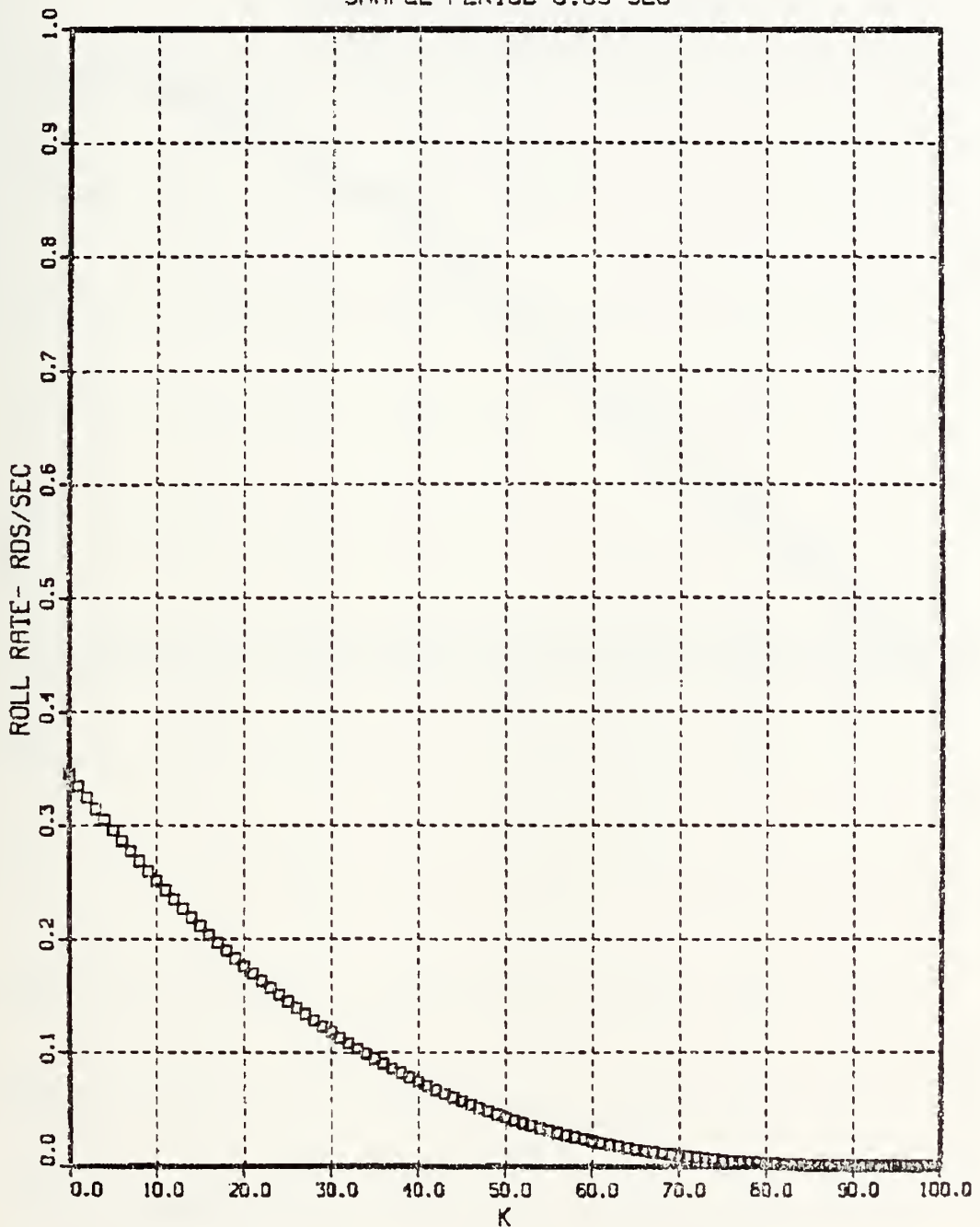


Figure 3.8 Commanded Roll Rate- Case 0.

CASE 0
INITIAL TARGET ACCELERATION--.5 G
INITIAL TARGET POSITION- 100 M
SAMPLE PERIOD-0.05 SEC

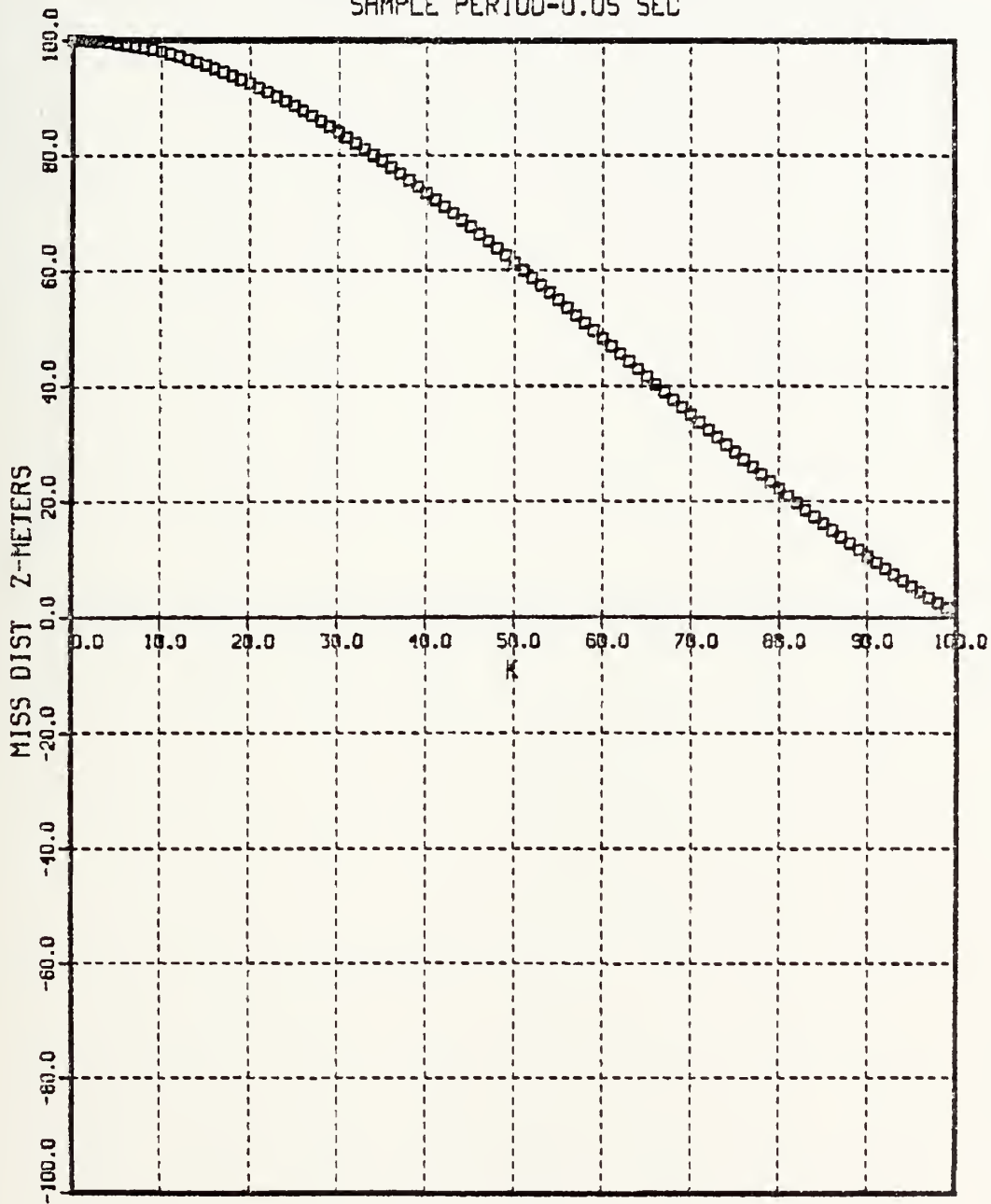


Figure 3.9 Miss Distance in Z Direction- Case 0.

CASE 0
INITIAL TARGET ACCELERATION--.5 G
INITIAL TARGET POSITION- 100 M
SAMPLE PERIOD-0.05 SEC

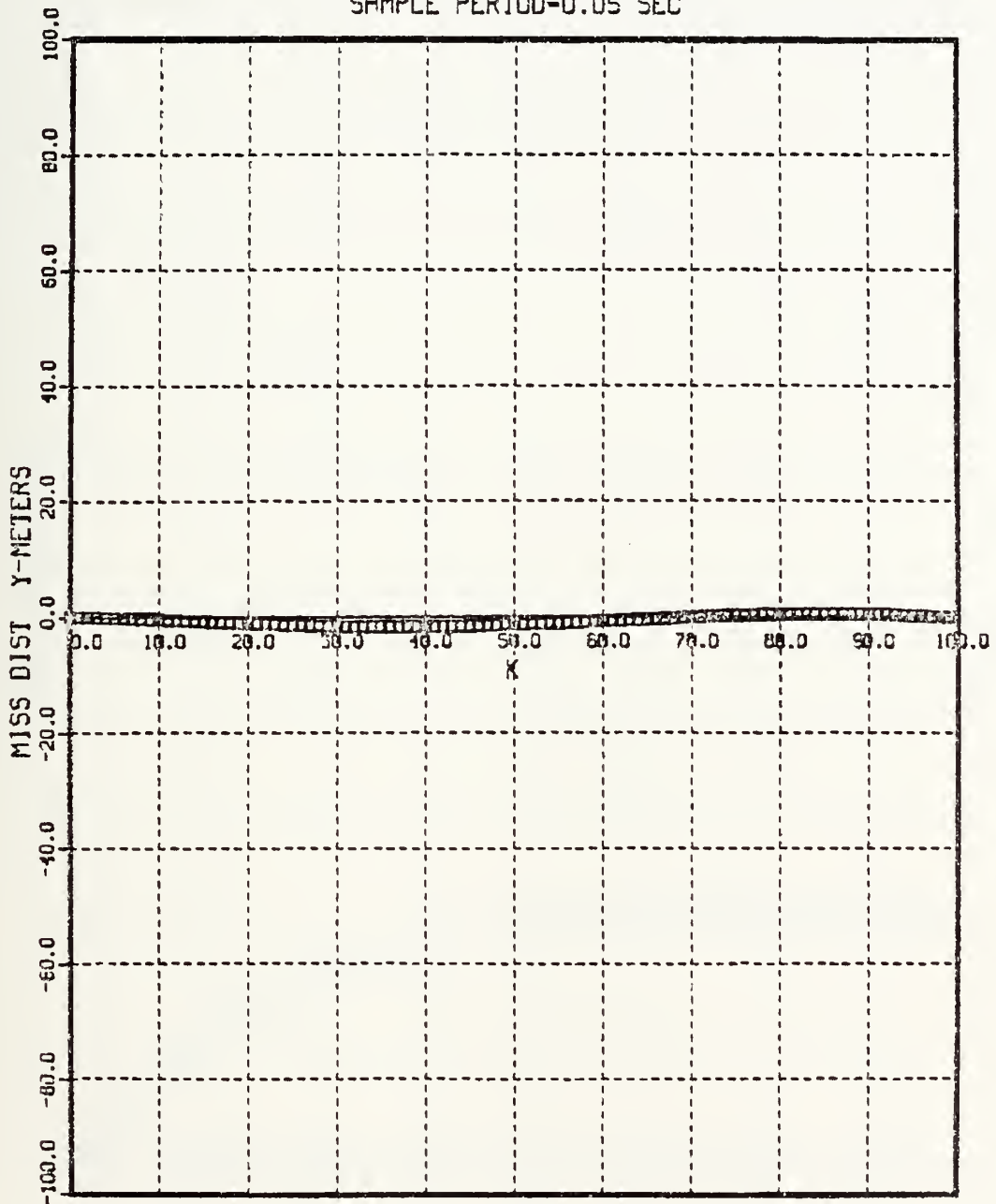


Figure 3.10 Miss Distance in Y Direction- Case 0.

CASE 0
INITIAL TARGET ACCELERATION--.5 G
INITIAL TARGET POSITION- 100 M
SAMPLE PERIOD-0.05 SEC

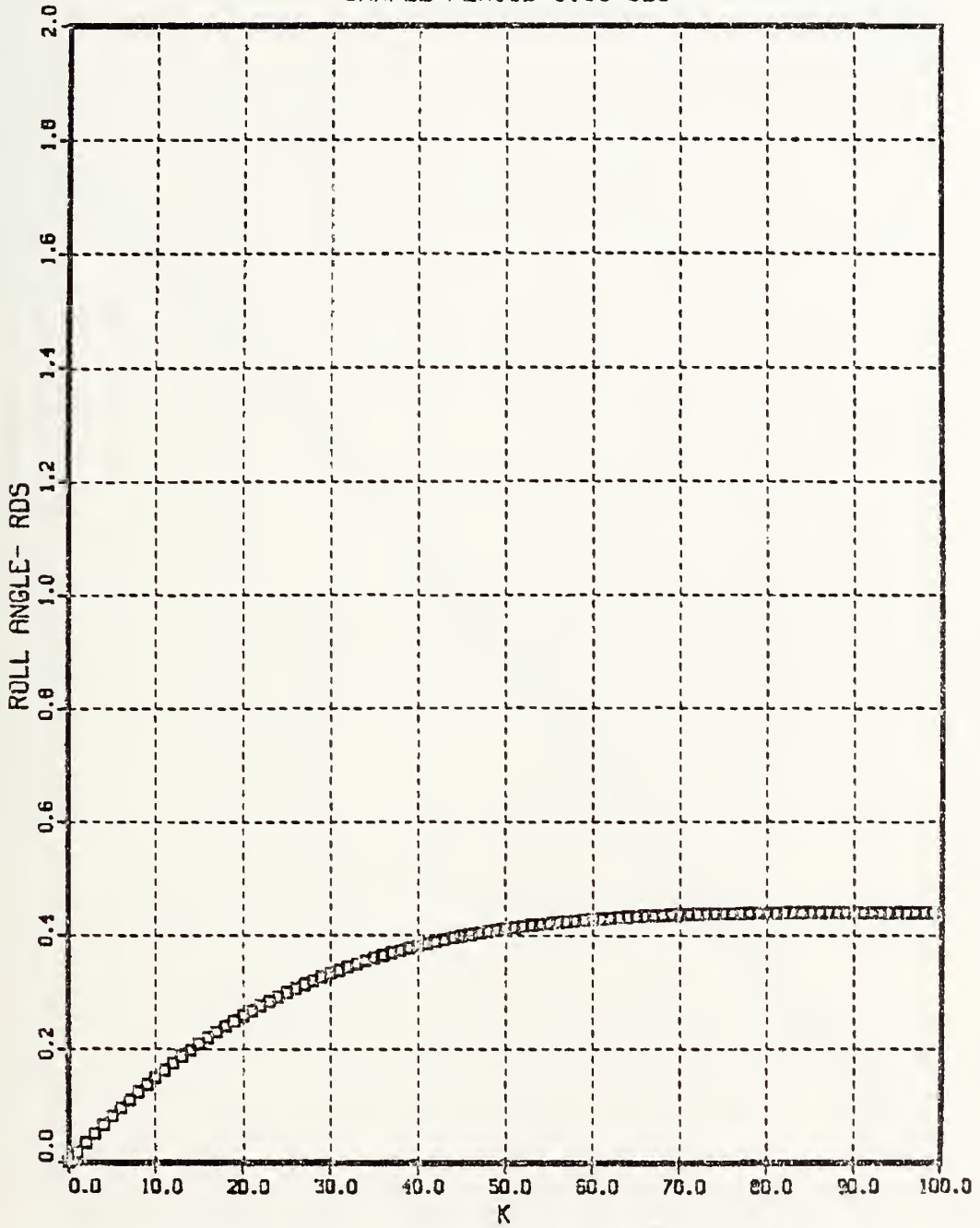


Figure 3.11 Roll Angle- Case 0.

1ST CASE
INITIAL TARGET ACCELERATION- -.5 G
INITIAL TARGET POSITION-100 M
SAMPLE PERIOD-0.05 SEC

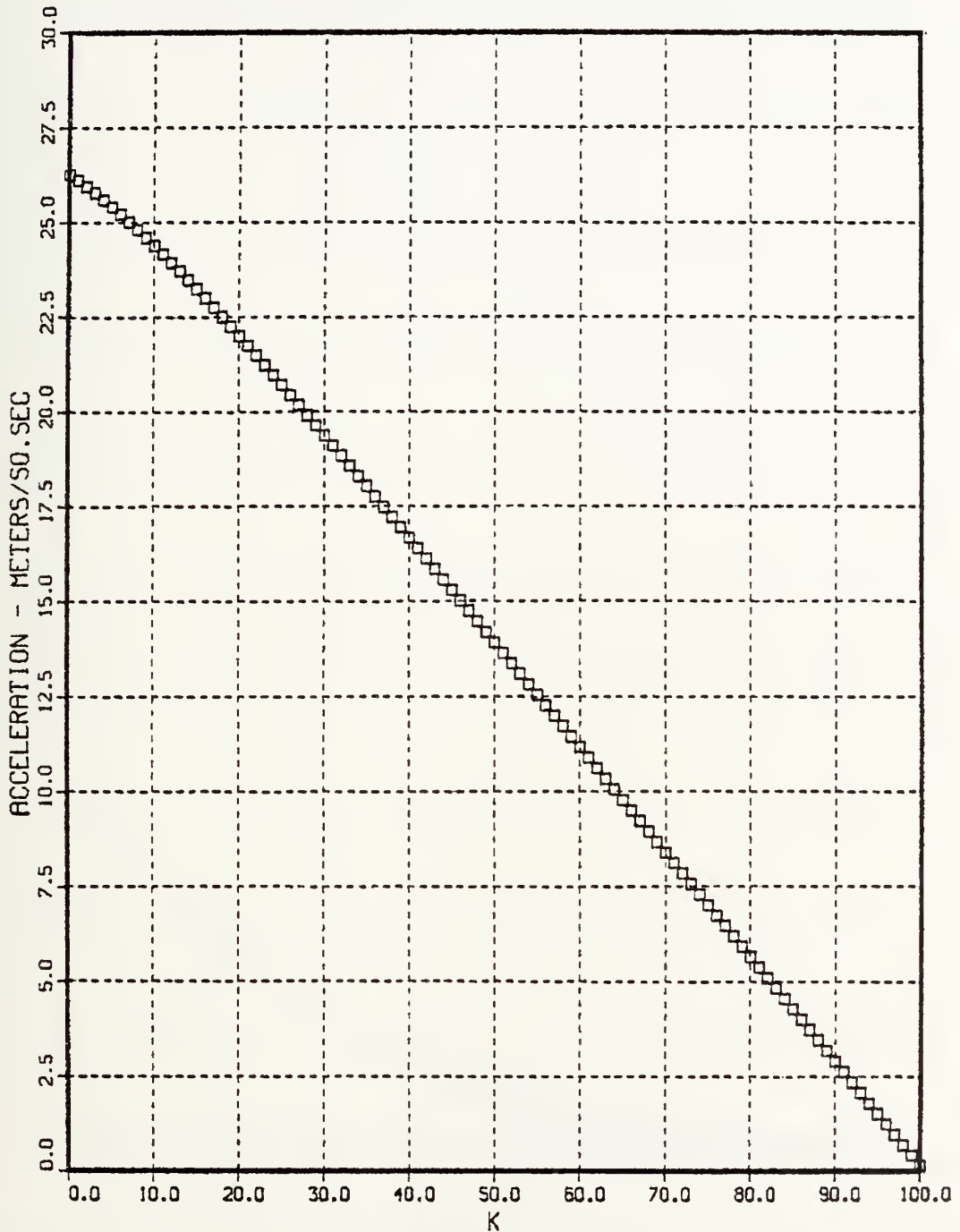


Figure 3.12 Commanded Acceleration- Case 1.

1ST CASE
INITIAL TARGET ACCELERATION- -.5 G
INITIAL TARGET POSITION-100 M
SAMPLE PERIOD-0.05 SEC

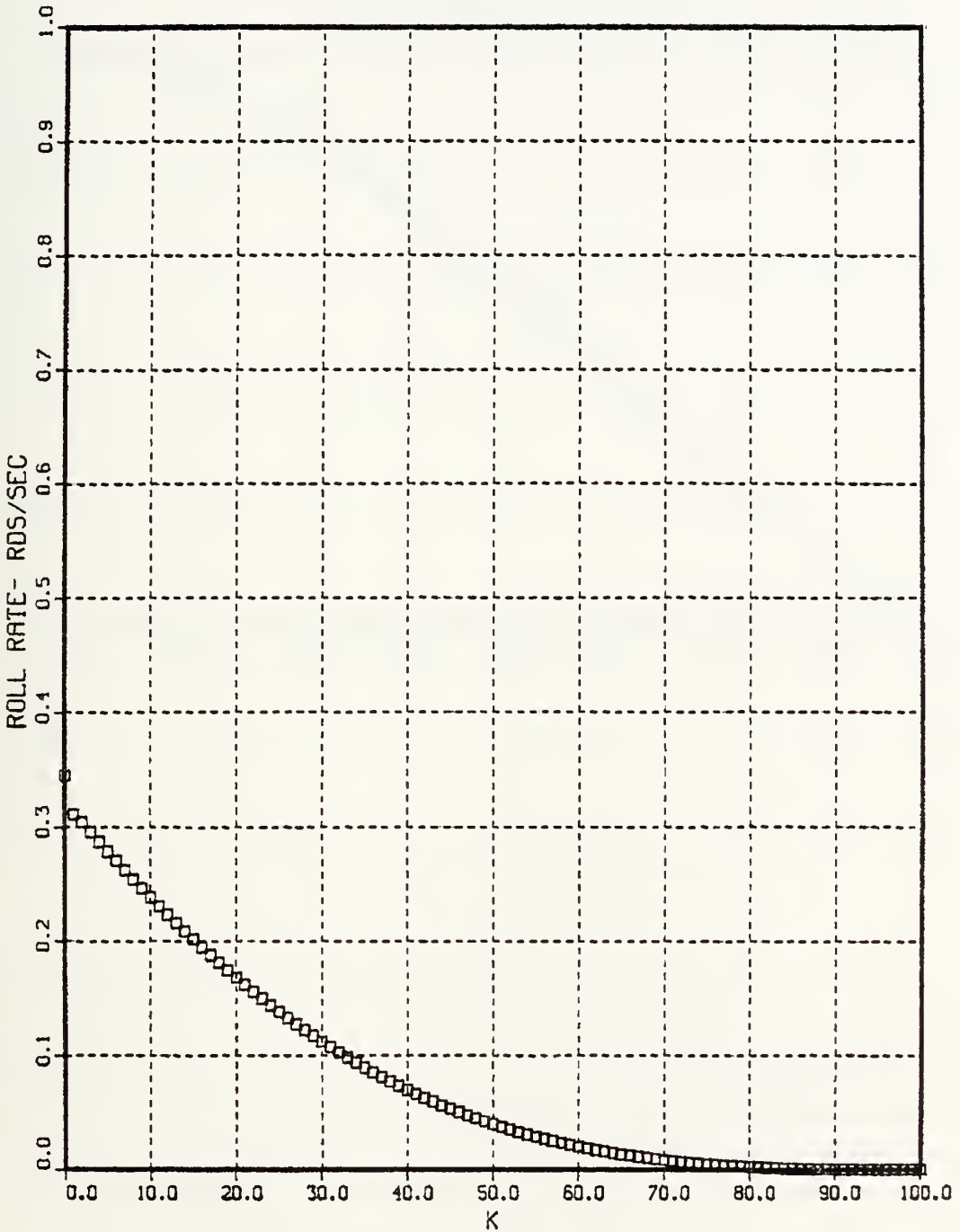


Figure 3.13 Commanded Roll Rate- Case 1.

1ST CASE
INITIAL TARGET ACCELERATION- -5 G
INITIAL TARGET POSITION-100 M
SAMPLE PERIOD-0.05 SEC

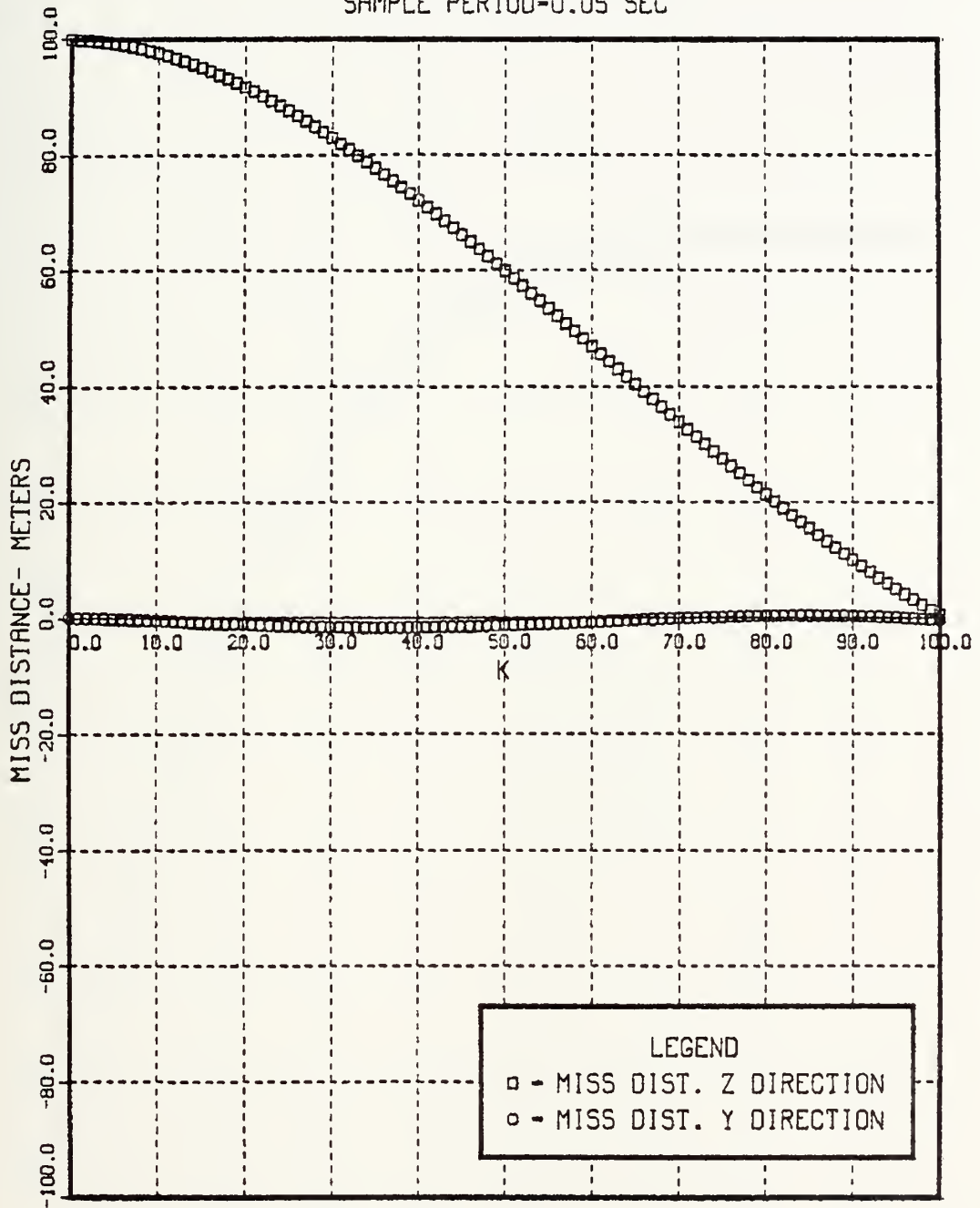


Figure 3.14 Miss Distance- Case1.

1ST CASE
INITIAL TARGET ACCELERATION= -.5 G
INITIAL TARGET POSITION=100 M
SAMPLE PERIOD=0.05 SEC

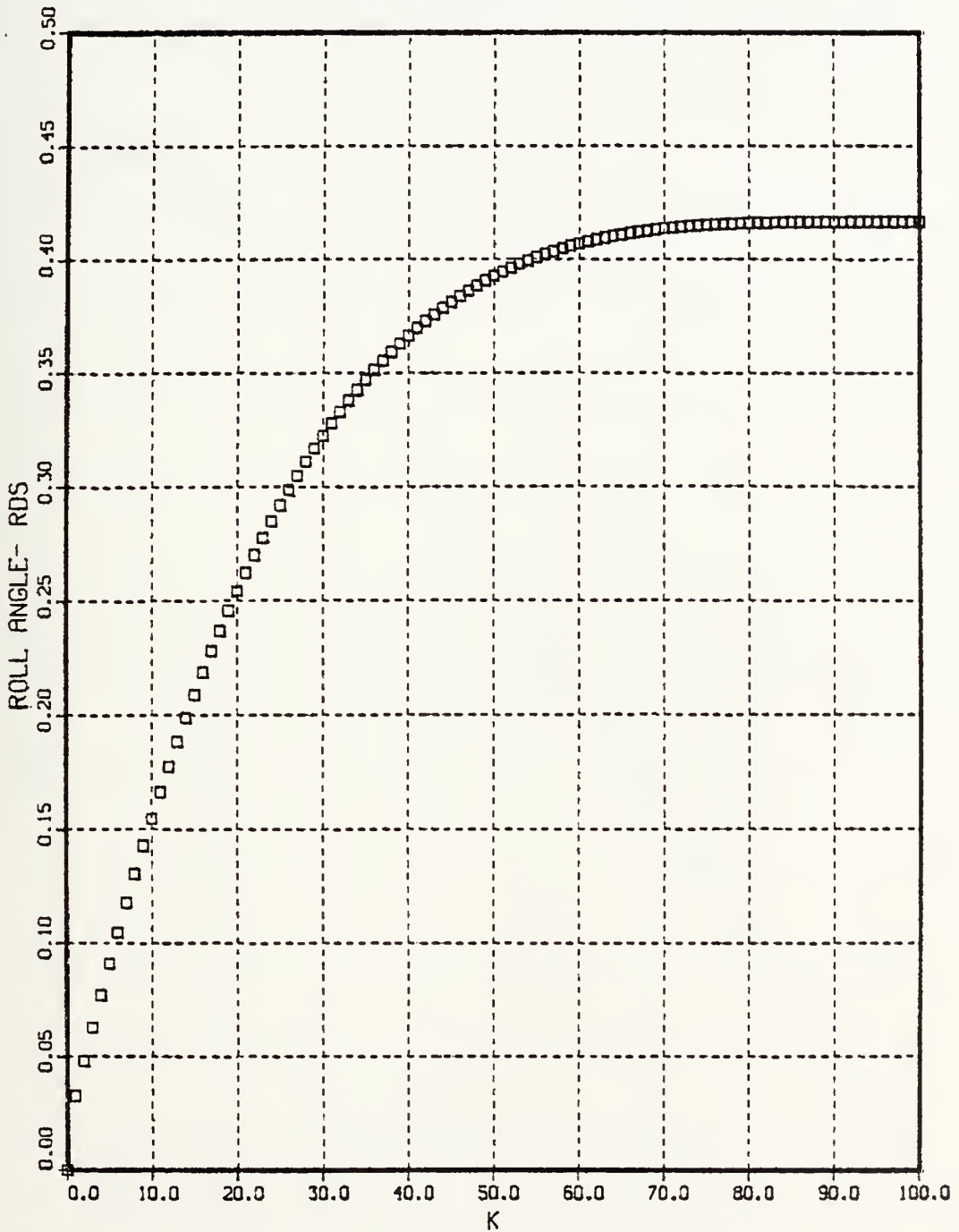


Figure 3.15 Roll Angle- Case 1.

2ND CASE
INITIAL TARGET ACCELERATION= -1. G
INITIAL TARGET POSITION=100 M
SAMPLE PERIOD=0.05 SEC

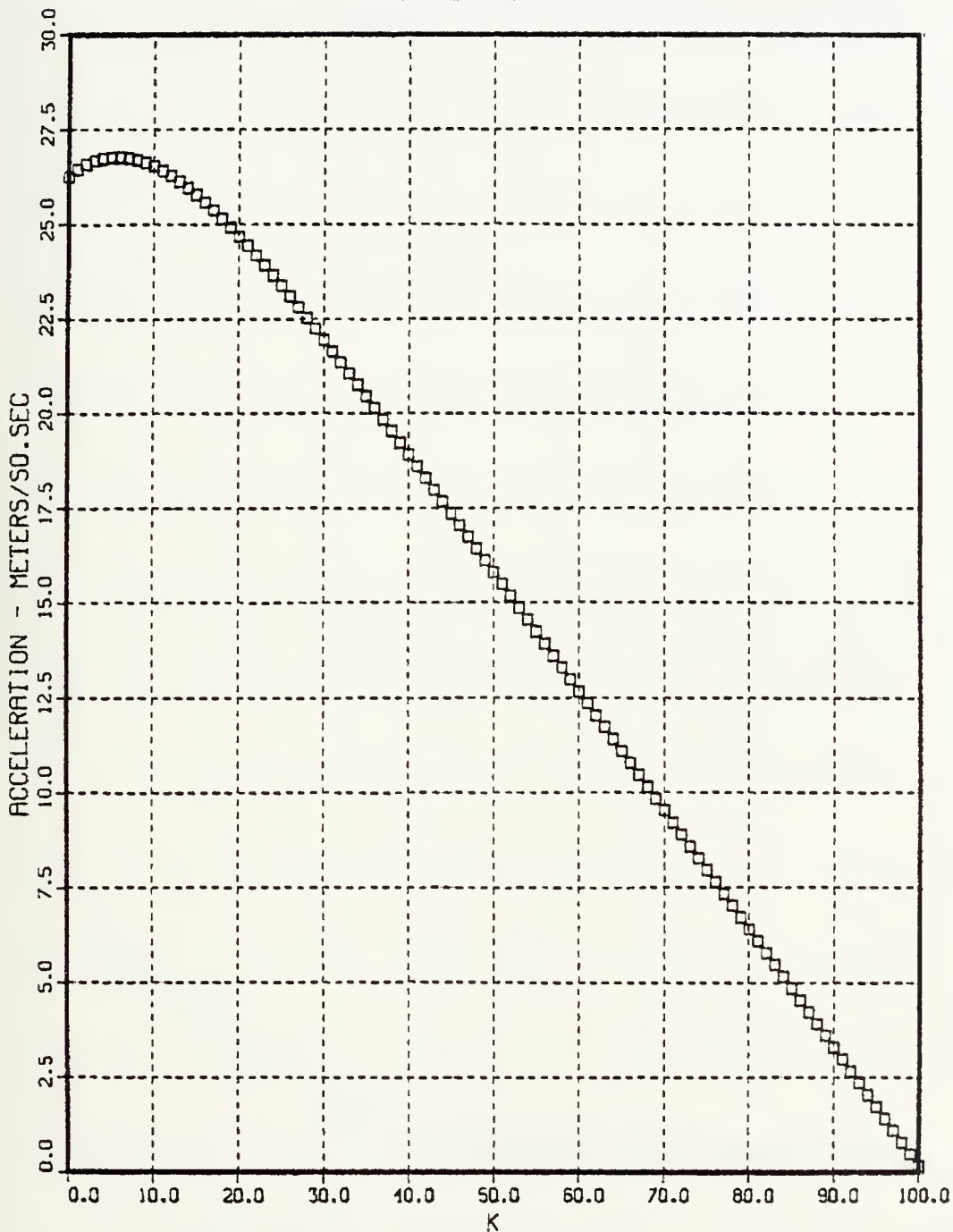


Figure 3.16 Commanded Acceleration- Case 2.

2ND CASE
INITIAL TARGET ACCELERATION- -1. G
INITIAL TARGET POSITION-100 M
SAMPLE PERIOD-0.05 SEC

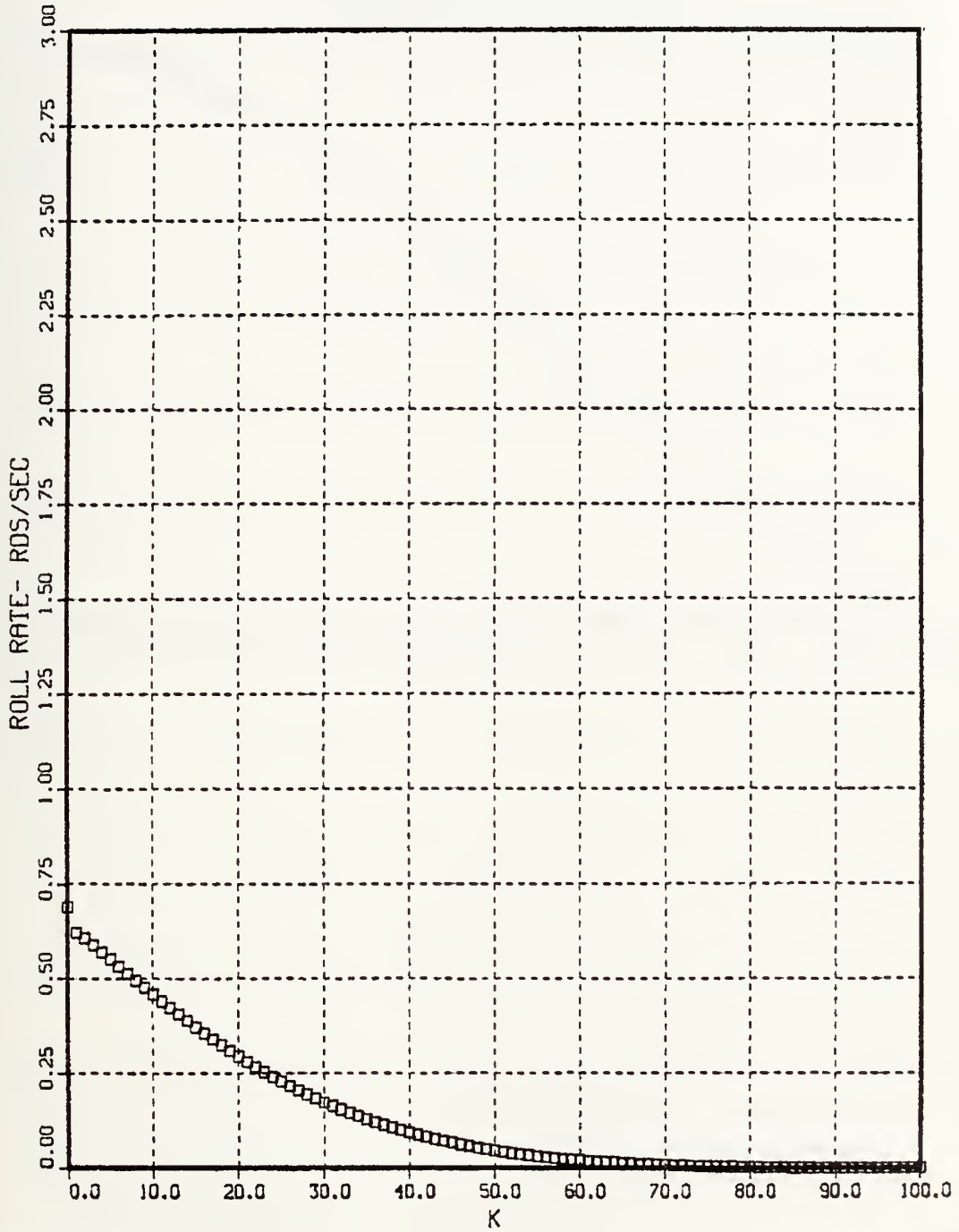


Figure 3.17 Commanded Roll Rate- Case 2.

2ND CASE
INITIAL TARGET ACCELERATION- -1. G
INITIAL TARGET POSITION-100 M
SAMPLE PERIOD=0.05 SEC

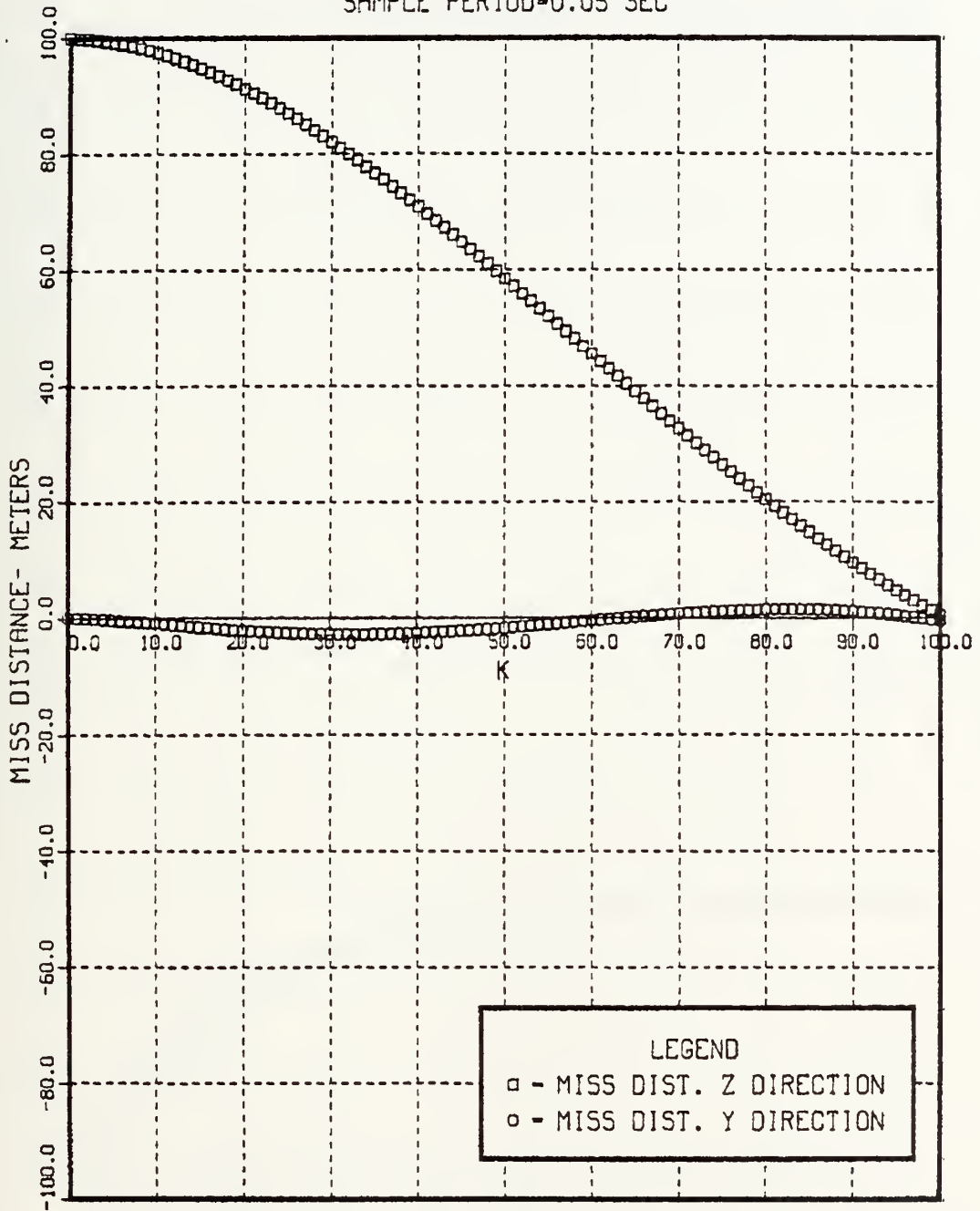


Figure 3.18 Miss Distance- Case 2.

2ND CASE
INITIAL TARGET ACCELERATION= -1. G
INITIAL TARGET POSITION=100 M
SAMPLE PERIOD=0.05 SEC

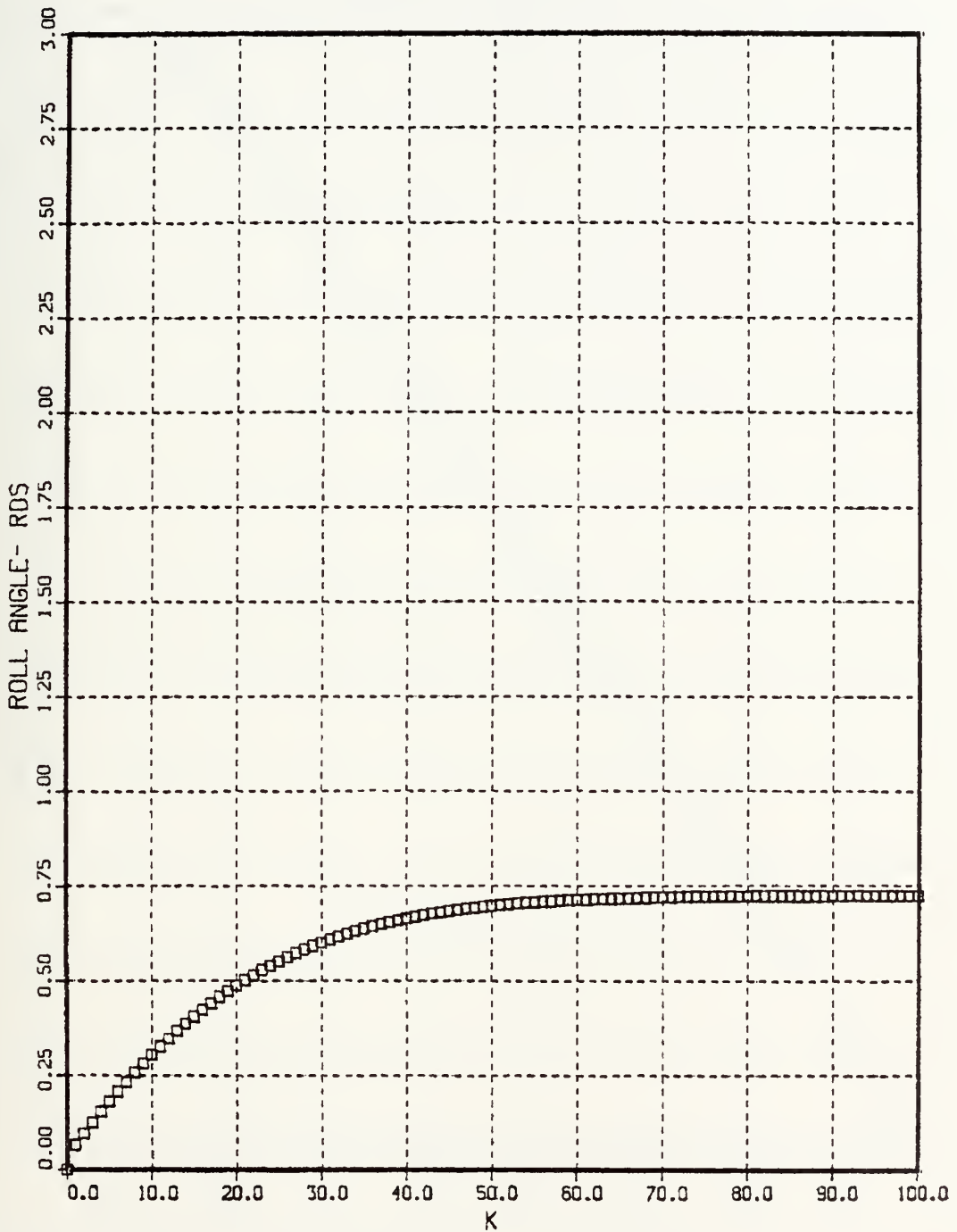


Figure 3.19 Roll Angle- Case 2.

3RD CASE
INITIAL TARGET ACCELERATION- -4. G
INITIAL TARGET POSITION-100 M
SAMPLE PERIOD-0.05 SEC

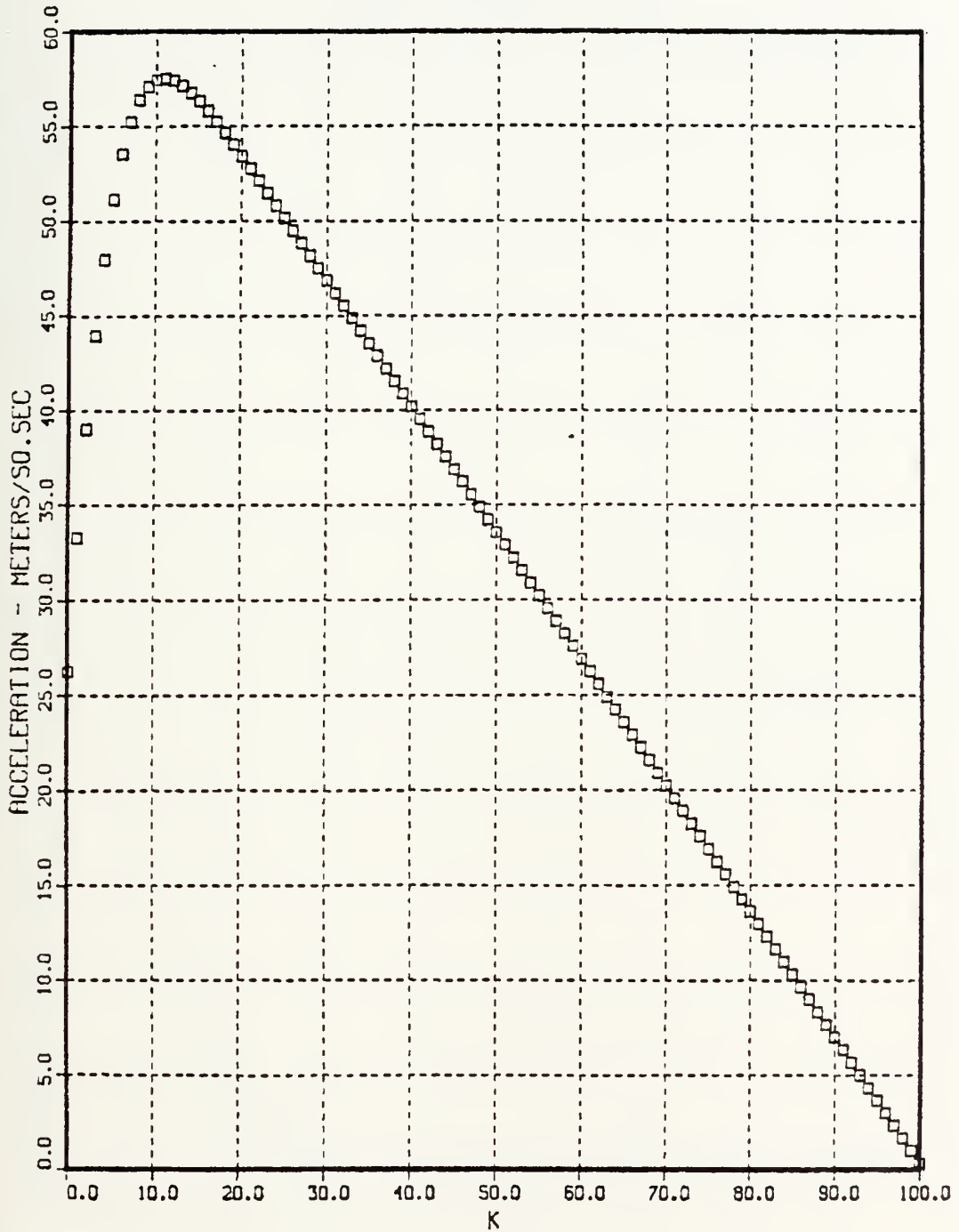


Figure 3.20 Commanded Acceleration- Case 3.

3RD CASE
INITIAL TARGET ACCELERATION- -4. G
INITIAL TARGET POSITION-100 M
SAMPLE PERIOD-0.05 SEC

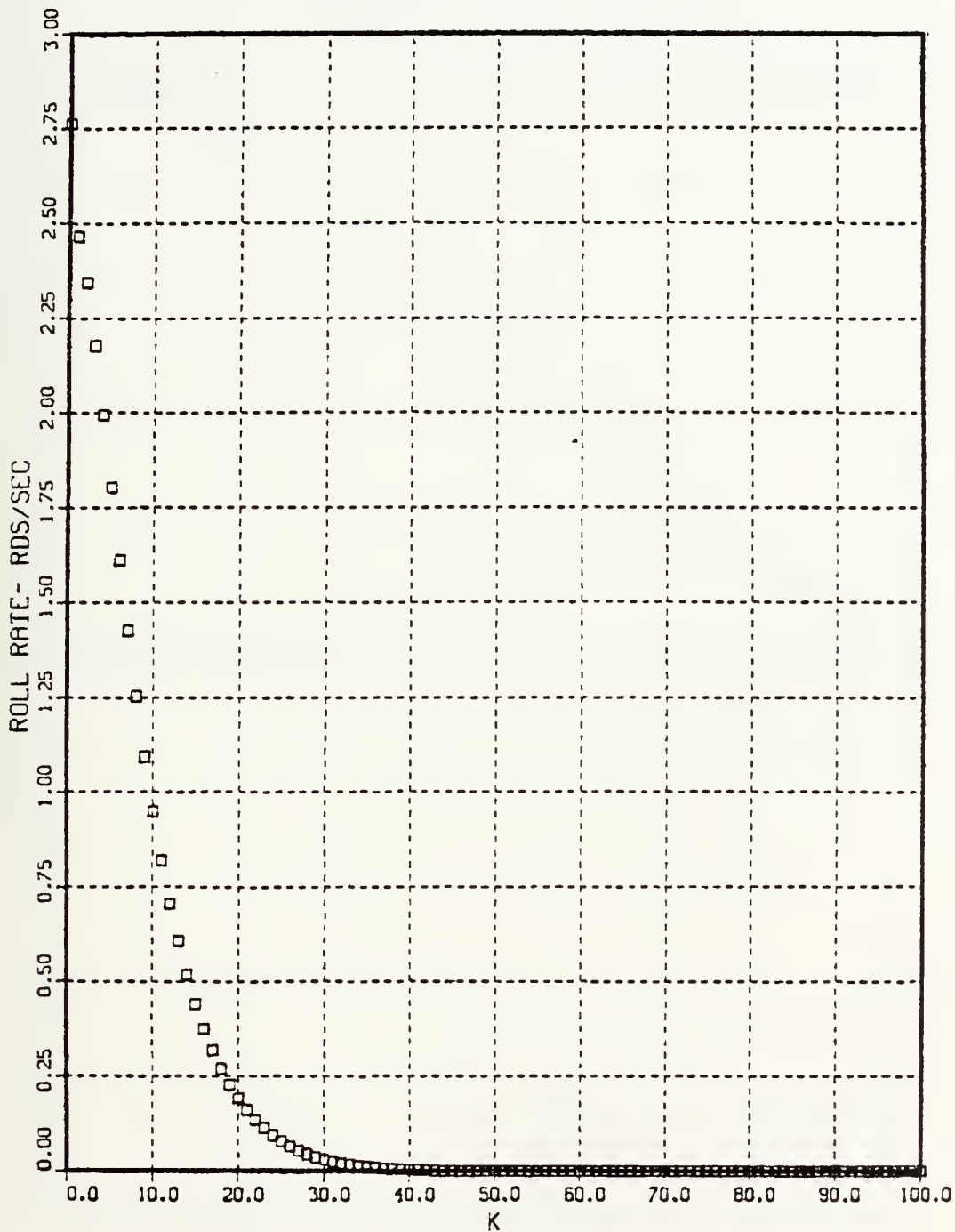


Figure 3.21 Commanded Roll Rate- Case 3.

3RD CASE
INITIAL TARGET ACCELERATION= -4. G
INITIAL TARGET POSITION=100 M
SAMPLE PERIOD=0.05 SEC

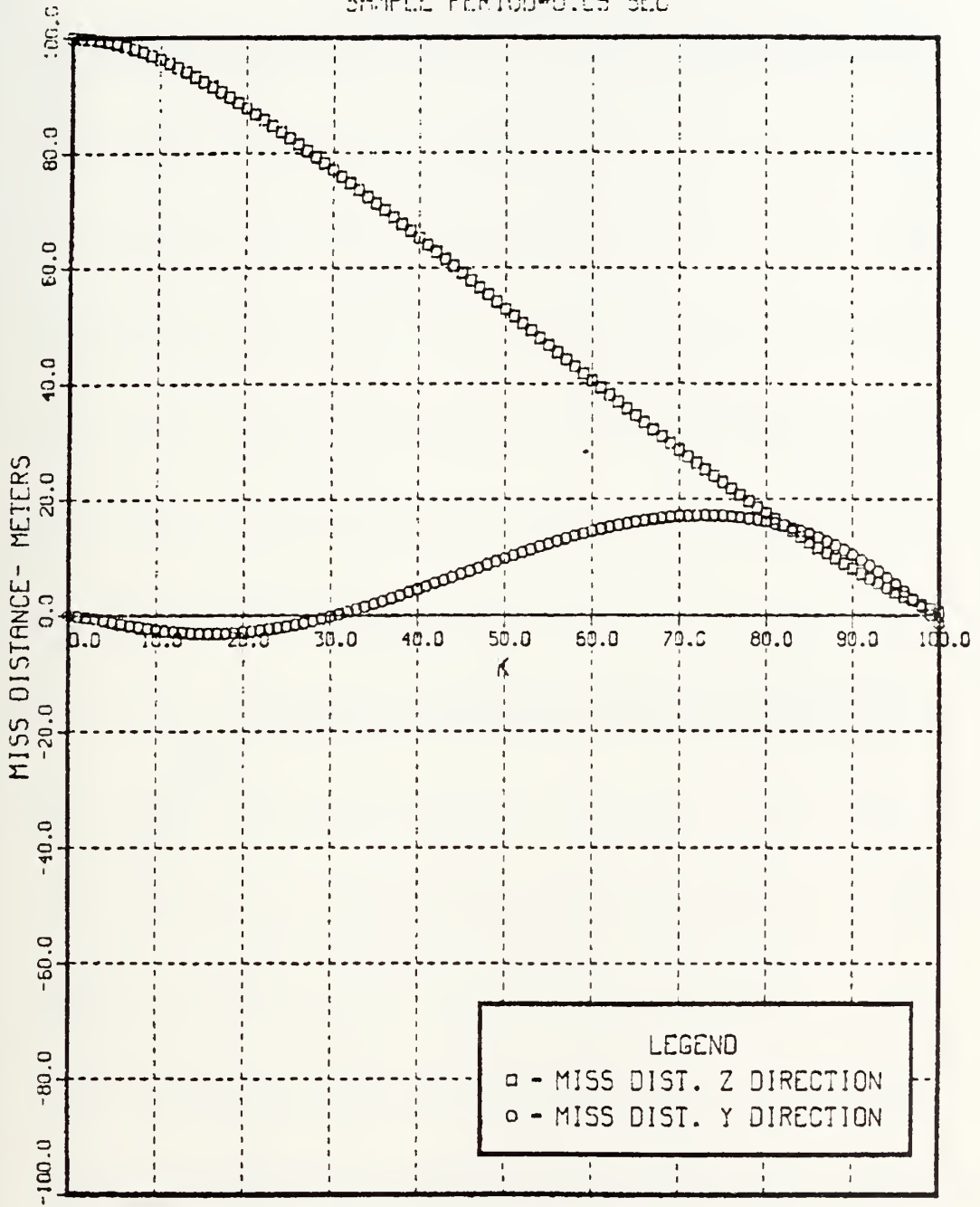


Figure 3.22 Miss Distance- Case3.

3RD CASE
INITIAL TARGET ACCELERATION- -4. G
INITIAL TARGET POSITION-100 M
SAMPLE PERIOD-0.05 SEC

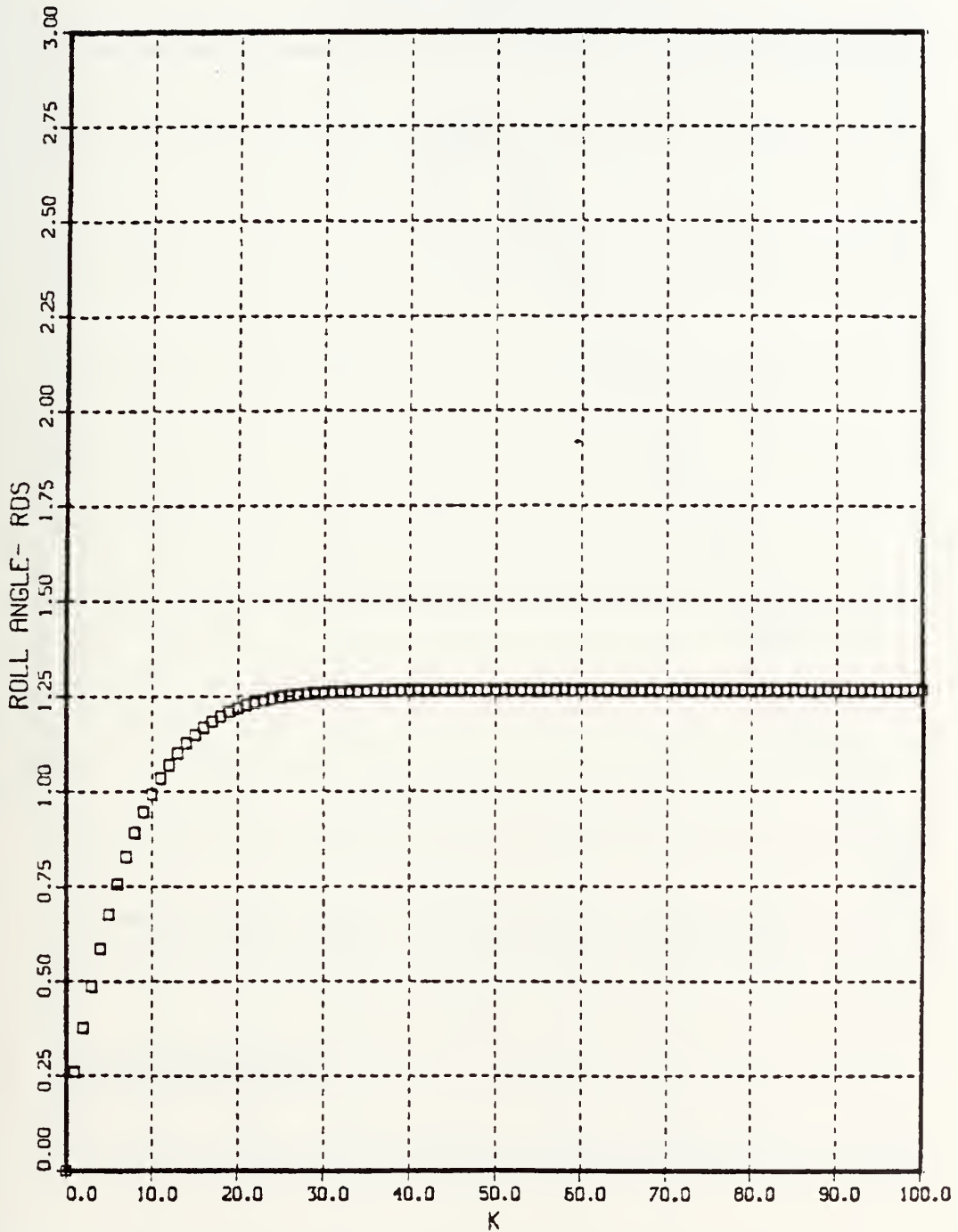


Figure 3.23 Roll Angle- Case 3.

4TH CASE
INITIAL TARGET ACCELERATION- -4. G
INITIAL TARGET POSITION--600 M
SAMPLE PERIOD-0.05 SEC

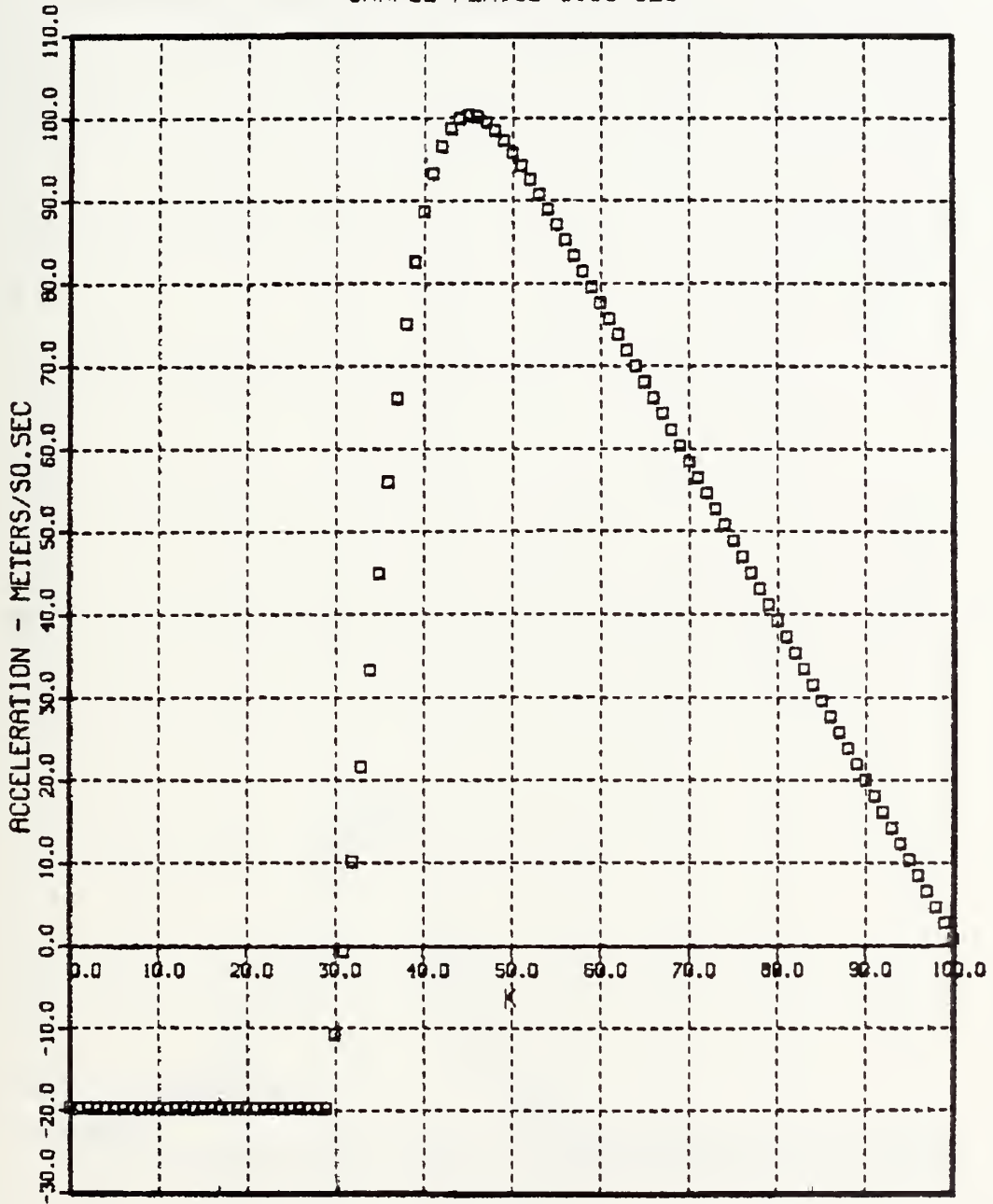


Figure 3.24 Commanded Acceleration- Case 4.

4TH CASE
INITIAL TARGET ACCELERATION- -4. G
INITIAL TARGET POSITION--600 M
SAMPLE PERIOD-0.05 SEC

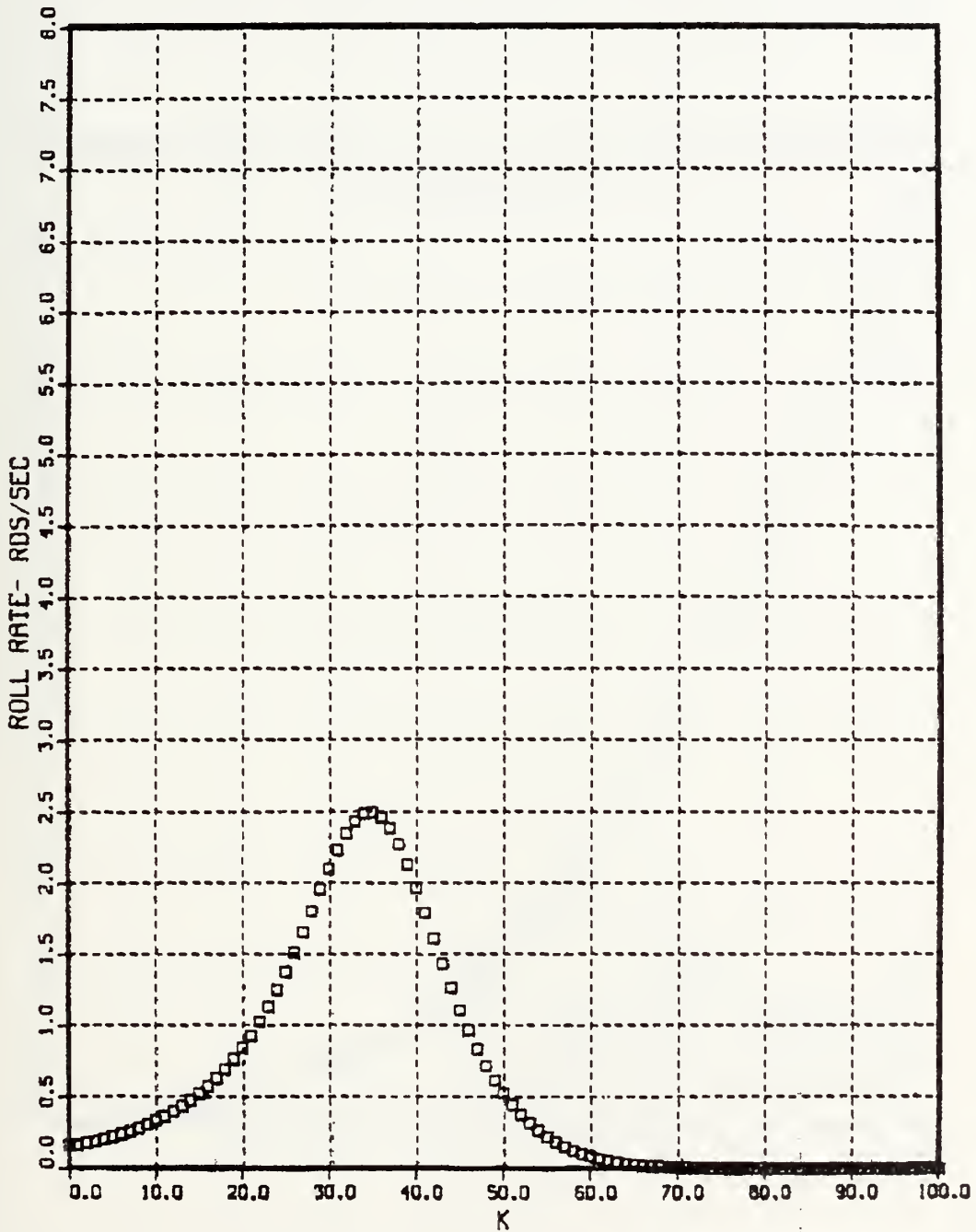


Figure 3.25 Commanded Roll Rate- Case 4.

4TH CASE
INITIAL TARGET ACCELERATION- -4. G
INITIAL TARGET POSITION--600 M
SAMPLE PERIOD-0.05 SEC

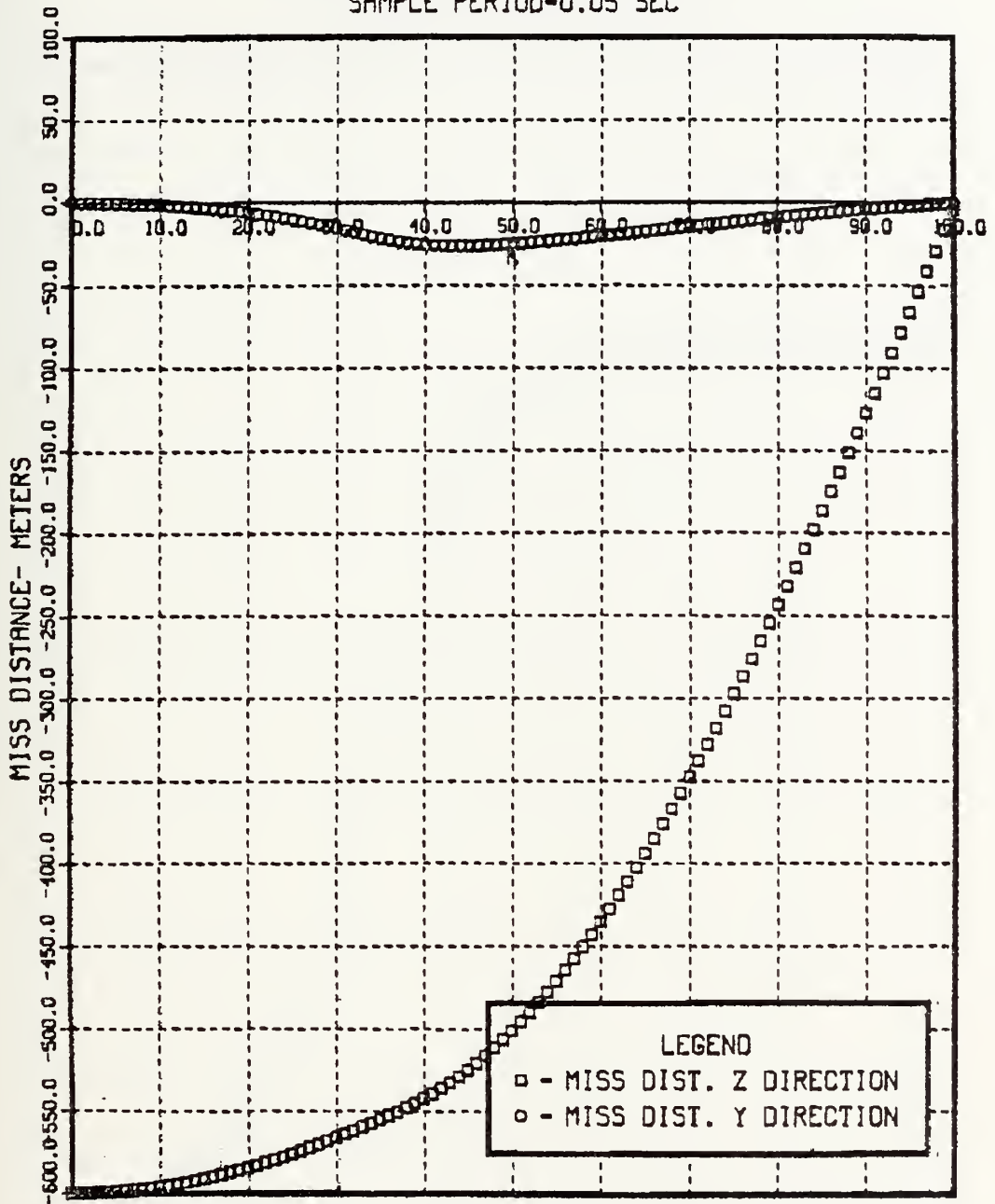


Figure 3.26 Miss Distance- Case 4.

4TH CASE
INITIAL TARGET ACCELERATION- -4. G
INITIAL TARGET POSITION--600 M
SAMPLE PERIOD-0.05 SEC

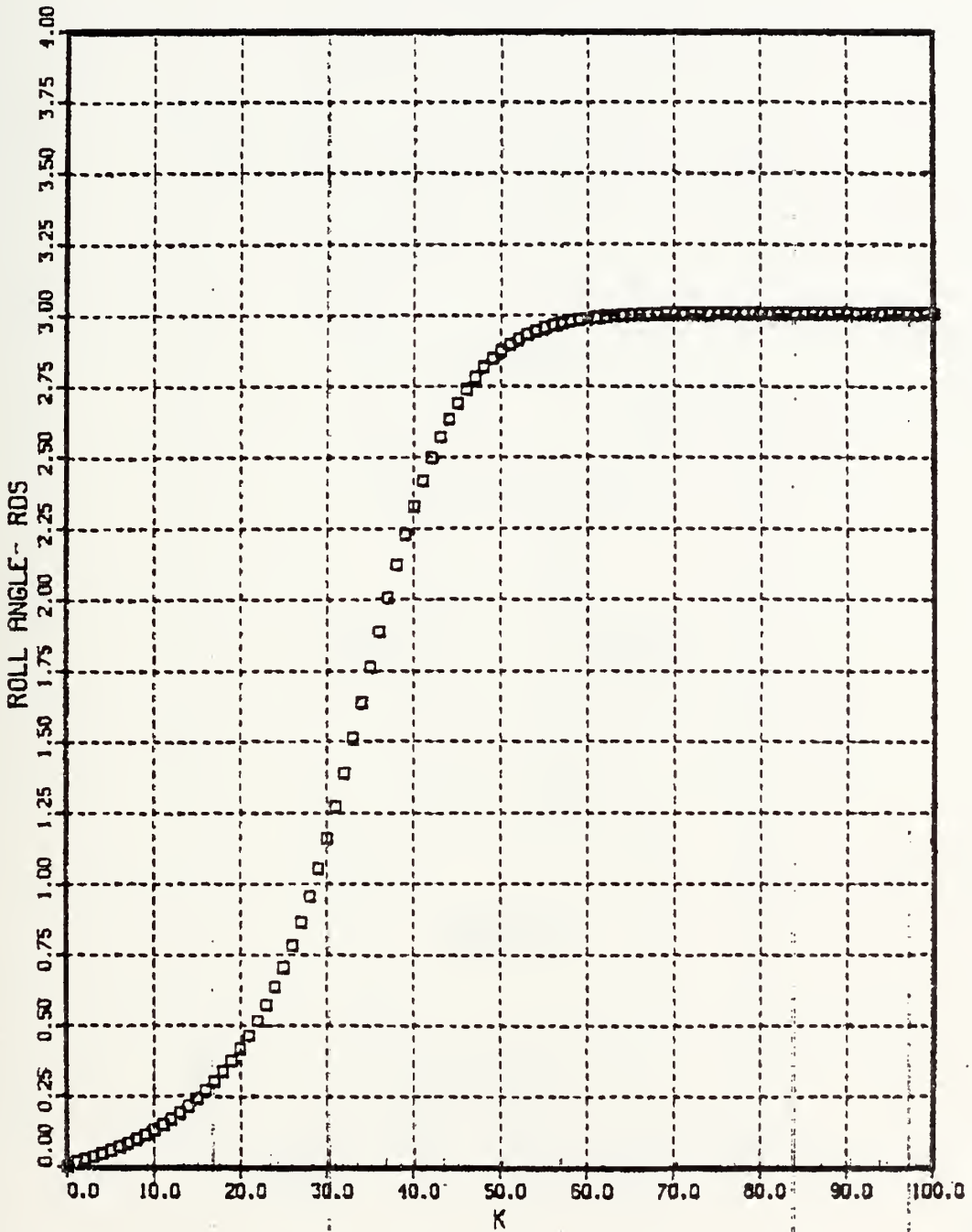


Figure 3.27 Roll Angle- Case 4.

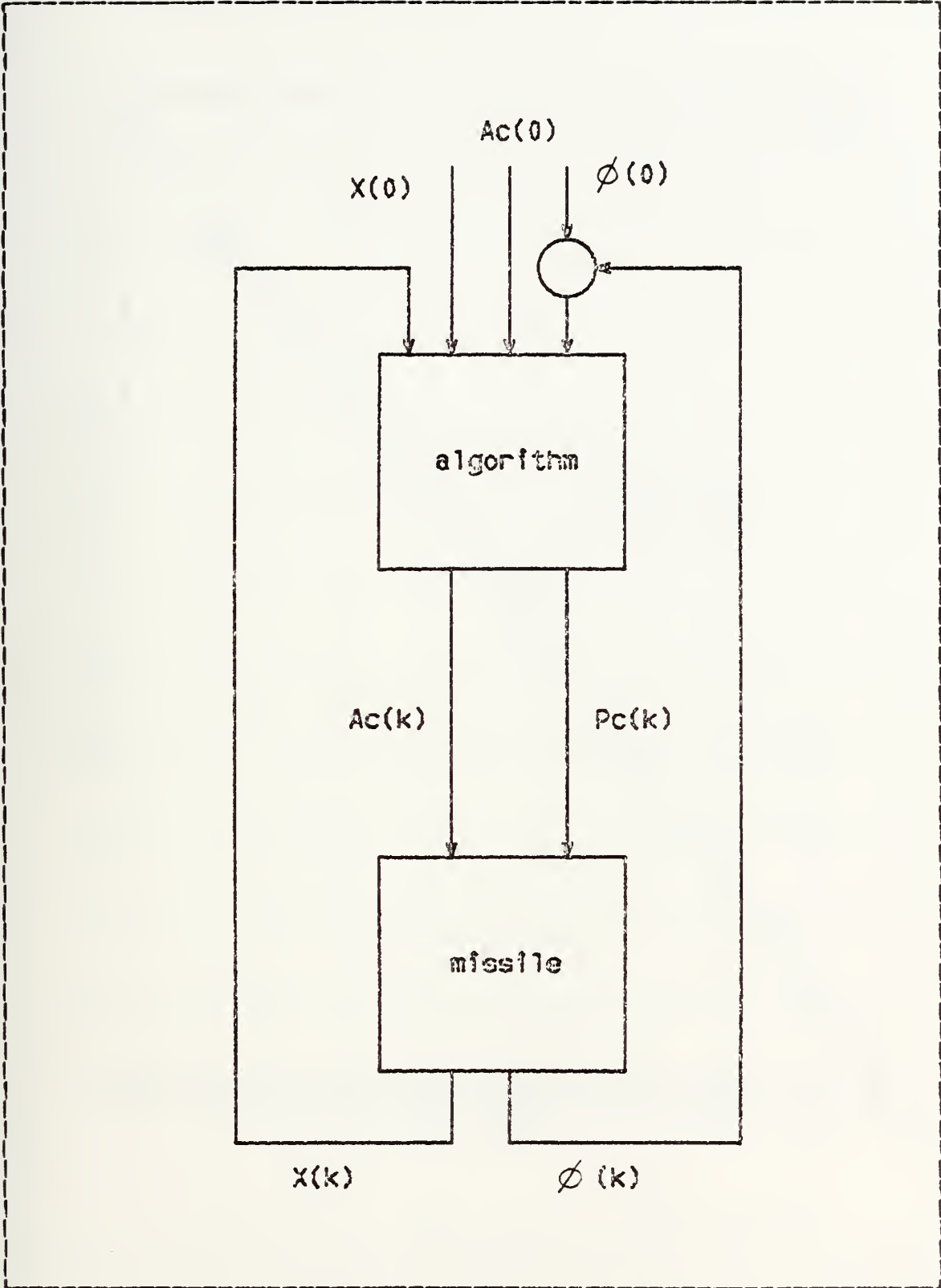


Figure 3.28 Corrected Model.

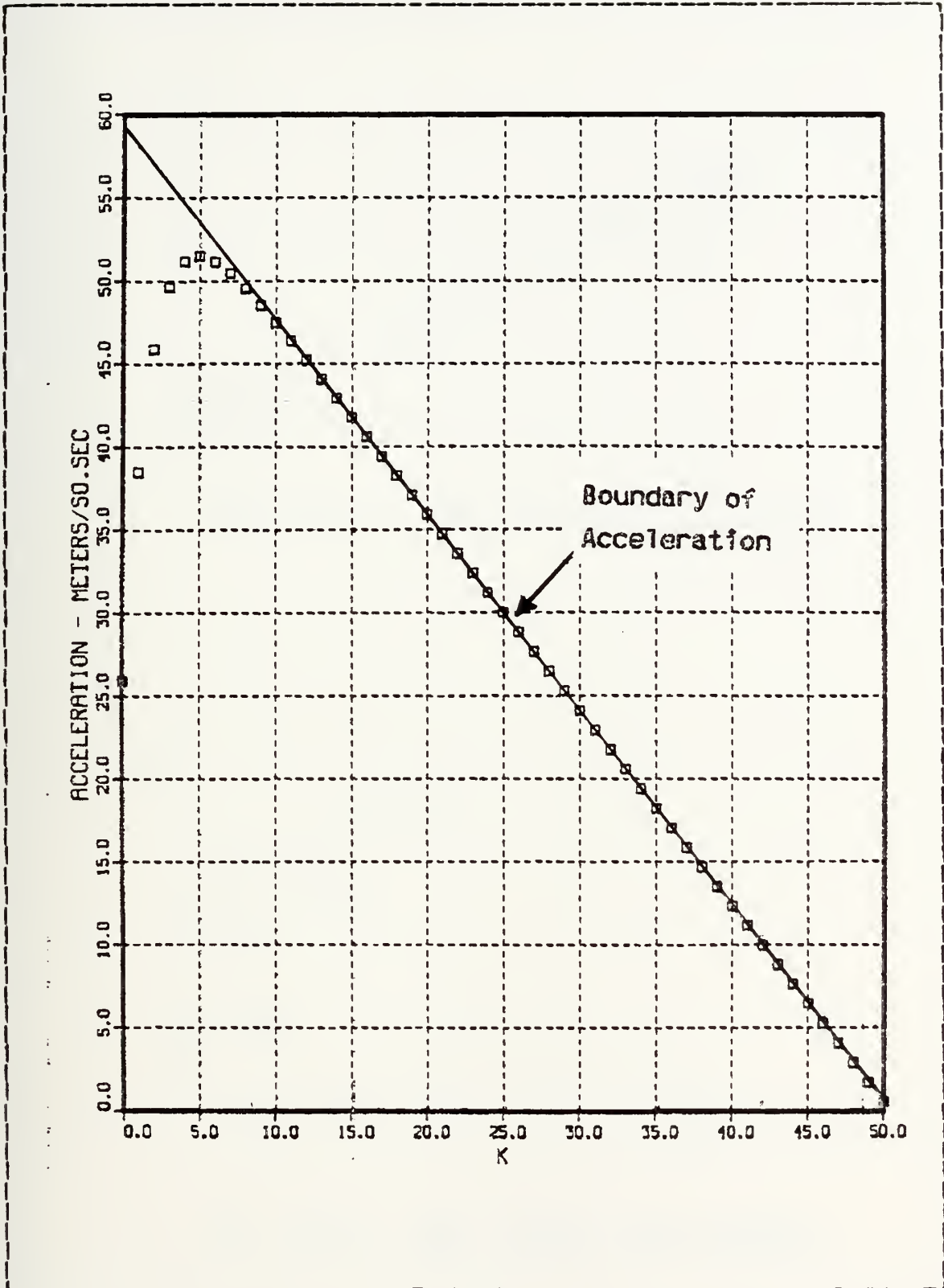


Figure 3.29 Boundary of the Commanded Acceleration.

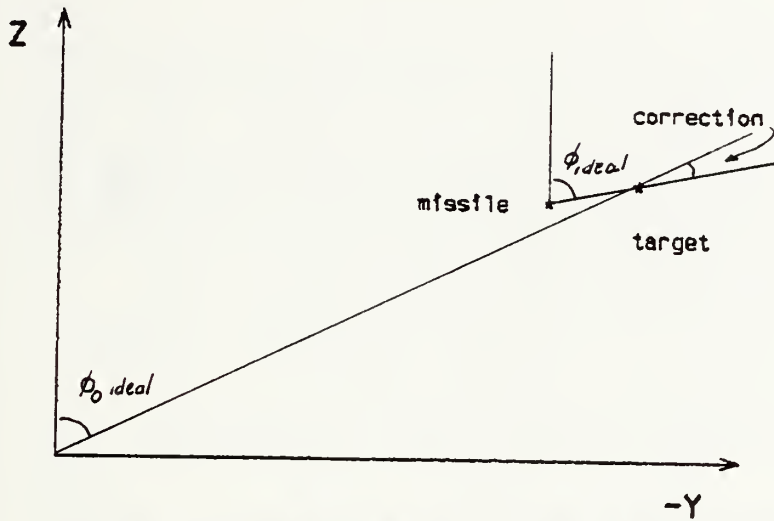


Fig. 3.30 a Large target accelerations

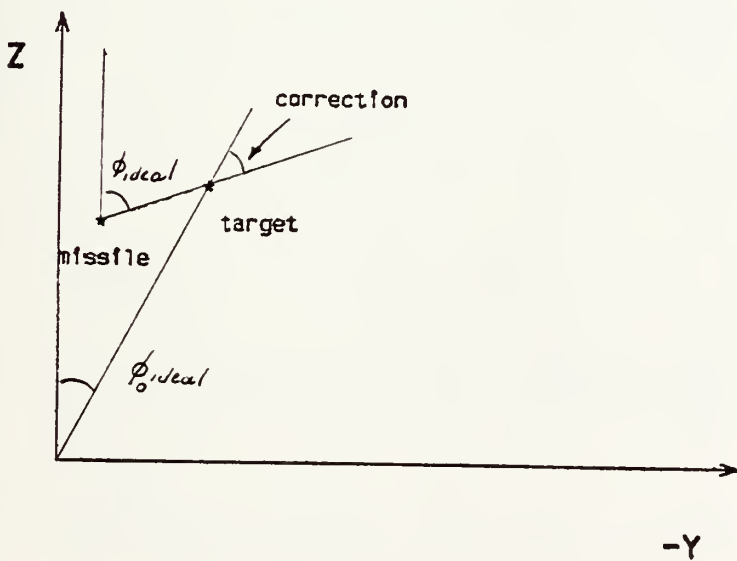


Fig. 3.30 b Small target accelerations

Figure 3.30 Corrections on the Roll Angle.

TABLE I
Results From Tests

case	t	AC (m/sec)	PC (rad/sec)	miss distance Y direction (m)	miss distance Z direction (m)	ϕ (rad)	CG-to-CG miss distance (m)
0	0	26.47	.345	0.0	100.	0.0	100.
	Tf	.133	0.0	-.542	1.50	.439	1.51
1	0	26.47	.345	0.0	100.	0.0	100.
	Tf	.138	0.0	-.383	.528	.416	.652
2	0	26.47	.691	0.0	100.	0.0	100.
	Tf	.157	0.0	-.575	.458	.724	.735
3	0	26.47	2.76	0.0	100.	0.0	100.
	Tf	.332	0.0	-1.47	.046	1.27	1.54
4	0	-19.6	.167	0.0	-600.	0.0	600.
	Tf	.959	0.0	.592	-4.39	3.01	4.44

IV. ANALISYS OF GAINS, SAMPLE RATE AND PITCH ANGLE

A. ANALISYS OF THE GAINS

In chapter 3 has been developed a solution for the optimal control of a system as:

$$x(k+1) = A(k) x(k) + B(k) u(k) + E g$$

It would be interesting to check if the optimal gains reach steady state, but at the moment that the extention for large roll excursions has been introduced, and the system is being feed with optimal commands which are varying each step of time, such idea can not be applied. However one can do such check in the model for small roll excursions, which is actually used to compute the optimal commands.

Doing this, one has the time history of those gains as in 4.1 and 4.2

One can notice in fig. 4.1 that the gain $FG(2,1)$ associated with the effect of gravity has no effect on the comanded roll rate, and that $FG(1,1)$, as shown in fig. 4.2, has a large effect on the commanded acceleration. Furthermore, this gain reaches steady state very fast, thus it can be assumed that the gain FG will be equal to the steady state value during all time.

From eqn. 3.19, and assuming steady state:

$$u(k) = -F(k) x(k) - FG(k) g \quad (4.1)$$

and substituting g :

$$u(k) = -F(k) x(k) - C \quad (4.2)$$

where the second term in the right hand side is a constant, and its value is exactly equal to the value of the commanded acceleration necessary at $t=0$ to correct the gravity fall of the missile (or to correct the initial ZEM due to gravity).

It might be supposed that one could solve the optimal control problem for the system represented by eqn. 4.1, just considering one reduced system represented by:

$$x(k+1) = A(k) x(k) + B(k) u(k) \quad (4.3)$$

with a bias in the control as:

$$u(k) = -F(k) x(k) + C \quad (4.4)$$

But as showed in the following analysis, this is not possible.

The constant term in the right hand side of eqn. 4.4 is calculated as follows:

from eqn.:

$$\text{initial ZEM due to gravity} = ZEM = \frac{1}{2} g t^2$$

$$C = \frac{ZEM g}{\left[\frac{t^2}{2} - \frac{t^3}{6T_i} \right] \cos \phi_0}$$

and the gains $F(k)$ are calculated using a Ricatti equation as usual.

Case 5 was tested using the above considerations, and using the same scenario of case 3.

Figures 4.3 and 4.4, show the time history of the controls. One can see that the commanded acceleration has begun at same values as in case 3, but the commanded acceleration reaches a peak considerable higher, then decreases does not following a linear law, with a final at 14.7 meters per second square, being this terminal value due to the constant term representing the effect of the gravity.

Referring to fig. 4.4, the commanded roll rate begins at a same value as in case 3, but as the control A_c is too high, it reaches negative values, going to zero almost at the end of the running time. This behaviour of the control leads to a large miss distance as seen in figure 4.5, and table II.

Figure 4.6 shows the time history of the roll angle, which rises to values close to 1.5 radians. As the acceleration at this point is larger than the correct value, the corrections are excessive and the roll angle decreases at the end of the running time to the value of .12 radians.

Thus, one can see that the gain due to the gravity's acceleration can not be replaced by its steady state value. This kind of simplification can thus not be done in the system being studied.

B. EFFECT OF THE SAMPLE RATE

Throughout all the simulations a sample period of .05 seconds has been used. In this section a brief study of the effect of the change of this sample rate is given.

Two best cases have been selected to illustrate the effect of the sample period.

The first case, case 6, has been run with a sample period of .1 seconds and consists of the same scenario as case 3.

As one can see in figure 4.7 and table III, there is no noticeable change in the commanded acceleration, but the commanded roll rate begins at smaller value than in case 3, as is seen in fig. 4.8. This initial decrease in roll rate, leads to a large miss distance in Y direction as shown in fig. 4.9, and to a small value of roll angle (see fig. 4.10).

The second case, case 7, has a sample period of 0.025 seconds. There is no noticeable change in the time history of the control A_c as shown in fig. 4.11. The commanded roll rate begins at a higher value than in case 3 as shows fig. 4.12, which leads to a final miss distance in Y direction of -2.22 meters and in Z direction smaller than case 6 (see fig. 4.13). Figure 4.14 shows that the final roll angle is increased and the missile cross the target with 1.28 radians and with a CG-to-CG distance of 2.5 meters.

In both cases, the miss distance was increased over the nominal value obtained with a sampling rate of 0.05 seconds. Thus, it would appear that there is an optimal value for the sampling rate, which may be connected with the geometry of the scenario and with time to go.

C. EFFECT OF THE INITIAL PITCH ANGLE

It is important at this step to remember that throughout this work as we have been discussing a dimensional model, where there is no information on the X coordinate, so it is impossible to verify the behavior of the pitch angle.

In this work, since in all the previous scenarios the initial angle θ was equal to zero, this value has been kept as a constant during all time, and considering that without any information of a third dimension it was not possible to correct the time to intercept, this time was also kept constant and equal to the nominal value of 5 seconds.

Notice that this assumption is likely to be correct if one has the horizontal initial distance from target to missile compared with the initial vertical distance between target and missile large enough in order to have small angles.

The question that rises is, how could this pitch angle affect the system if it was not small?

As seen in fig.4.15, the missile velocity in the X direction would be:

$$V_{mx} = V_m \cos\theta + g \cos\theta \sin\theta t \quad (4.5)$$

which has an effect not only from the pitch angle, represented by the $\cos\theta$, but also from the gravity's acceleration, which will lead to a different time to intercept.

Considering the same physical scenario as in case 4, but changing the initial pitch angle, in order to have the missile pointing to the target (see fig.4.16), and keeping the missile's velocity of 1000 m/sec in the X direction, one has a completely different geometry of the problem as seen from the flight path reference frame.

With this new situation (see fig. 4.16), case 8 has been run. Figures 4.17 and 4.18 show that now the missile is commanding large positive accelerations, and the roll rate at the beginning of the flight is too high, going to zero in a very small period of time. The miss distance as seen in fig.4.19 are increased in the initial part of the flight and as the missile corrects its trajectory it is decreased to reach a final CG-to-CG miss distance of 2.17 m. The roll angle, due to the large control Pc is oscillatory in the beginning and becomes constant with a value of .57 radians (see fig.4.20 and table IV).

Notice that the high values of acceleration needed are in some part due to a vertical component of target's velocity, which is seen from the flight path frame as the target was manouvering in the Z direction with constant velocity. These large accelerations leads to roll rates too large for the physical integrity of the missile. This means that although although the good results obtained, if compared with case 4, they are not practical.

In order to get rid of the vertical manouever of the target, case 9 has been run. In this case, the scenario is the same as before with the target also pointing down, with the same pitch angle as the missile, and has a X velocity equal to the previous case (see fig.4.16).

From fig.4.21, one can see that the decrease in the control A_c is substantial if compared with case 8, but the commanded roll rate is still too large as shows fig.4.22. The time history of the miss distance is better, resulting in a final CG-to-CG distance of about 50% of case 8 (see fig.4.23). The roll angle is not oscillatory as seen in fig.4.24 and the missile cross the target with 1.3 radians in roll. (see tableIV).

The results obtained in the two previous cases, suggests that the algorithm developed in this work could be readily applied to air-to-surface missiles. In the latter, the scenario would be favorable to the missile than in either previous cases, since one can consider that the target could be essentially stationary in comparison with the missile speed.

Case 10 has been run with this assumption, and the scenario as in fig. 4.16. The target is with zero velocity and acceleration, and the missile begins its flight 600 meters above it, with the same initial pitch angle as before.

Fig.4.25 shows the time history of the commanded acceleration, where one can see that as there is no roll rate to

be commanded, the acceleration is following a straight line with very reasonable values. The miss distance is shown in figure 4.27, which shows the final CG-to-CG distance of .31 meters.

Based in the results of these tests, one can see that there will be some effect of the pitch angle on the miss distance, not only due to its effect on the time to intercept, but also because at the moment that there is a pitch angle different from zero, even if the target is keeping its flight level, in the flight path frame a component of the target's velocity will show up leading the missile to command large accelerations and roll rates. Although this results harm the performance in an air-to-air missile, in the case of air-to-surface missiles, when the target has been considered with no motion, good results have been obtained.

D. EFFECT OF TIME TO INTERCEPT

In the simulation of case 1 and 2 in chapter 3, it has been observed that when the target was at small accelerations, the missile did larger corrections on its roll angle, with respect to the ideal initial roll angle, than when the target was with large accelerations. One can think that must be some kind of compromise between the velocity rate of target and missile (which will be reflected on the time to intercept), and the relative position between them, which will affect the miss distance.

In order to do a brief analysis on this, case 11 and 12 has been run.

In case 11, the scenario of case 2 has been kept, with the exception that the missile's velocity was changed to 2000 m/sec., which means that T_i was changed to 2.5 seconds.

Figure 4.29 shows that the acceleration is largely increased due to the small time required to correct the ZEM, and the commanded roll rate is almost twice of case 2 (see fig. 4.30). The final miss distance is more than four times the value obtained in case 2, as seen in fig. 4.31 and table V. The final roll angle is about half as in case 2, since the projected final position of the target in the Y direction is less than in case 2 (see fig. 4.32).

Case 12 was run with a scenario less favorable to the missile, where all the conditions of the previous case was kept, except the target position that has been increased to 200 meters above the missile.

Now, the commanded acceleration are much larger, with a initial A_{co} of 103 m/sec², being almost impossible to see the difference of the time history of the acceleration from one straight line, as shown in fig. 4.33. The commanded roll rate is small, about the same as in case 2 (see fig. 4.34). The change in the miss distance is noticeable, with a final CG-to-CG distance of 4.8 meters as in table V, and figure 4.35. The final roll angle explain the shape of the acceleration curve, since with the small roll angle as shown in fig. 4.36, the system is behaving as for small roll excursions.

Notice that from this analysis, one has to realize that there is some kind of envelope where the 2-D system is valid. And in order to determine this envelope, one has to take in account not only the geometry of the scenario, but also the time to intercept, which is determined not only by the relation of velocities of missile and target, but the pitch angle too.

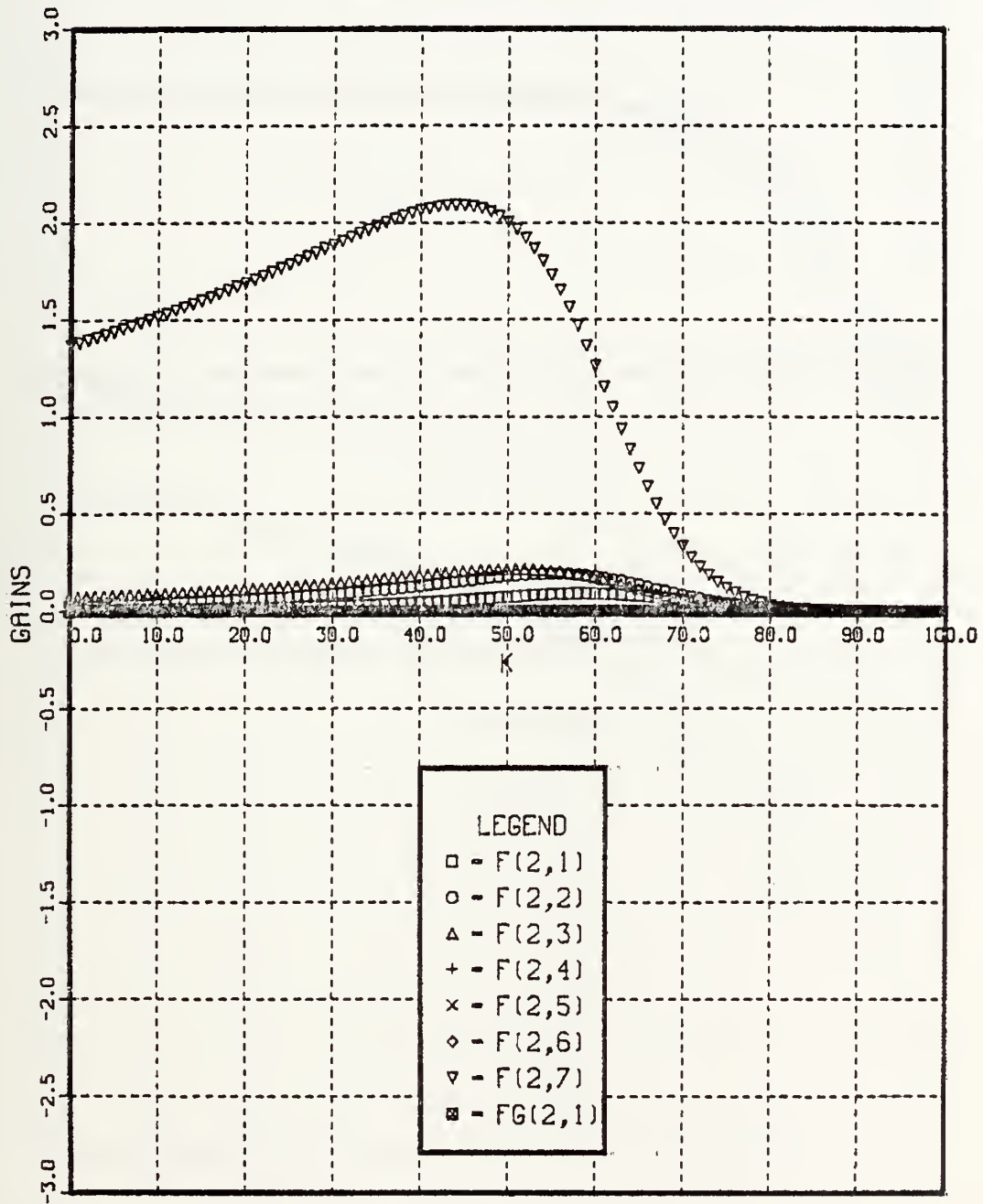


Figure 4.1 Gains affecting the commanded acceleration.

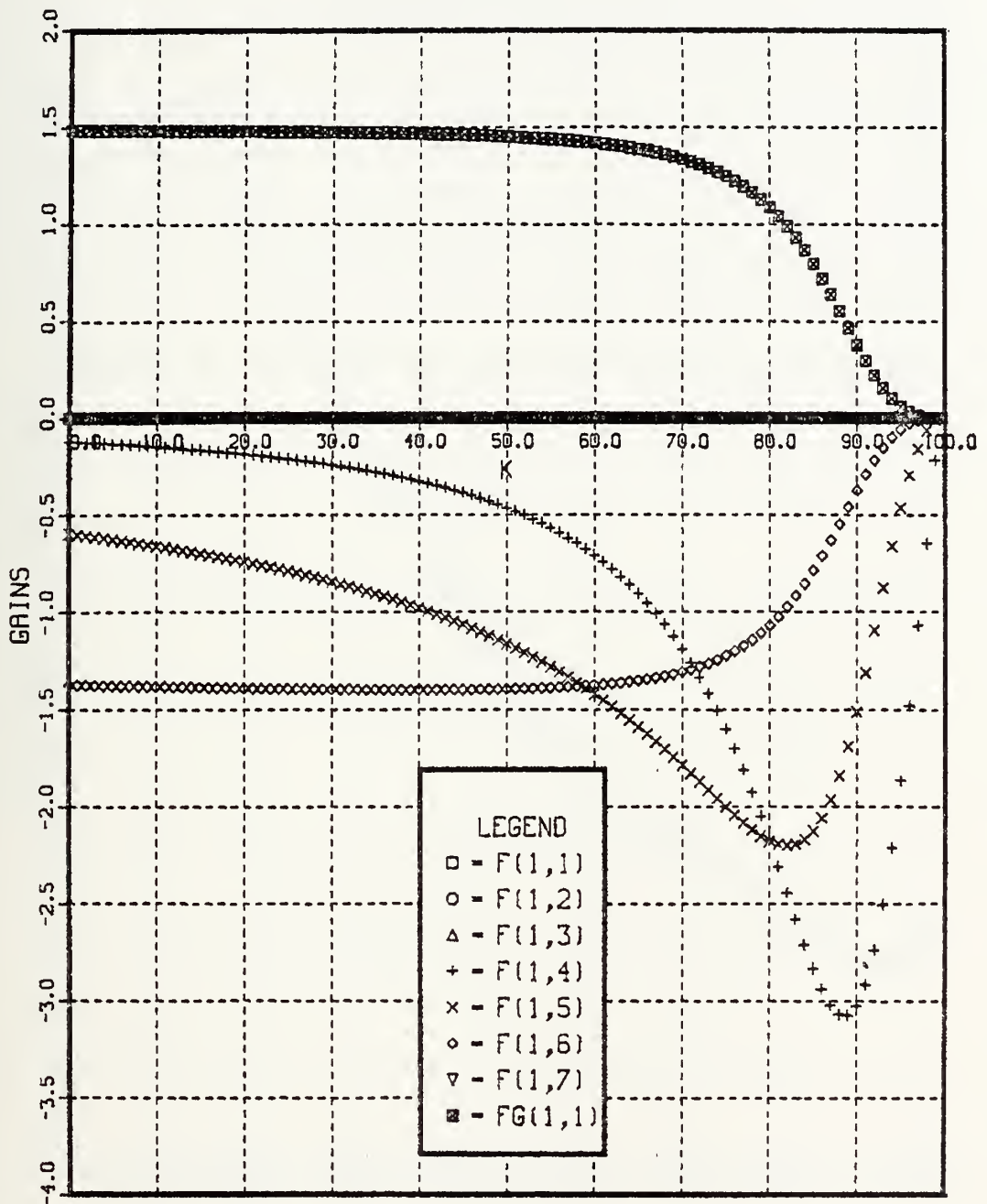


Figure 4.2 Gains Affecting the Commanded Roll Rate.

5TH CASE
INITIAL TARGET ACCELERATION- -4. G
INITIAL TARGET POSITION-100 M
SAMPLE PERIOD-0.05 SEC

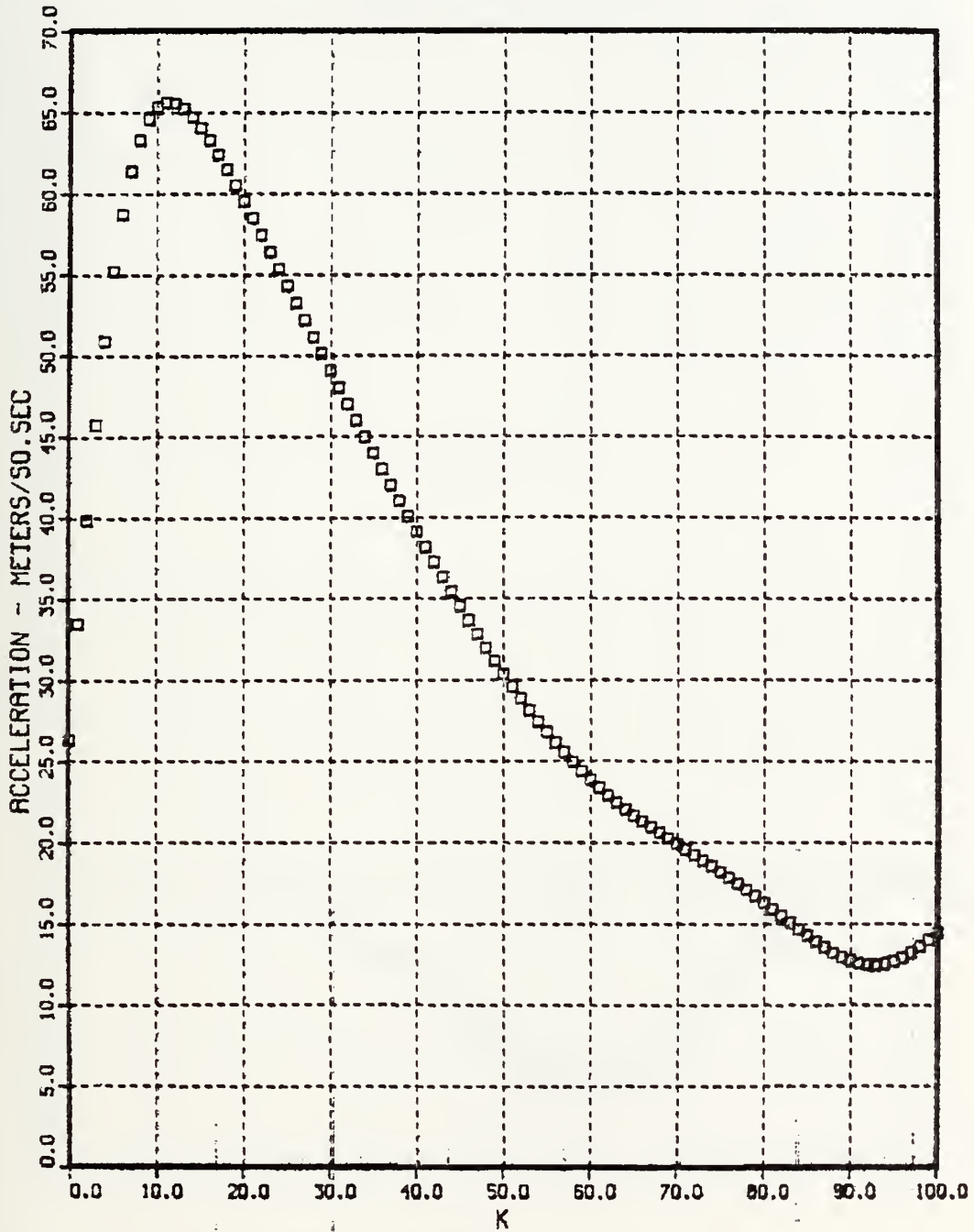


Figure 4.3 Commanded Acceleration-Case 5.

5TH CASE
INITIAL TARGET ACCELERATION- -4. G
INITIAL TARGET POSITION-100 M
SAMPLE PERIOD-0.05 SEC

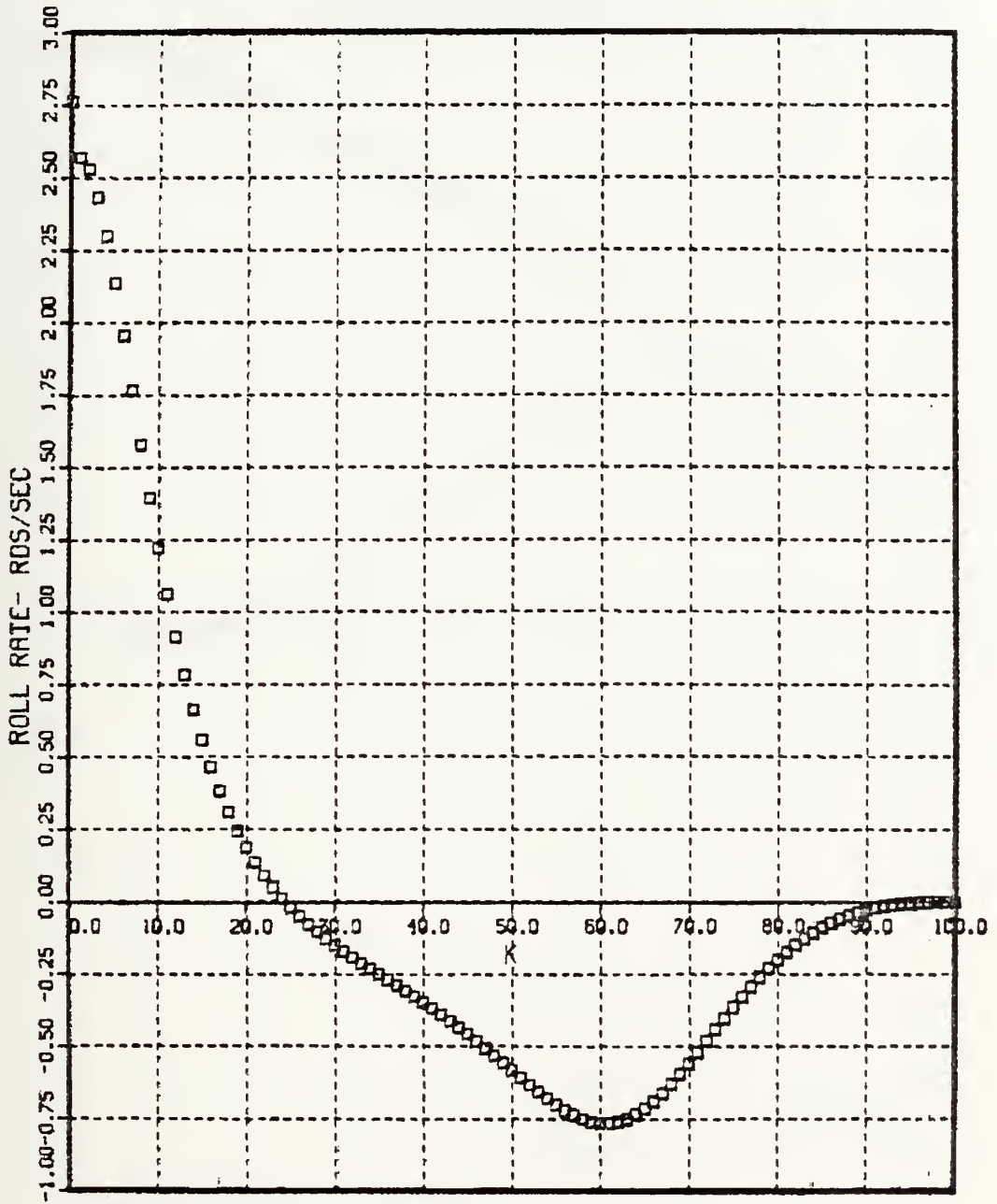


Figure 4.4 Commanded Roll Rate-Case 5.

5TH CASE
INITIAL TARGET ACCELERATION- -4. G
INITIAL TARGET POSITION-100 M
SAMPLE PERIOD-0.05 SEC

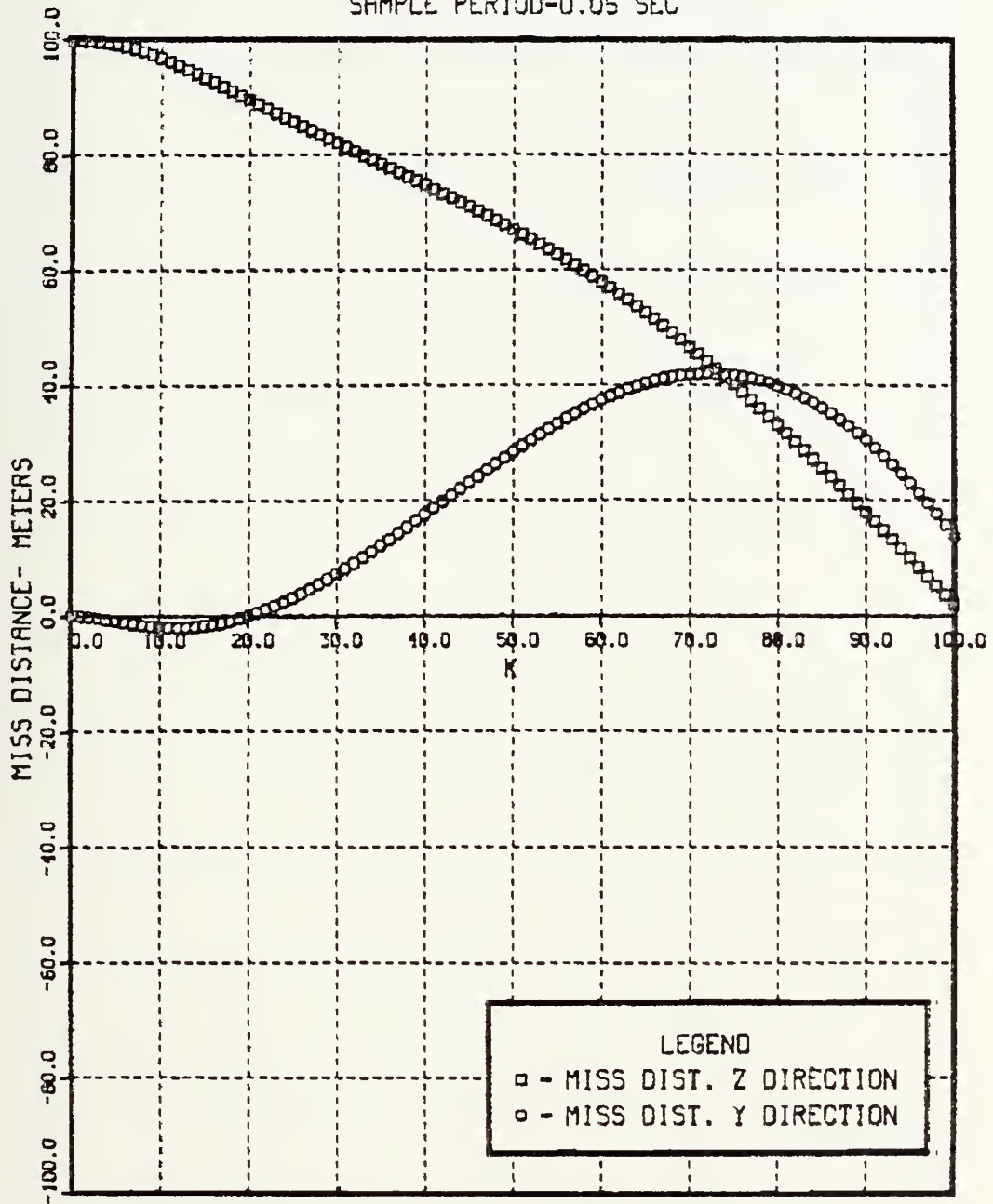


Figure 4.5 Miss Distance-Case 5.

5TH CASE
INITIAL TARGET ACCELERATION- -4. G
INITIAL TARGET POSITION-100 M
SAMPLE PERIOD-0.05 SEC

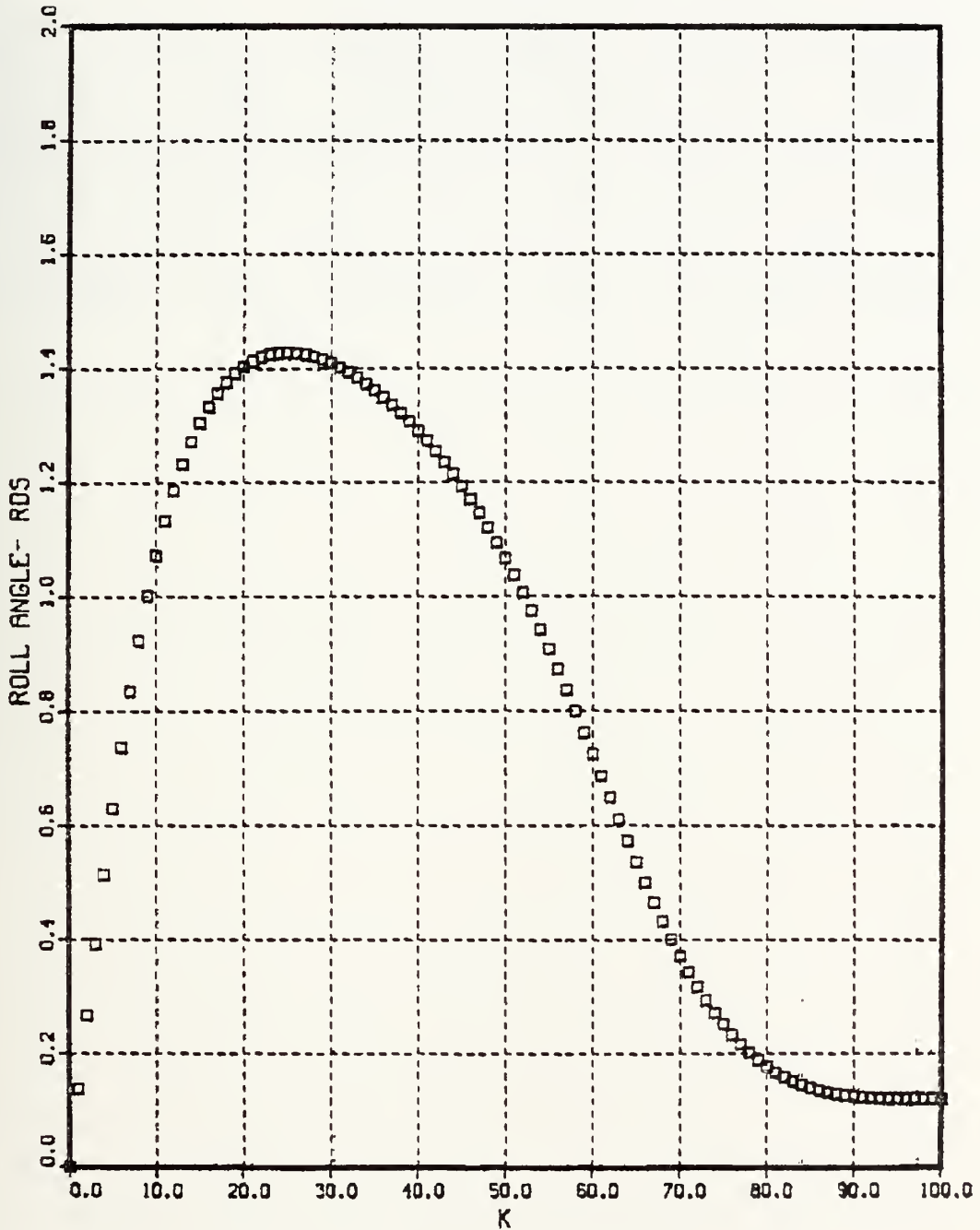


Figure 4.6 Roll Angle-Case 5.

TABLE II
Results from Biased Control

t	Ac (m/sec)	Pc (rad/sec)	miss distance Y direction (m)	miss distance Z direction (m)	ϕ (rad)	CG-to-CG miss distance (m)
0	26.37	2.76	0.0	100.	0.0	100.
Tf	14.47	0.0	13.78	2.00	.119	13.93

6TH CASE
INITIAL TARGET ACCELERATION- -4. G
INITIAL TARGET POSITION-100 M
SAMPLE PERIOD-0.10 SEC

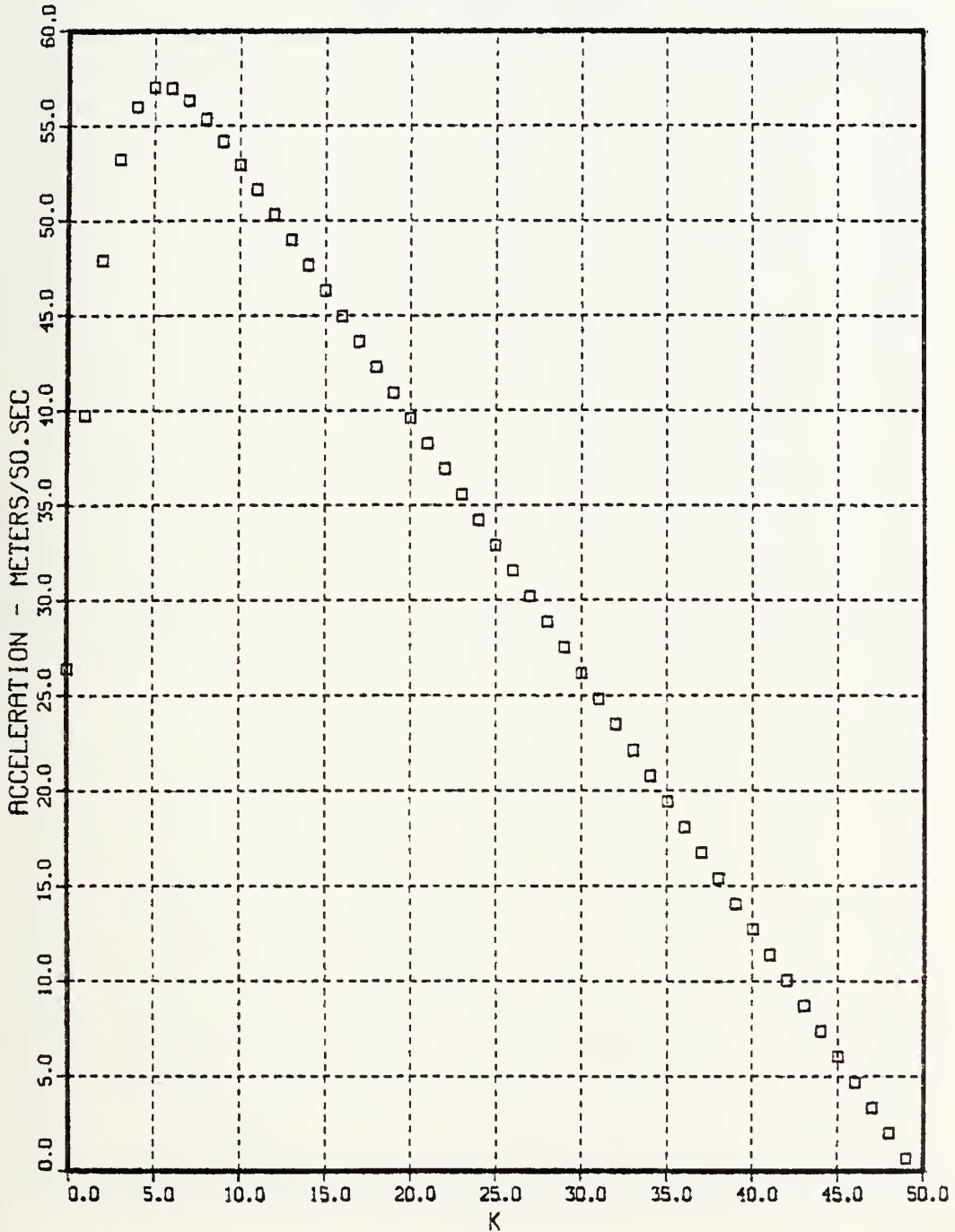


Figure 4.7 Commanded Acceleration-Case 6.

6TH CASE
INITIAL TARGET ACCELERATION= -4. G
INITIAL TARGET POSITION=100 M
SAMPLE PERIOD=0.10 SEC

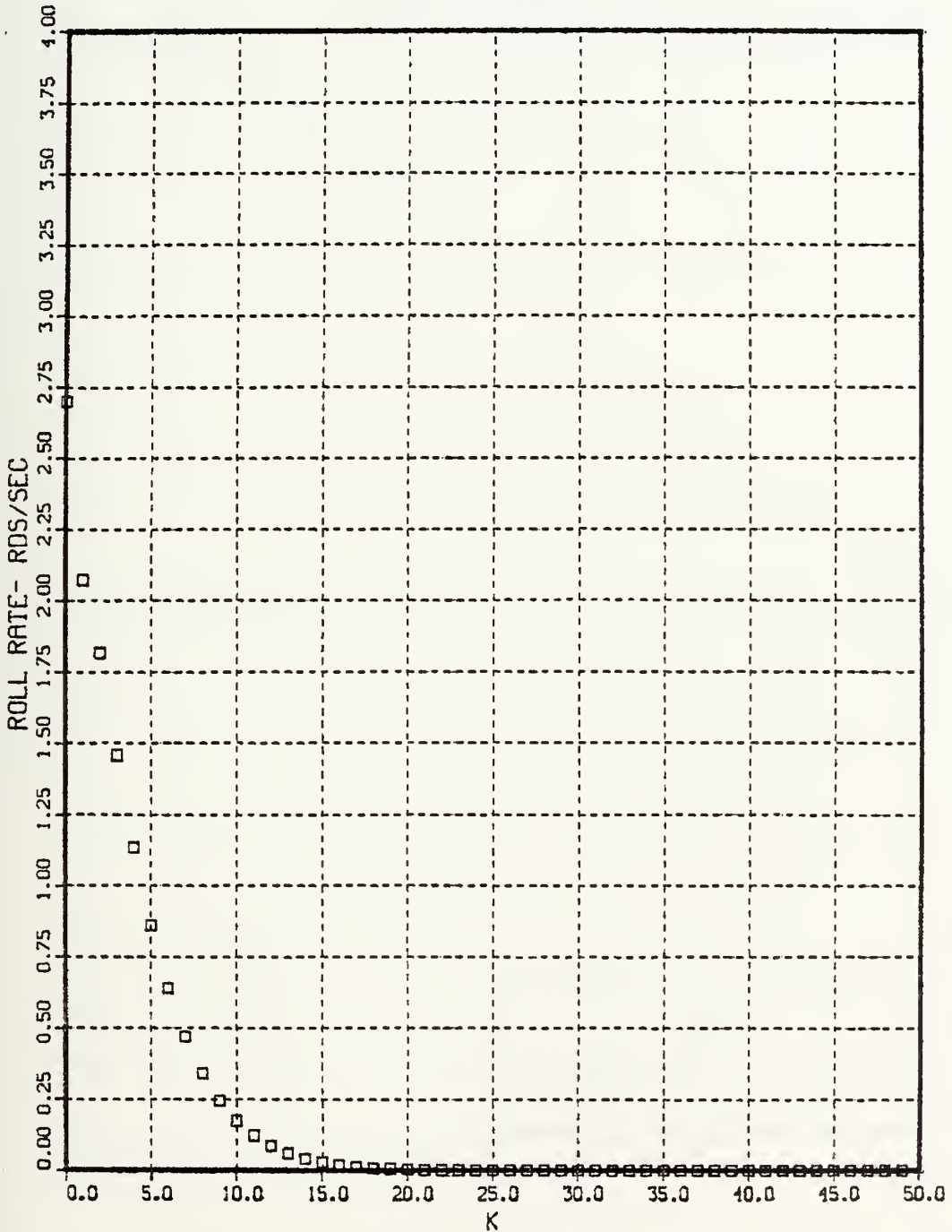


Figure 4.8 Commanded Roll Rate-Case 6.

6TH CASE
INITIAL TARGET ACCELERATION- -4. G
INITIAL TARGET POSITION-100 M
SAMPLE PERIOD-0.10 SEC

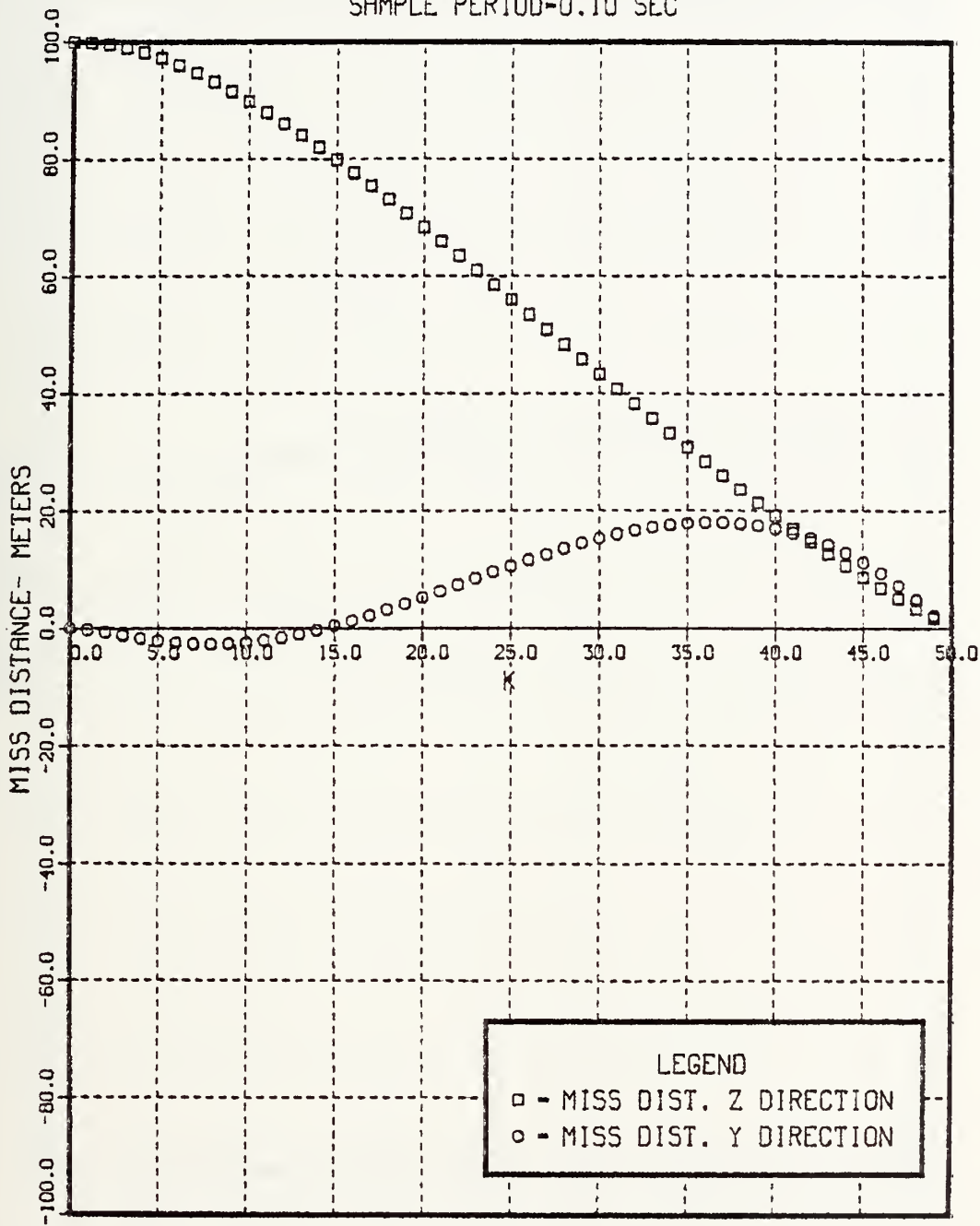


Figure 4.9 Miss Distance-Case 6.

6TH CASE
INITIAL TARGET ACCELERATION= -4. G
INITIAL TARGET POSITION=100 M
SAMPLE PERIOD=0.05 SEC

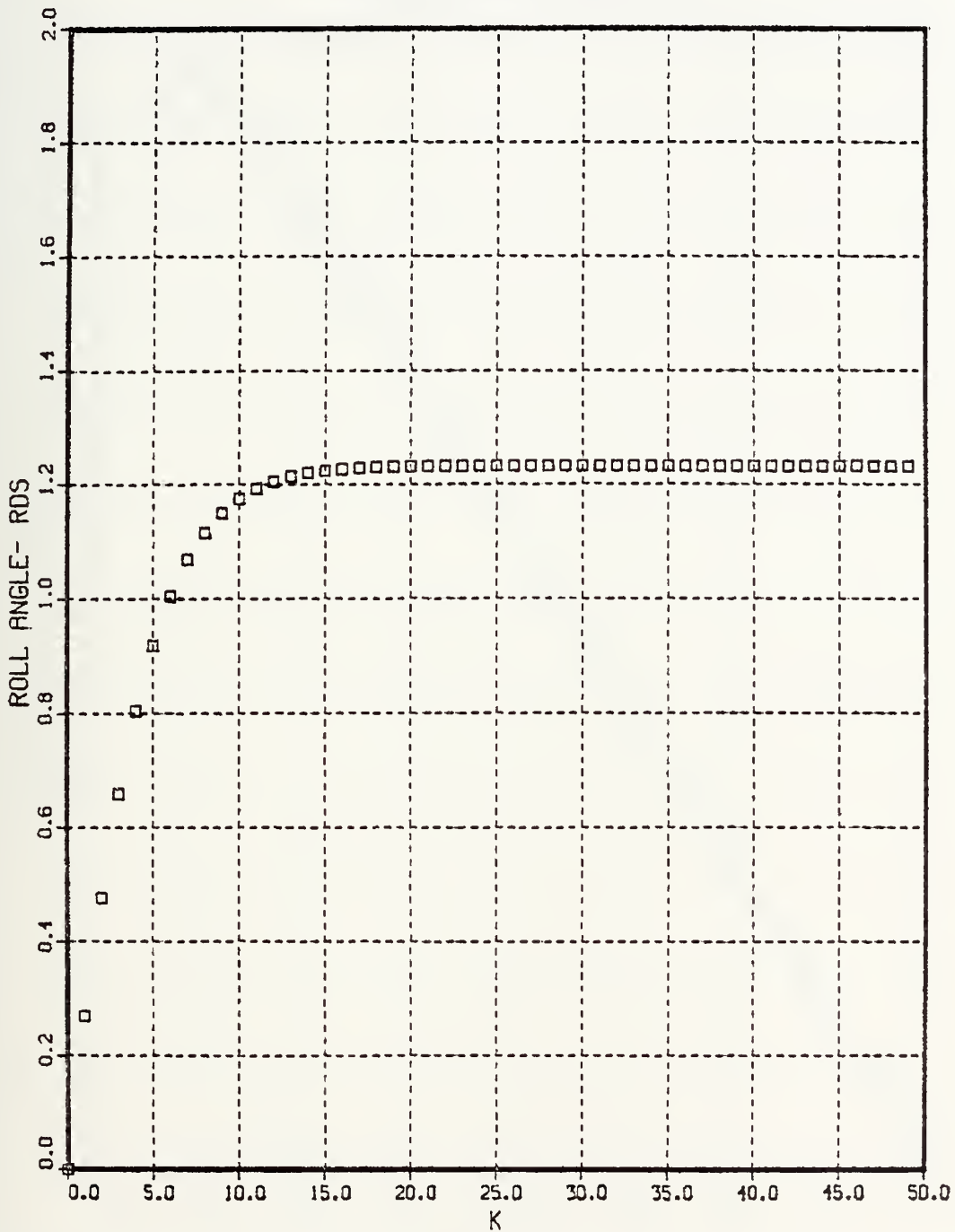


Figure 4.10 Roll Angle-Case 6.

7TH CASE
INITIAL TARGET ACCELERATION- -4. G
INITIAL TARGET POSITION-100 M
SAMPLE PERIOD-0.025 SEC

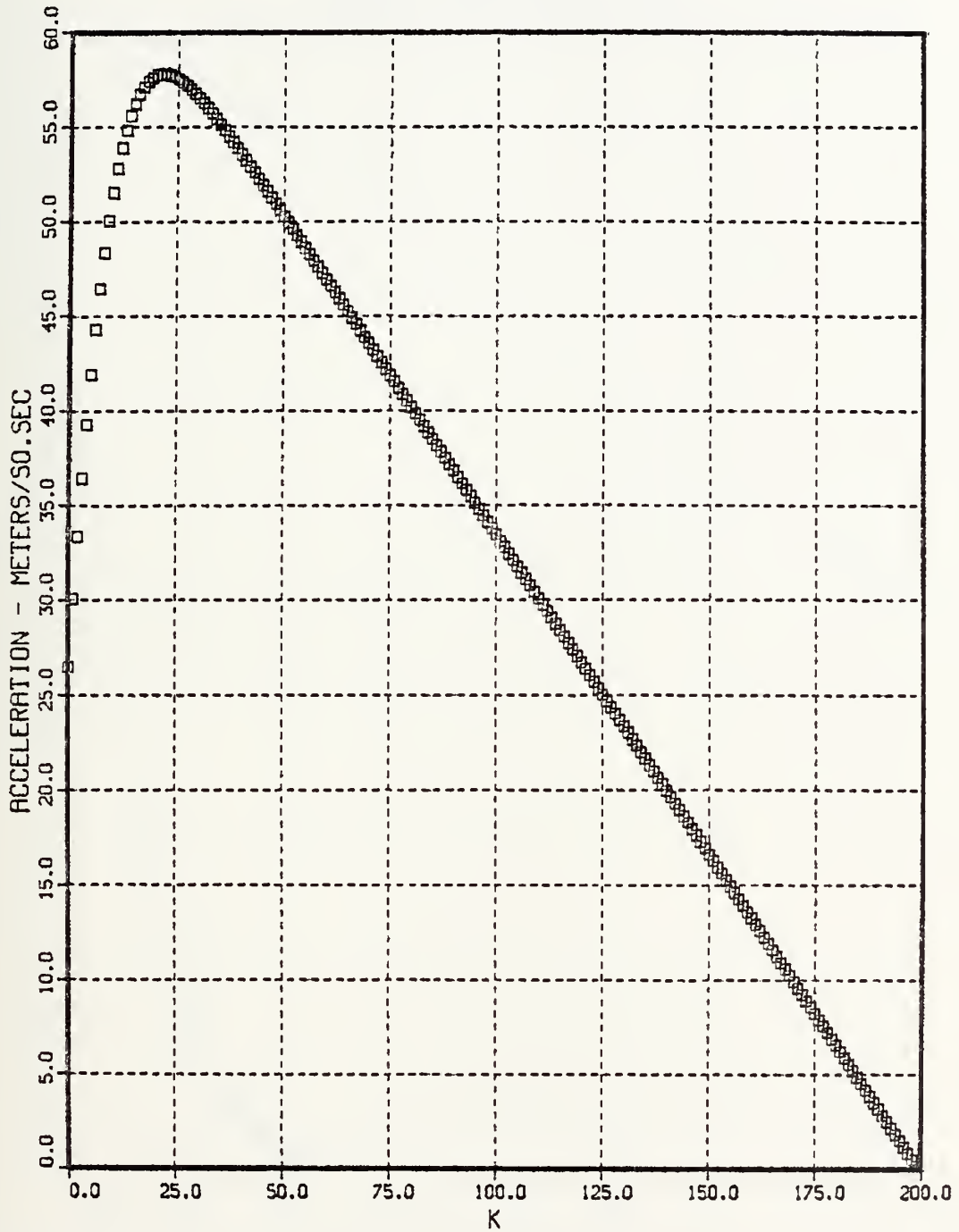


Figure 4.11 Commanded Acceleration-Case 7.

7TH CASE
INITIAL TARGET ACCELERATION= -4. G
INITIAL TARGET POSITION=100 M
SAMPLE PERIOD=0.025 SEC

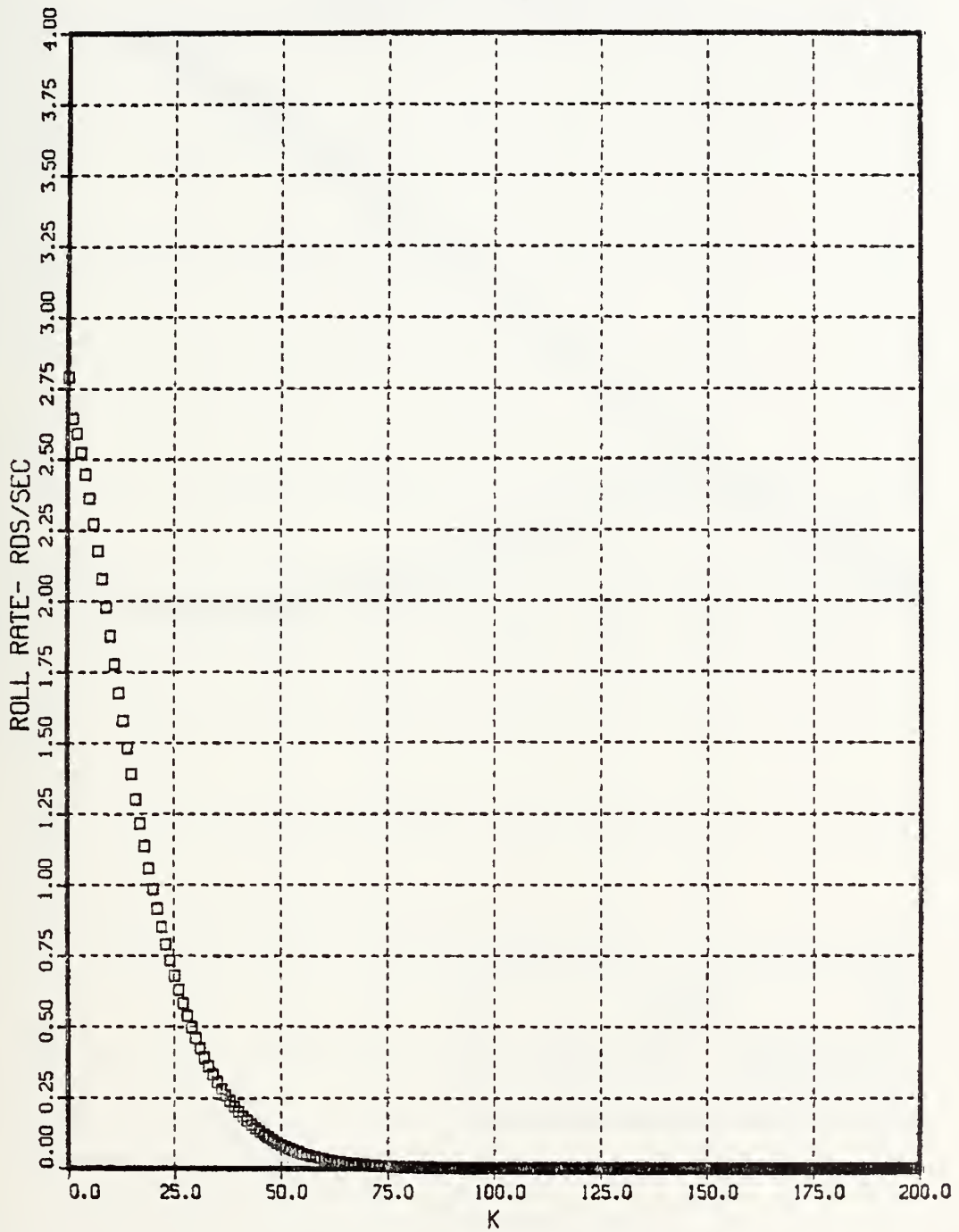


Figure 4.12 Commanded Roll Rate-Case 7.

7TH CASE
 INITIAL TARGET ACCELERATION- -4. G
 INITIAL TARGET POSITION-100 M
 SAMPLE PERIOD-0.025 SEC

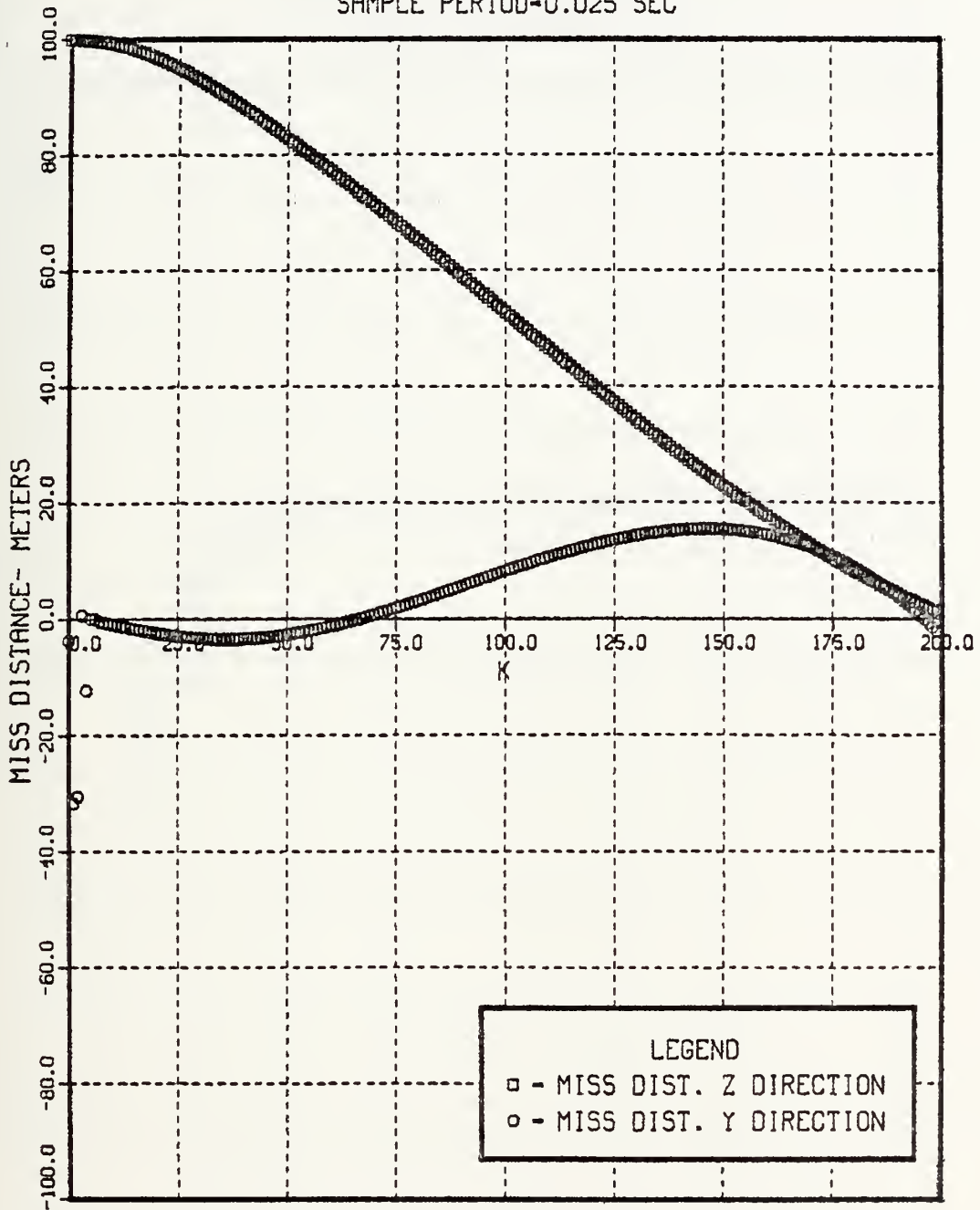


Figure 4.13 Miss distance-Case 7.

7TH CASE
INITIAL TARGET ACCELERATION- -4. G
INITIAL TARGET POSITION-100 M
SAMPLE PERIOD-0.025 SEC

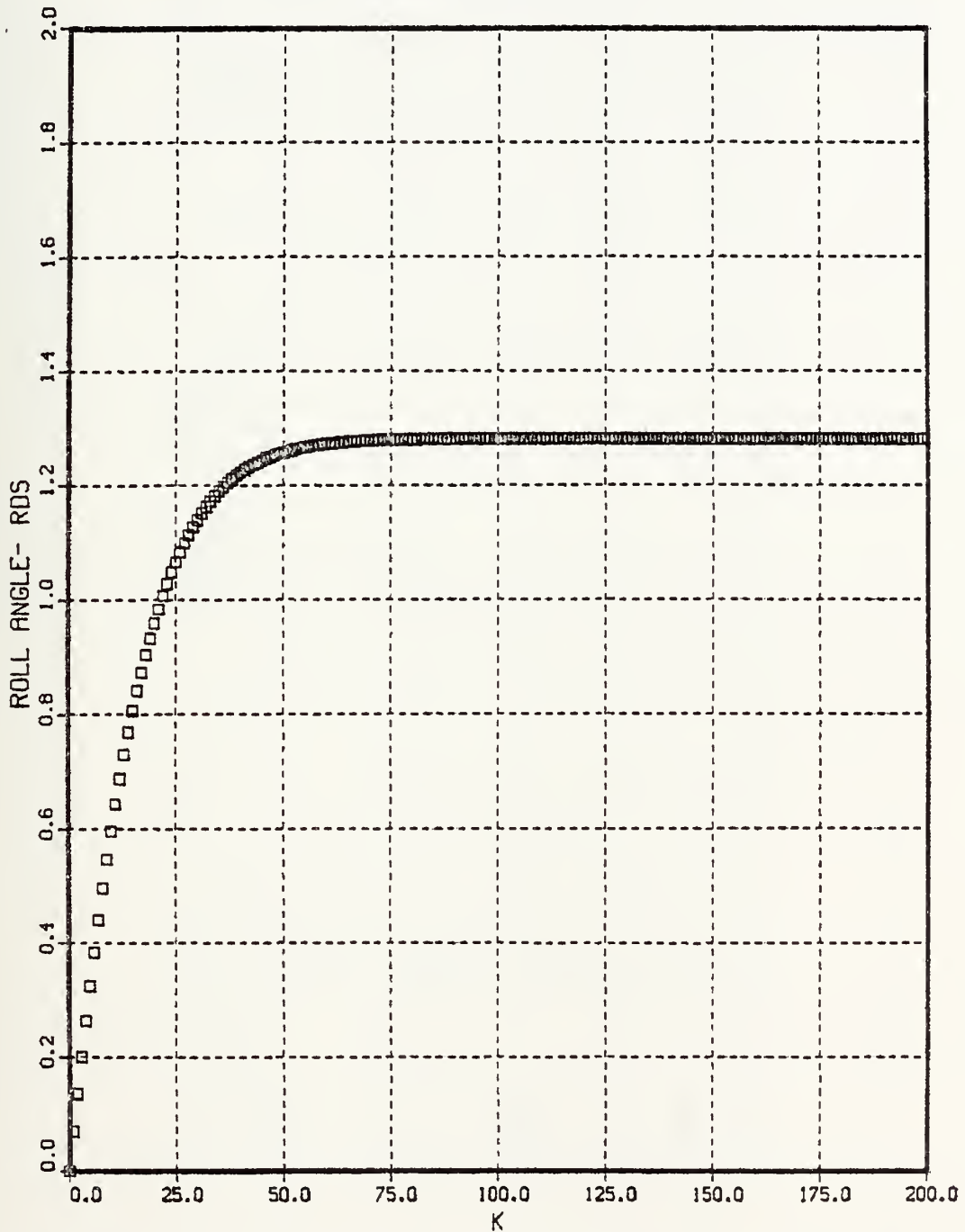


Figure 4.14 Roll Angle-Case 7.

TABLE III
Results for Different Sample Periods

T (sec)	case	t	AC (m/sec)	PC (rad/sec)	miss distance Y direction (m)	miss distance Z direction (m)	ϕ (rad)	CG-to-CG miss distance (m)
.1	6	0	26.40	2.70	0.0	100.	0.0	100.
		Tf	.67	0.0	2.23	1.77	1.23	2.85
.025	7	0	26.48	2.79	0.0	100.	0.0	100.
		Tf	.68	0.0	2.22	1.20	1.28	2.53
.05	3	0	26.47	2.76	0.0	100.	0.0	100.
		Tf	.33	0.0	-1.47	.046	1.27	1.54

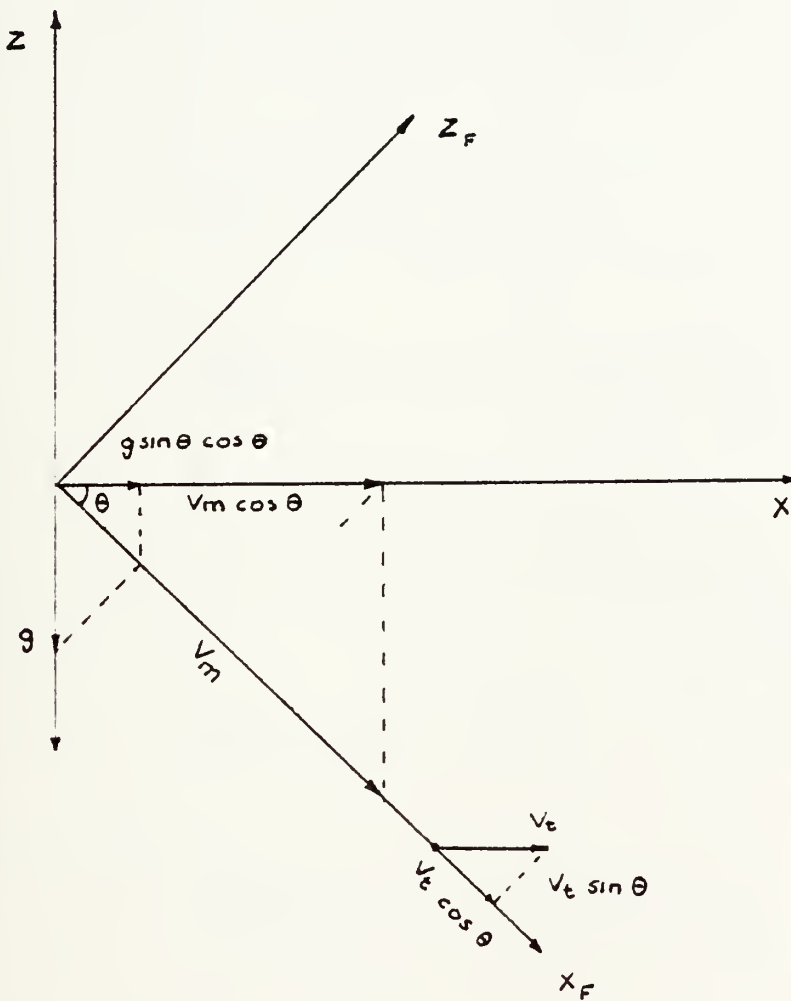


Figure 4.15 Effect of Initial Pitch Angle.

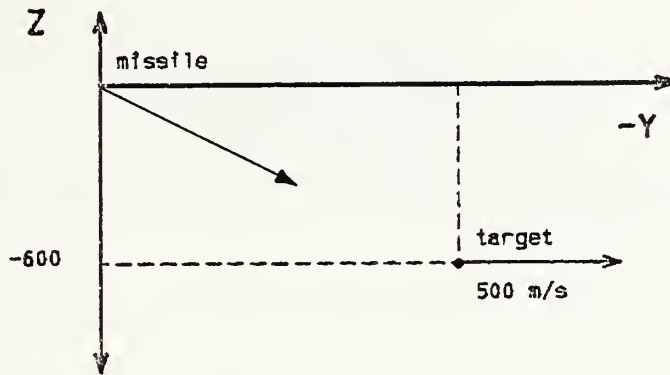


Figure 4.16a Case 8

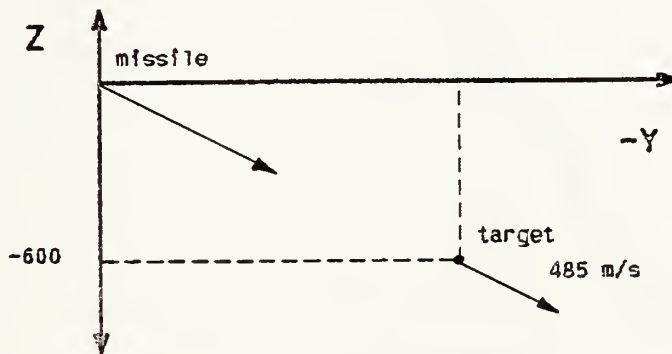


Figure 4.16b Case 9

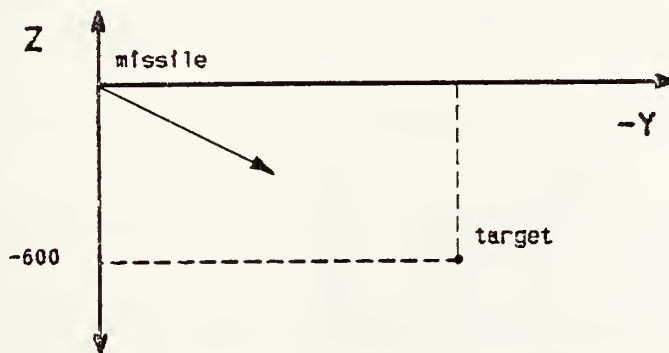


Figure 4.16c Case 10

Figure 4.16 Scenarios With Pitch Angle.

8TH CASE
INITIAL TARGET ACCELERATION- -4. G
INITIAL TARGET POSITION--600 M
SAMPLE PERIOD-0.05 SEC

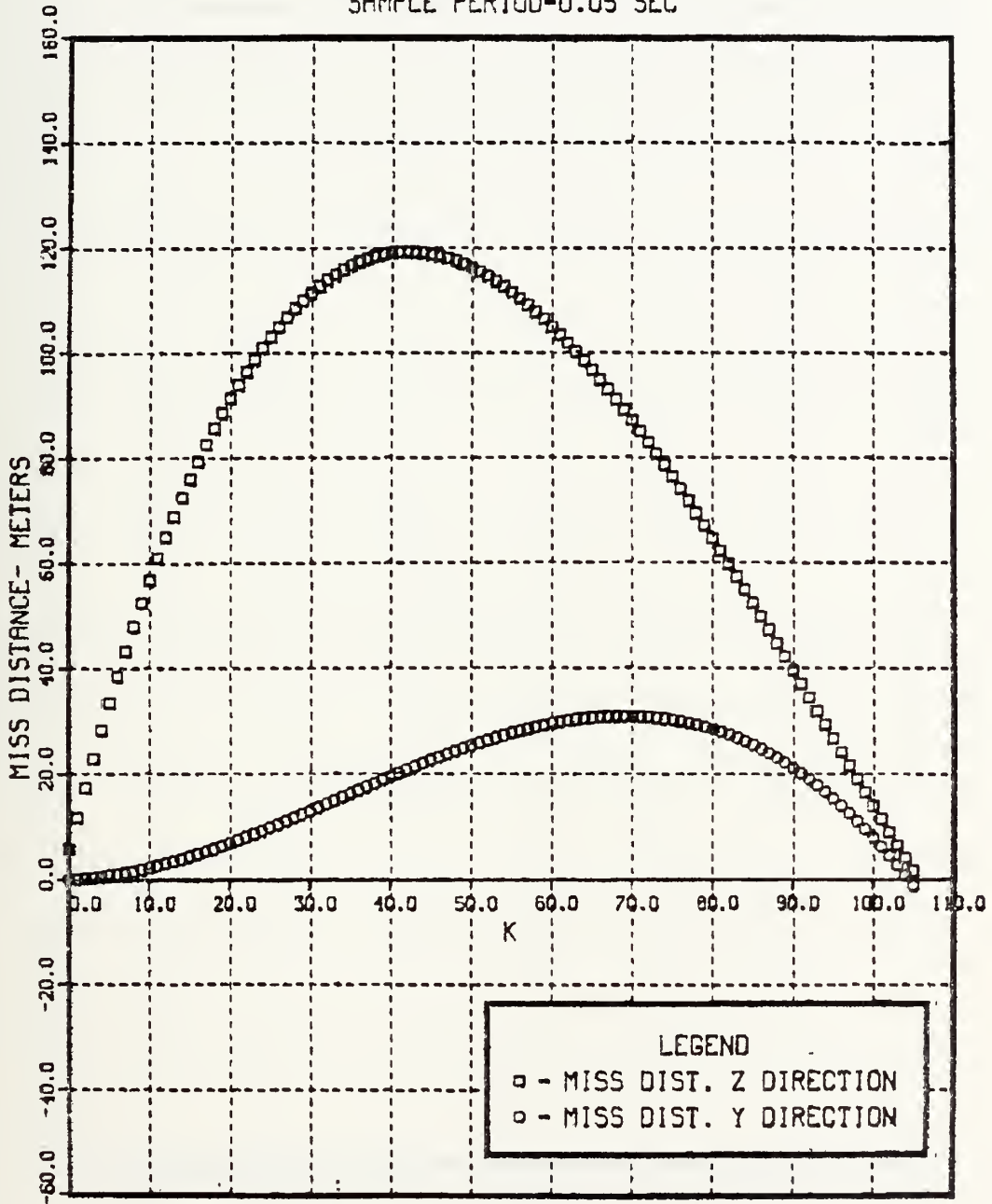


Figure 4.17 Commanded Acceleration-Case 8.

8TH CASE
INITIAL TARGET ACCELERATION- -4. G
INITIAL TARGET POSITION--600 M
SAMPLE PERIOD-0.05 SEC

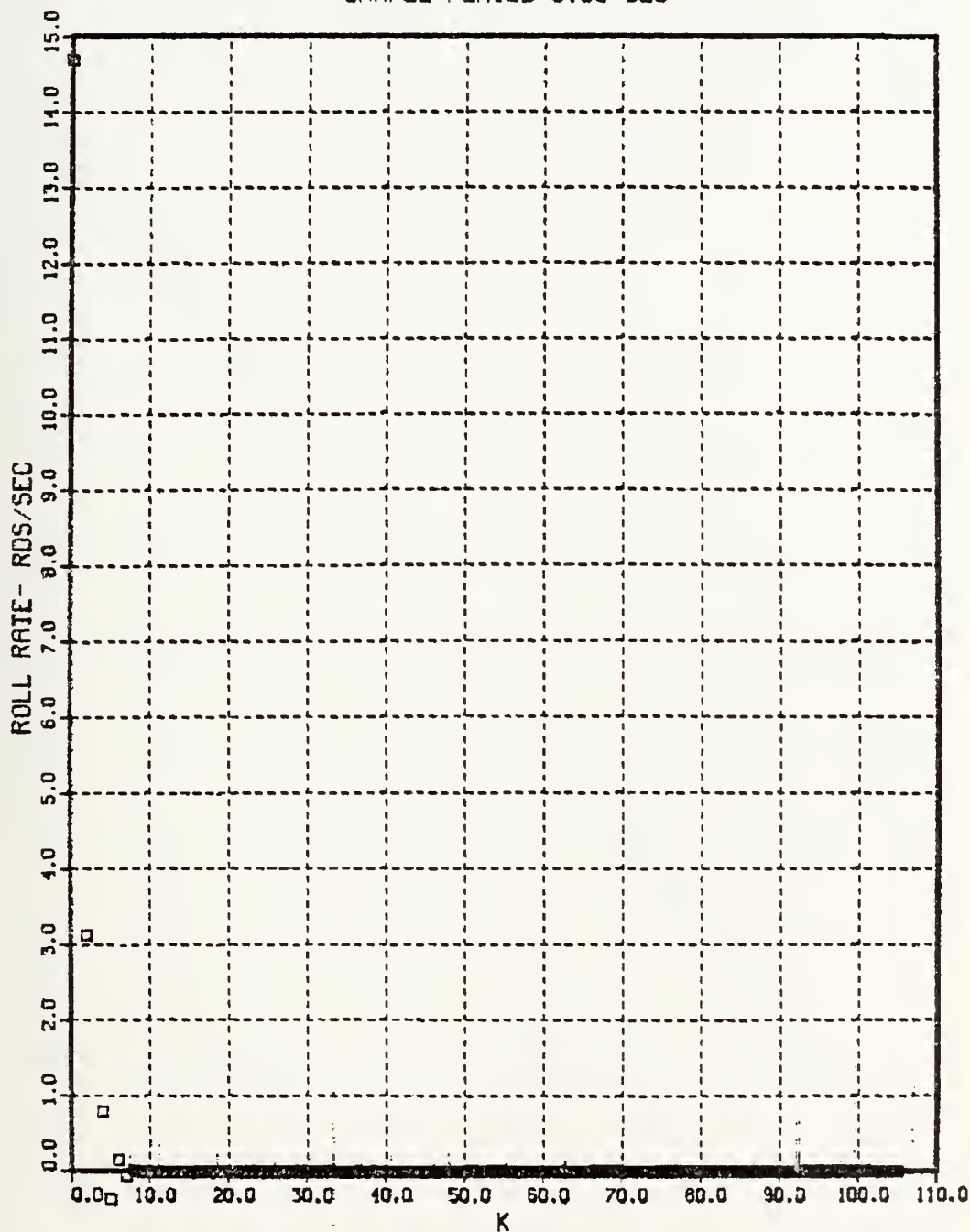


Figure 4.18 Commanded Roll Rate-Case 8.

8TH CASE
INITIAL TARGET ACCELERATION-- -4. G
INITIAL TARGET POSITION--600 M
SAMPLE PERIOD--0.05 SEC

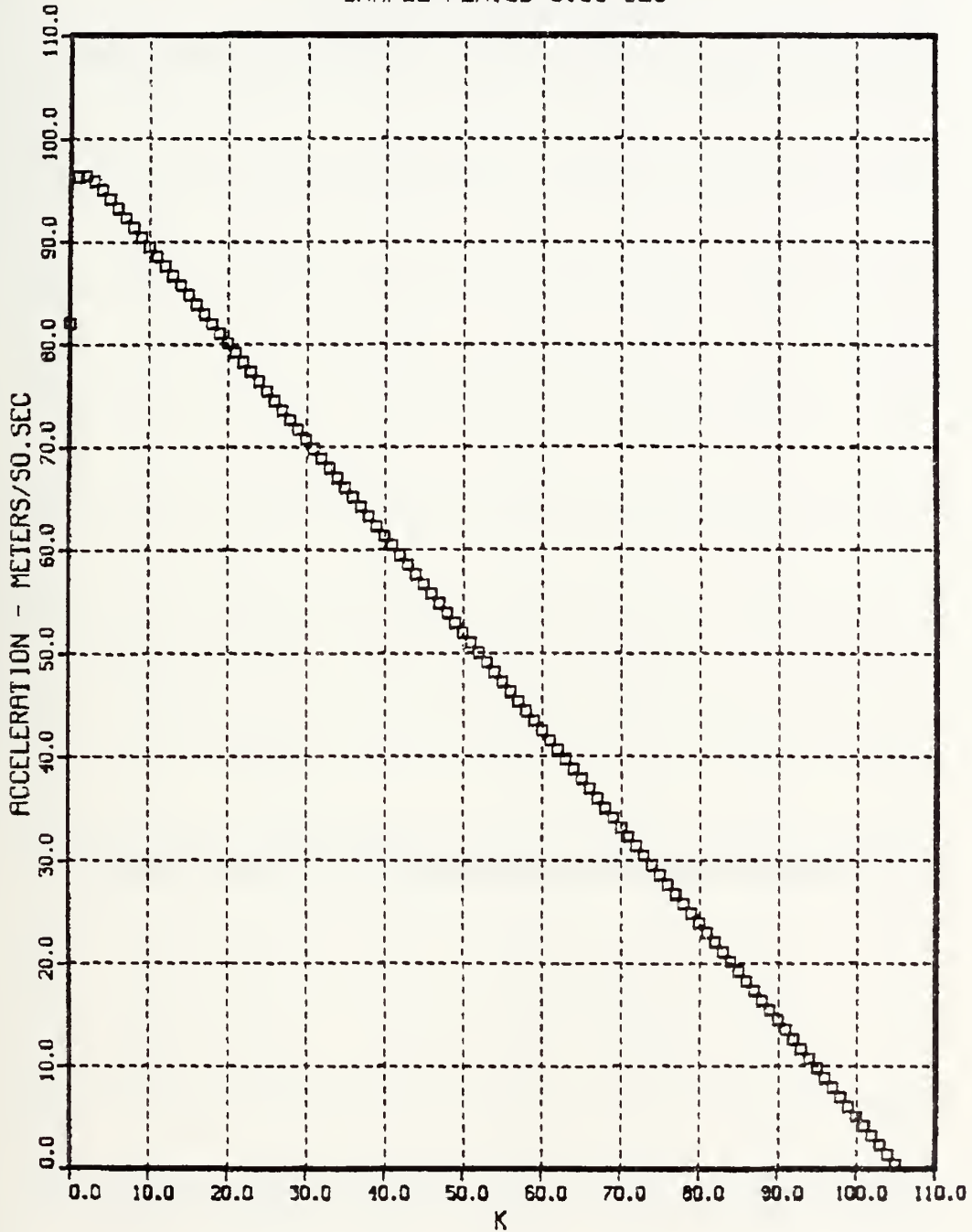


Figure 4.19 Miss Distance-Case 8.

8TH CASE
INITIAL TARGET ACCELERATION--4. G
INITIAL TARGET POSITION--600 M
SAMPLE PERIOD--0.05 SEC

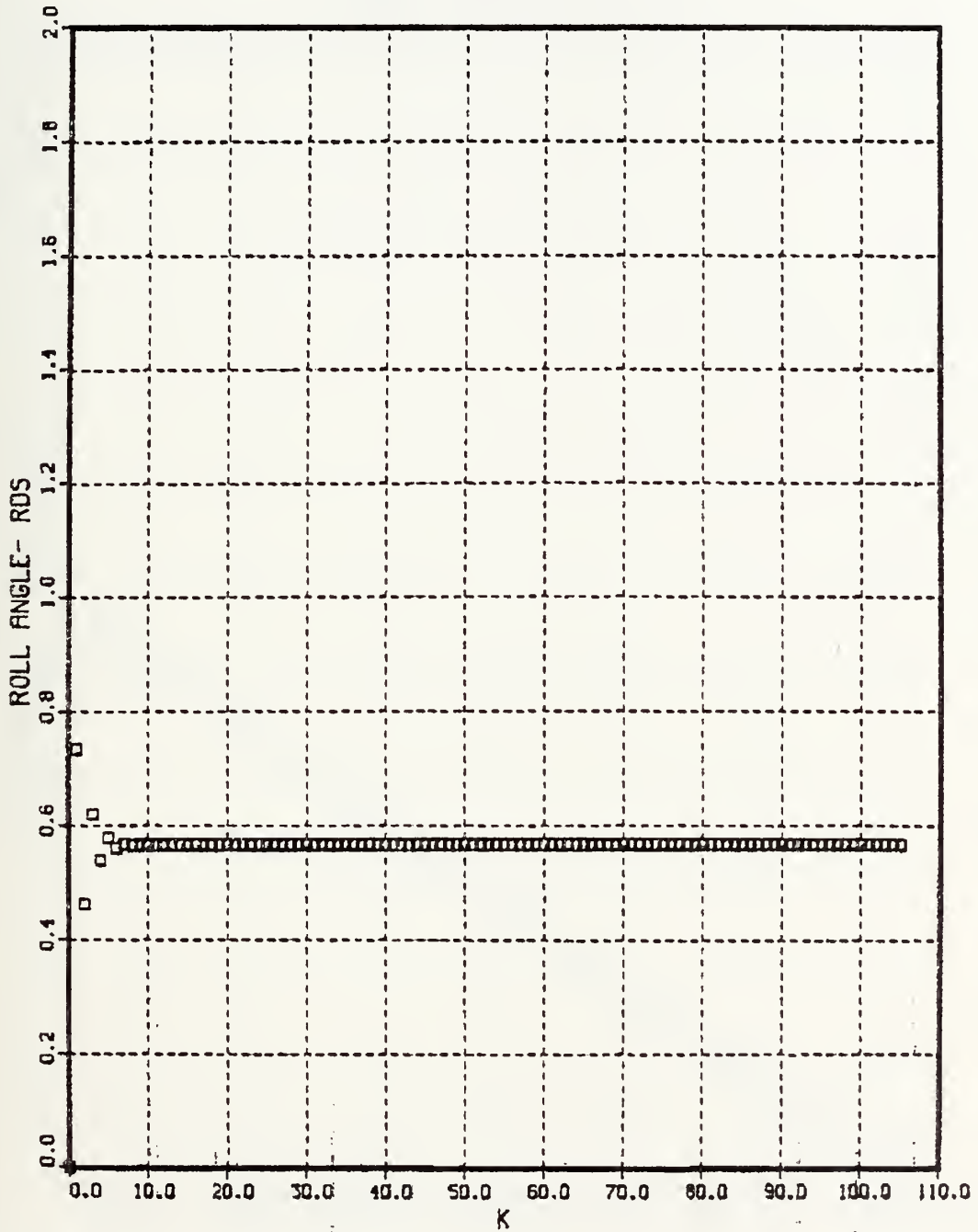


Figure 4.20 Roll Angle-Case 8.

9TH CASE
INITIAL TARGET ACCELERATION- -4. G
INITIAL TARGET POSITION--600 M
SAMPLE PERIOD-0.05 SEC

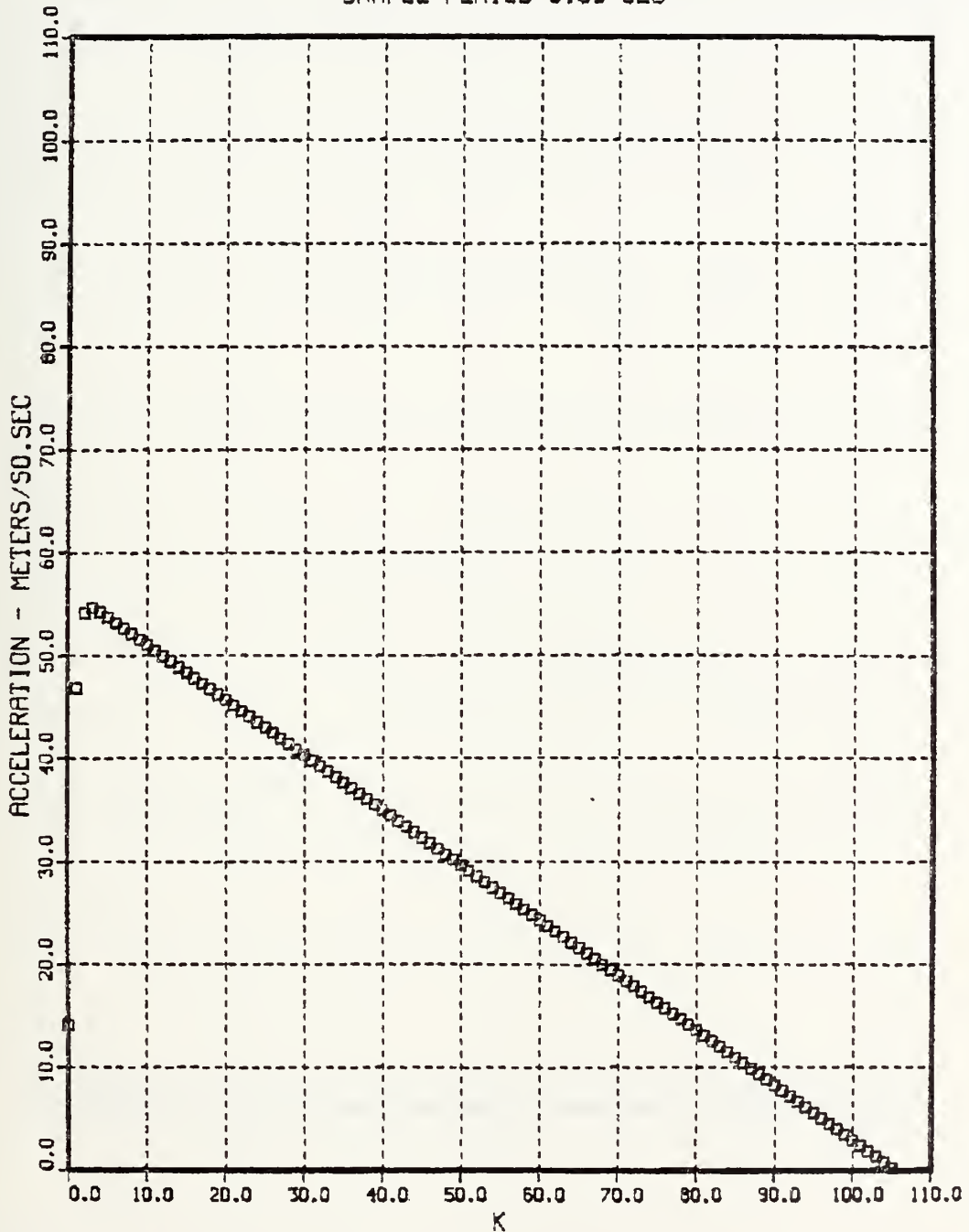


Figure 4.21 Commanded Acceleration-Case 9.

9TH CASE
INITIAL TARGET ACCELERATION- -4. G
INITIAL TARGET POSITION--600 M
SAMPLE PERIOD-0.05 SEC

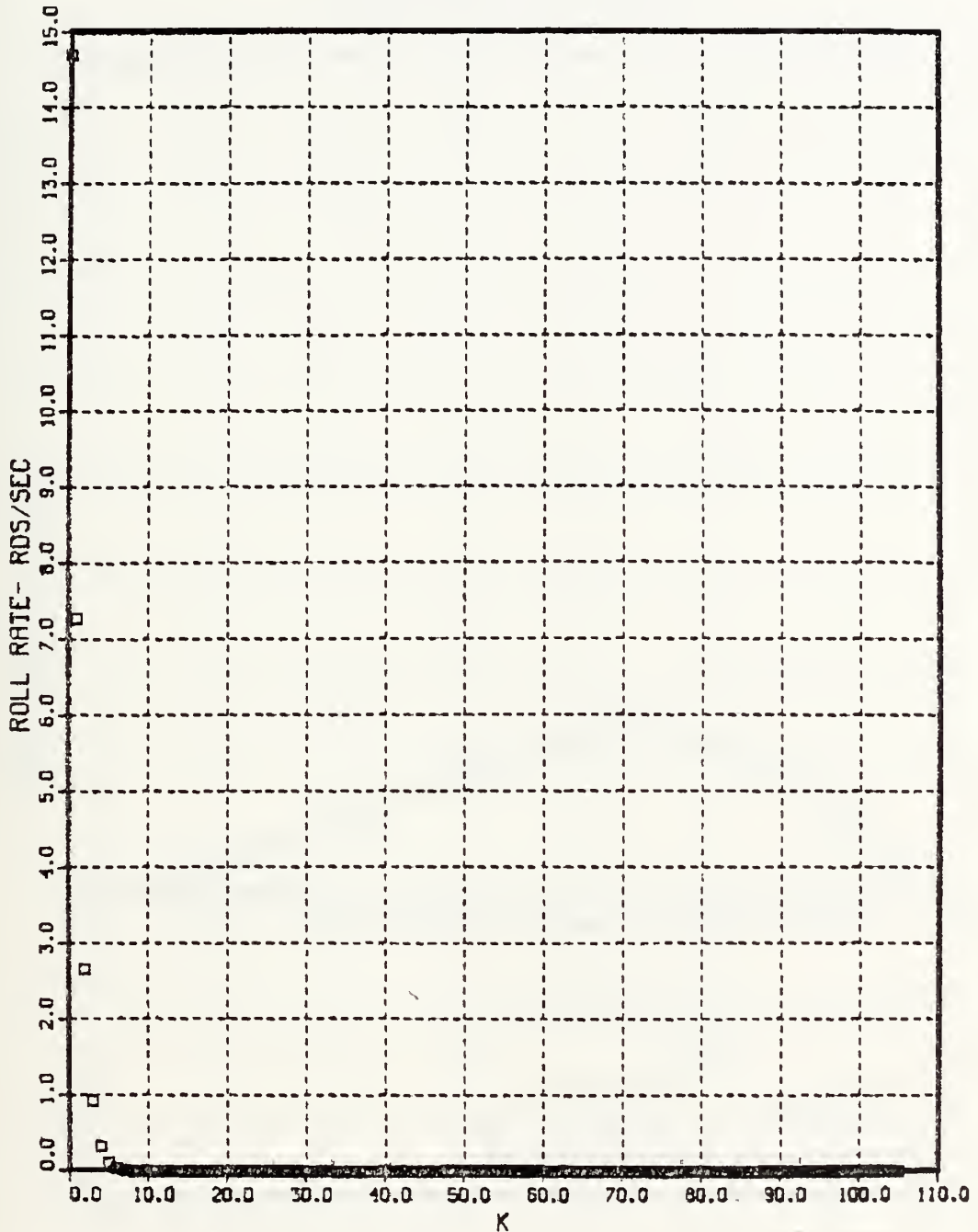


Figure 4.22 Commanded Roll Rate-Case 9.

9TH CASE
 INITIAL TARGET ACCELERATION- -4. G
 INITIAL TARGET POSITION--600 M
 SAMPLE PERIOD-0.05 SEC

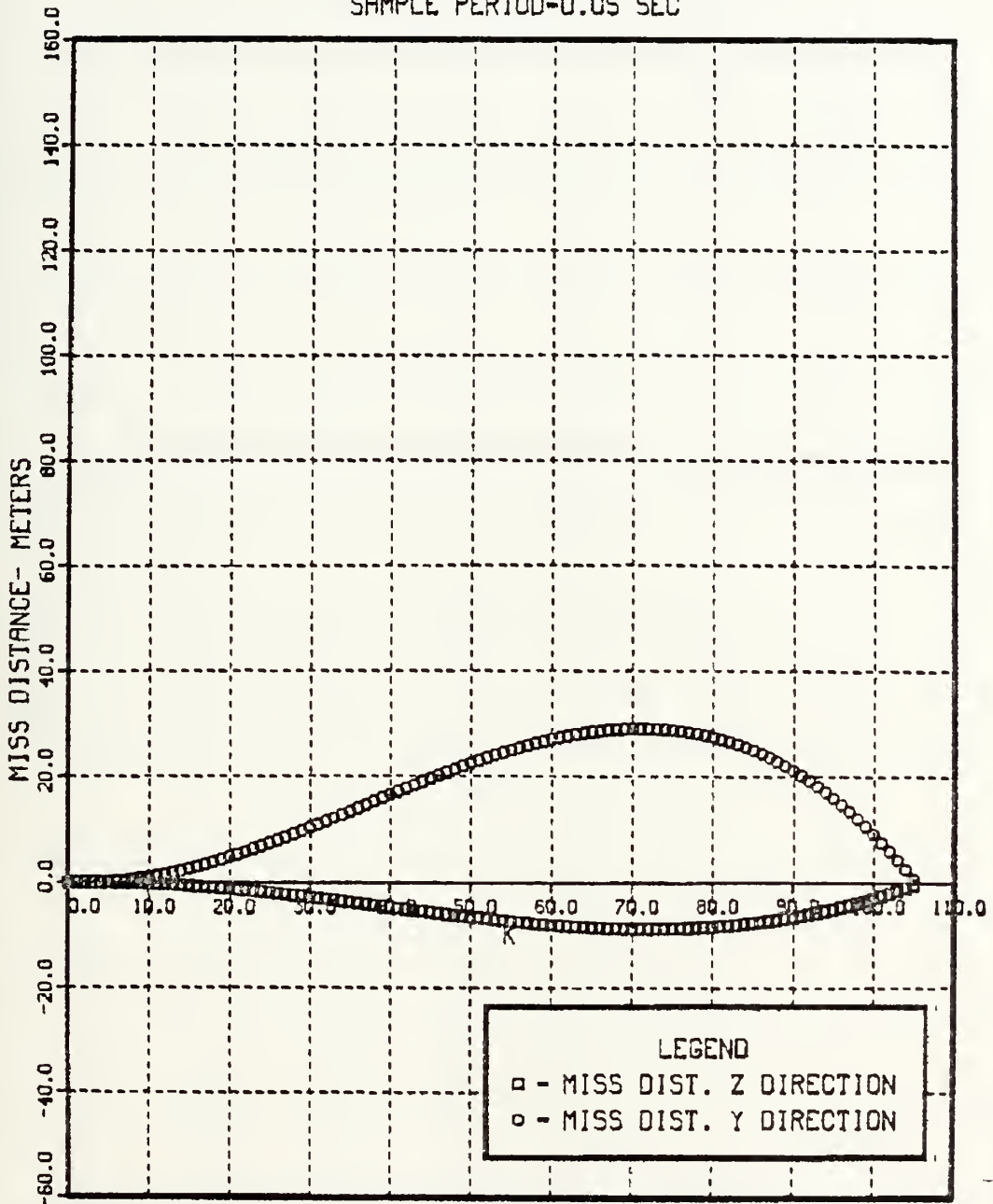


Figure 4.23 Miss Distance-Case 9.

9TH CASE
INITIAL TARGET ACCELERATION- -4. G
INITIAL TARGET POSITION--600 M
SAMPLE PERIOD-0.05 SEC

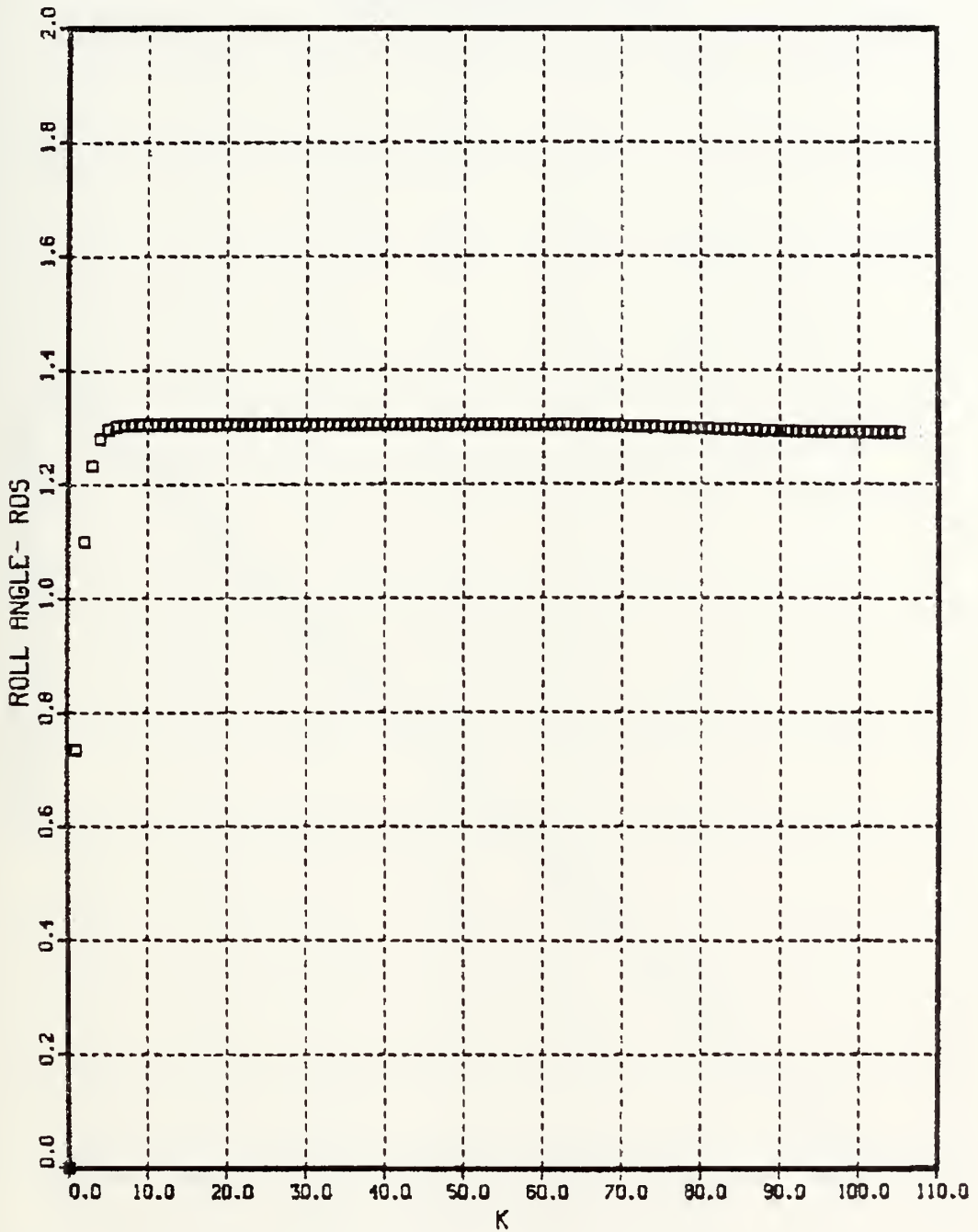


Figure 4.24 Roll Angle-Case 9.

10TH CASE
INITIAL TARGET ACCELERATION-- -4. G
INITIAL TARGET POSITION--600 M
SAMPLE PERIOD--0.05 SEC

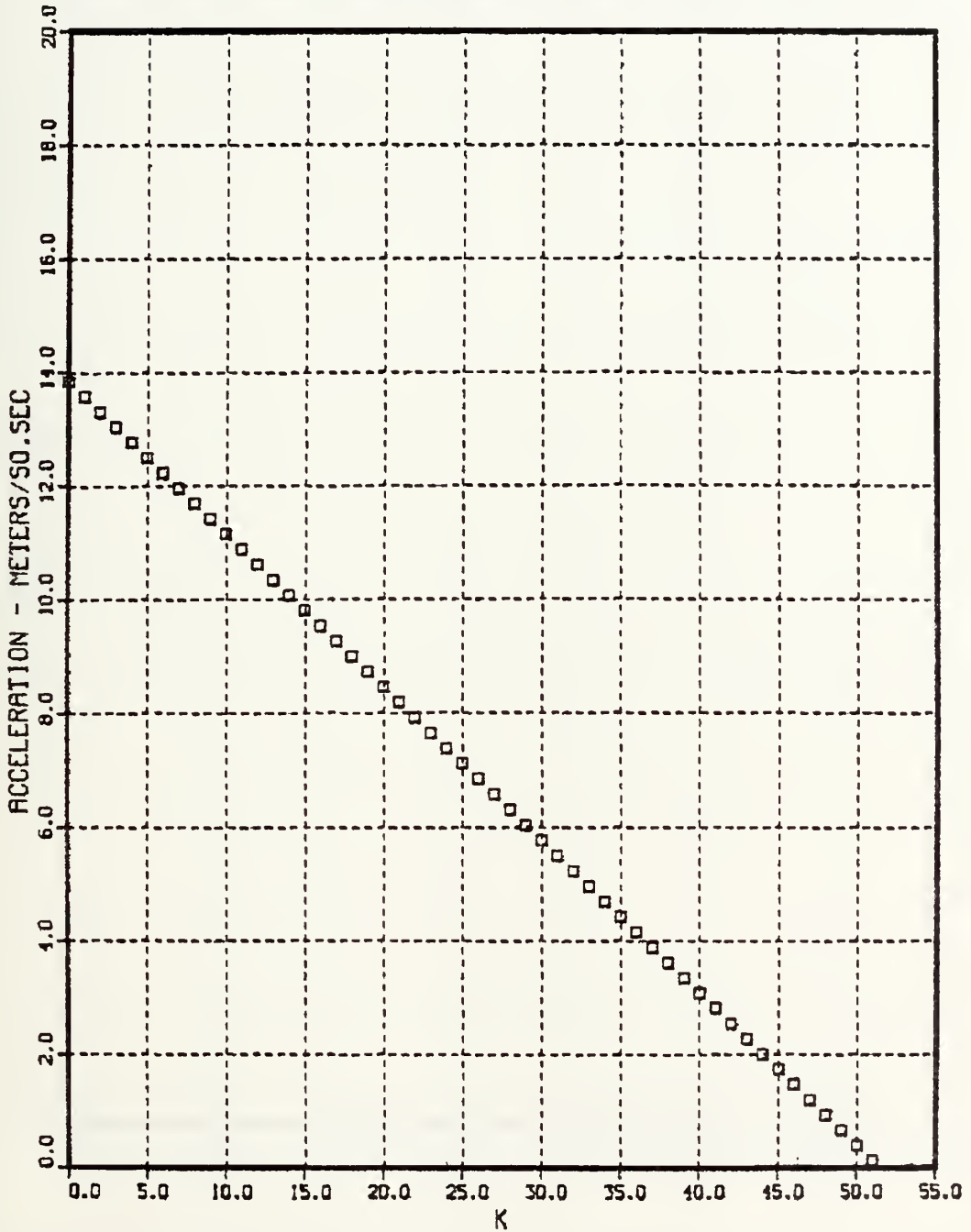


Figure 4.25 Commanded Acceleration-Case 10.

10TH CASE
INITIAL TARGET ACCELERATION- -4. G
INITIAL TARGET POSITION--600 M
SAMPLE PERIOD-0.05 SEC

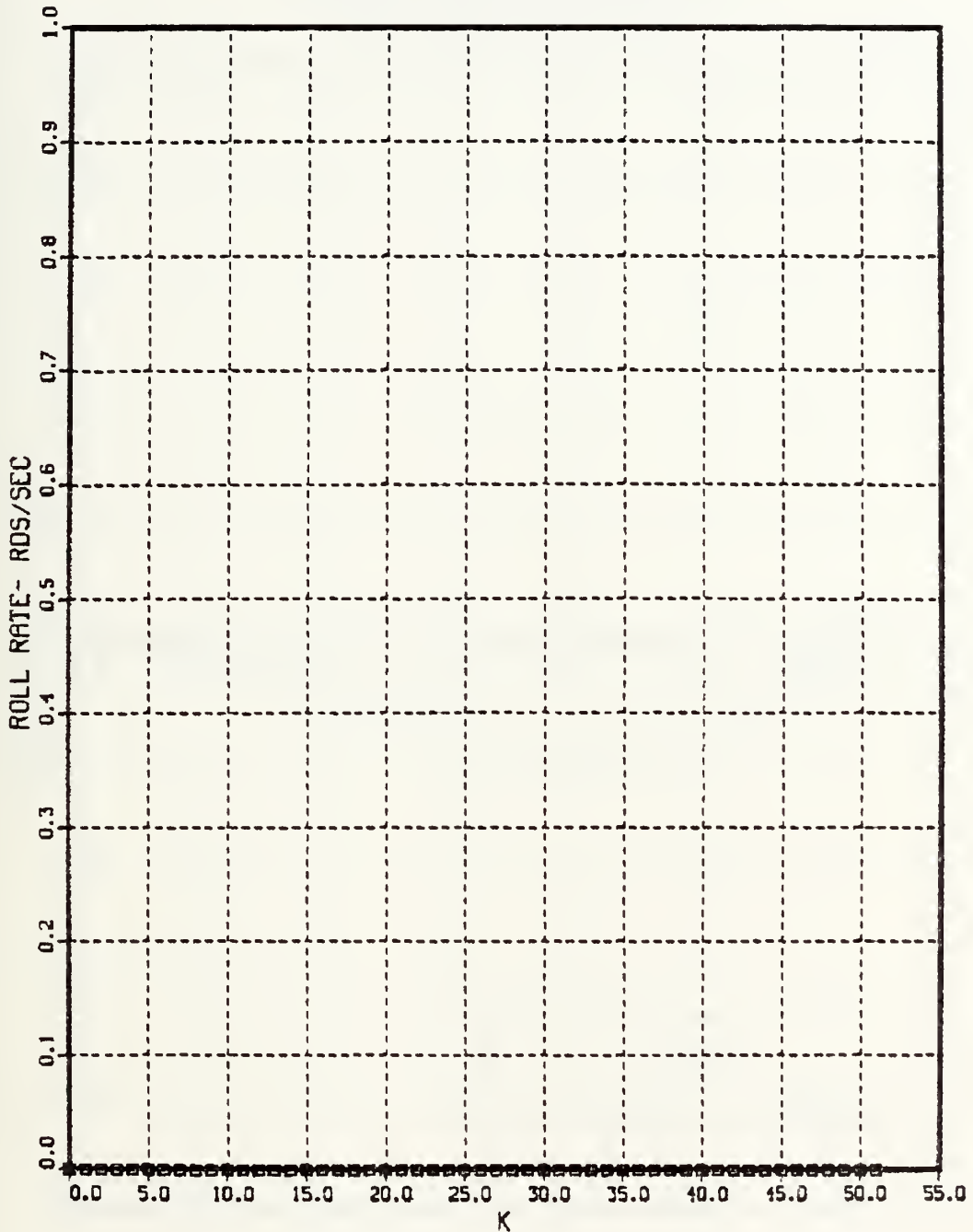


Figure 4.26 Commanded Roll Rate-Case 10.

10TH CASE
 INITIAL TARGET ACCELERATION- -4. G
 INITIAL TARGET POSITION--600 M
 SAMPLE PERIOD-0.05 SEC

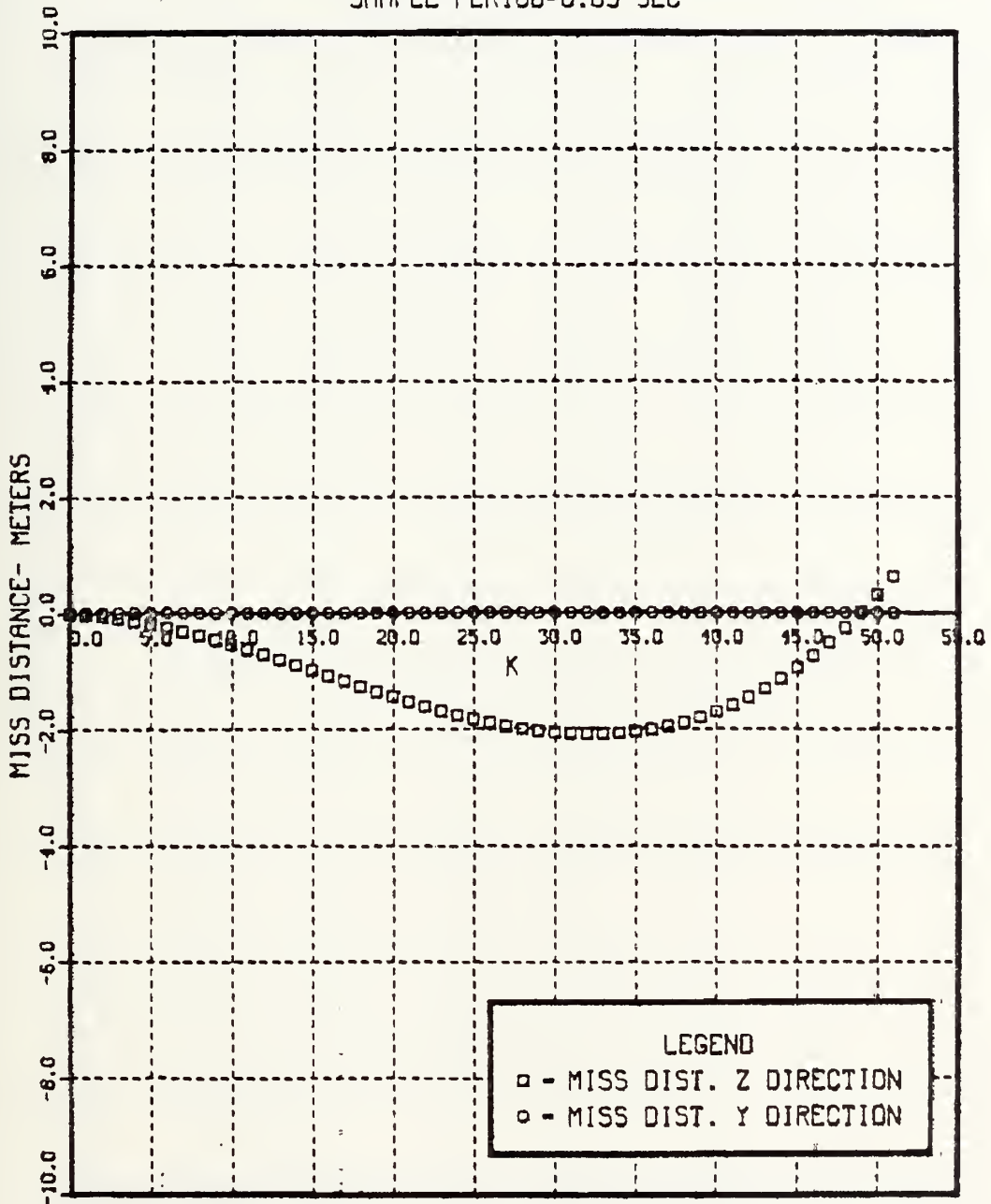


Figure 4.27 Miss Distance-Case 10.

10TH CASE
INITIAL TARGET ACCELERATION-- -4. G
INITIAL TARGET POSITION--600 M
SAMPLE PERIOD-0.05 SEC

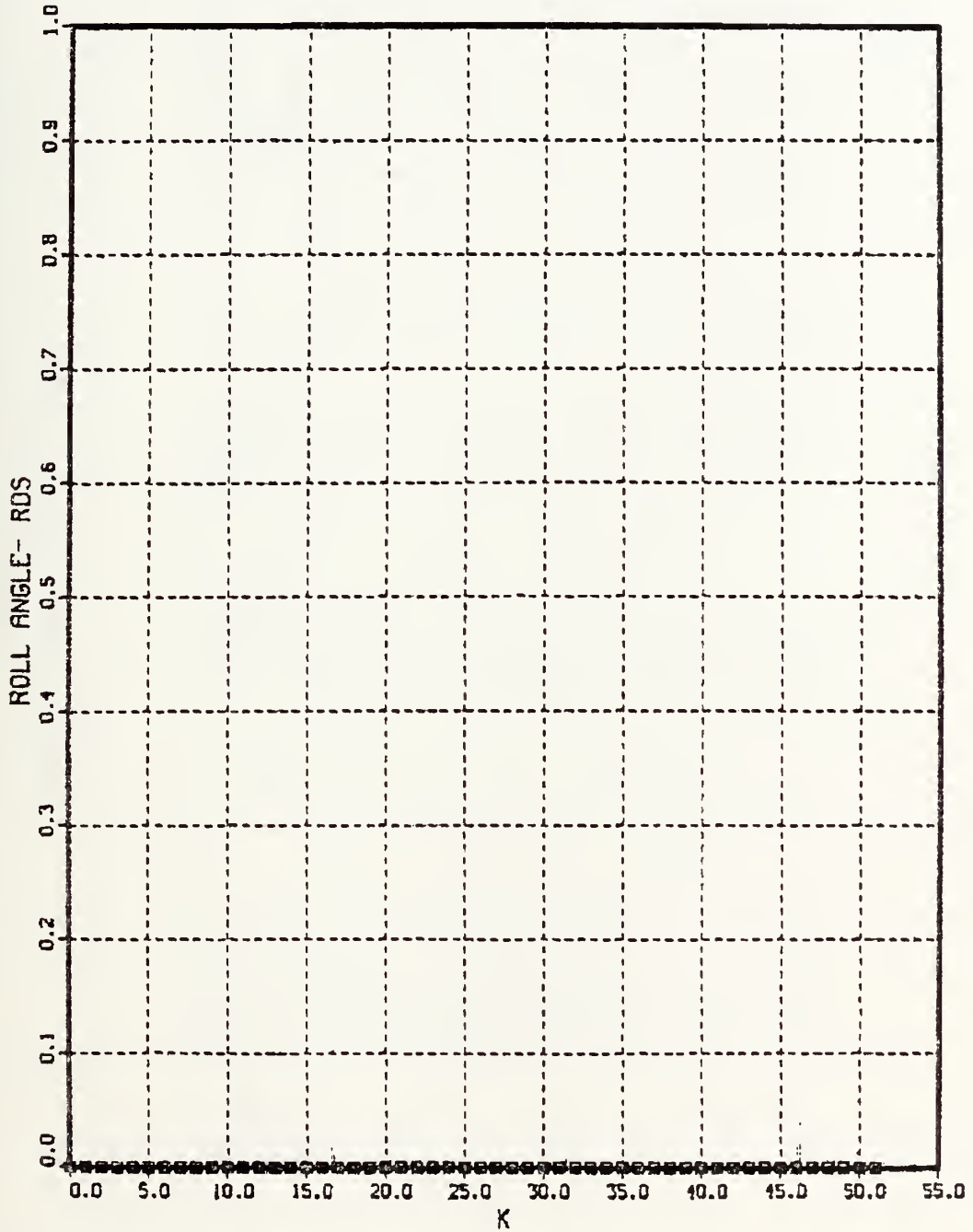


Figure 4.28 Roll Angle-Case 10.

TABLE IV
Results Using Pitch Angle

case	t	AC (m/sec)	PC (rad/sec)	miss distance Y direction (m)	miss distance Z direction (m)	(rad)	CG-to-CG miss distance (m)
8	0	82.13	14.71	0.0	-600	0.0	600
	π	.466	0.0	-1.17	.188	.562	2.17
9	0	14.16	14.71	0.0	-600	0.0	600
	π	.268	0.0	-1.12	.176	1.29	1.249
10	0	13.83	0.0	0.0	-600	0.0	600
	π	.135	0.0	0.0	.307	0.0	.307

11ST CASE
INITIAL TARGET ACCELERATION- -1. G
INITIAL TARGET POSITION-100 M
SAMPLE PERIOD-0.05 SEC

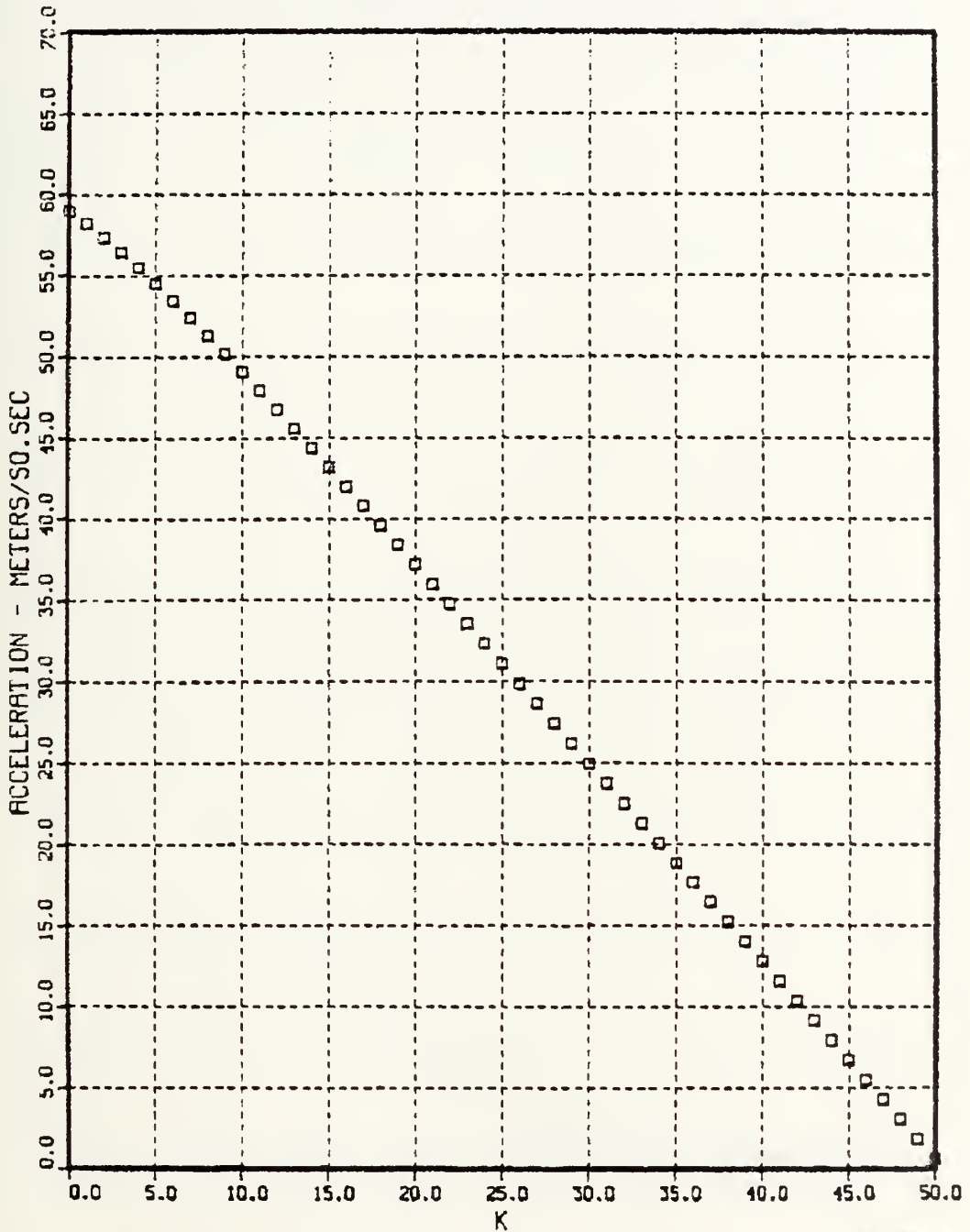


Figure 4.29 Commanded Acceleration-Case 11.

11ST CASE
INITIAL TARGET ACCELERATION- -1. G
INITIAL TARGET POSITION-100 M
SAMPLE PERIOD-0.05 SEC

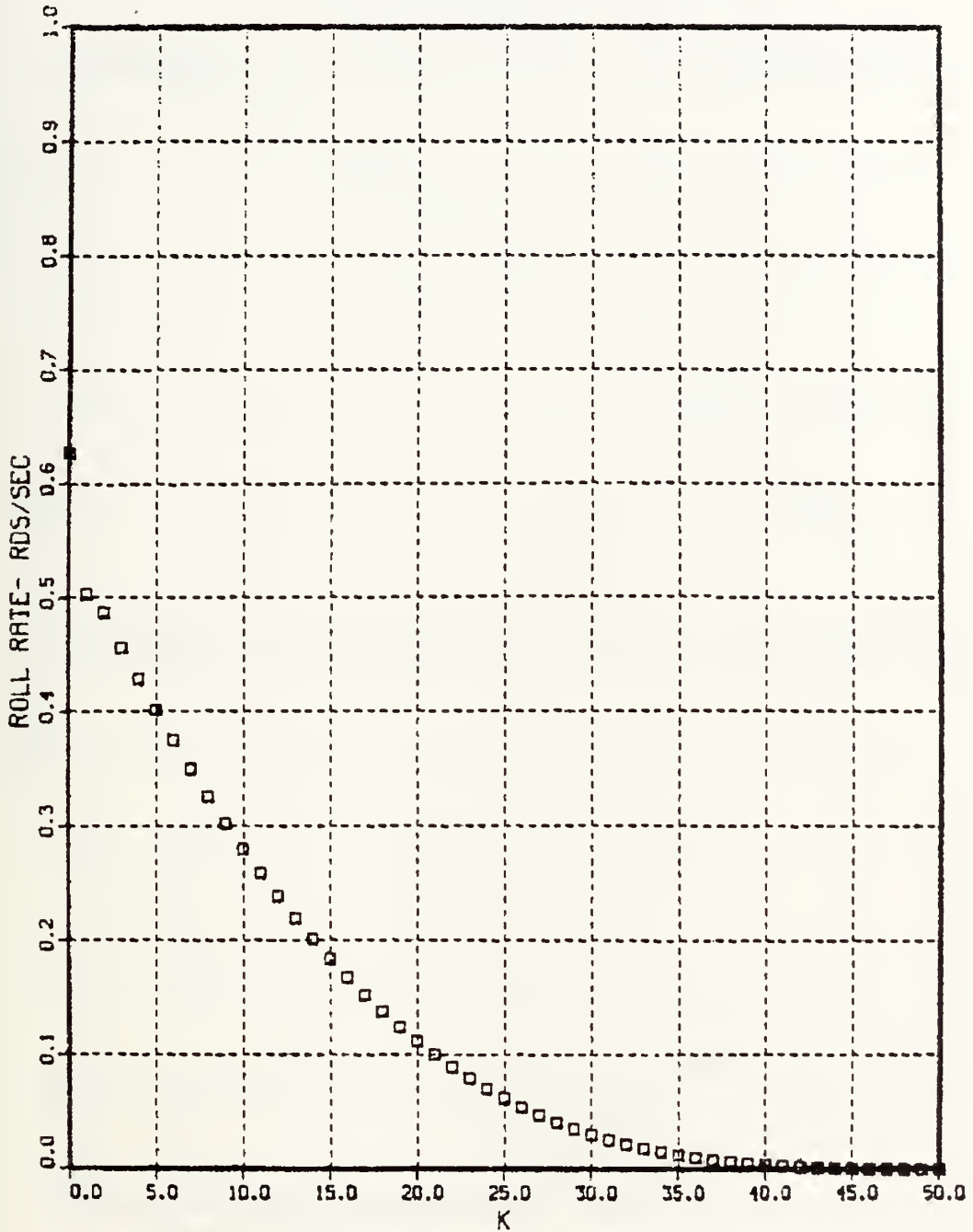


Figure 4.30 Commanded Roll Rate-Case 11.

11ST CASE
INITIAL TARGET ACCELERATION- -1. G
INITIAL TARGET POSITION-100 M
SAMPLE PERIOD-0.05 SEC

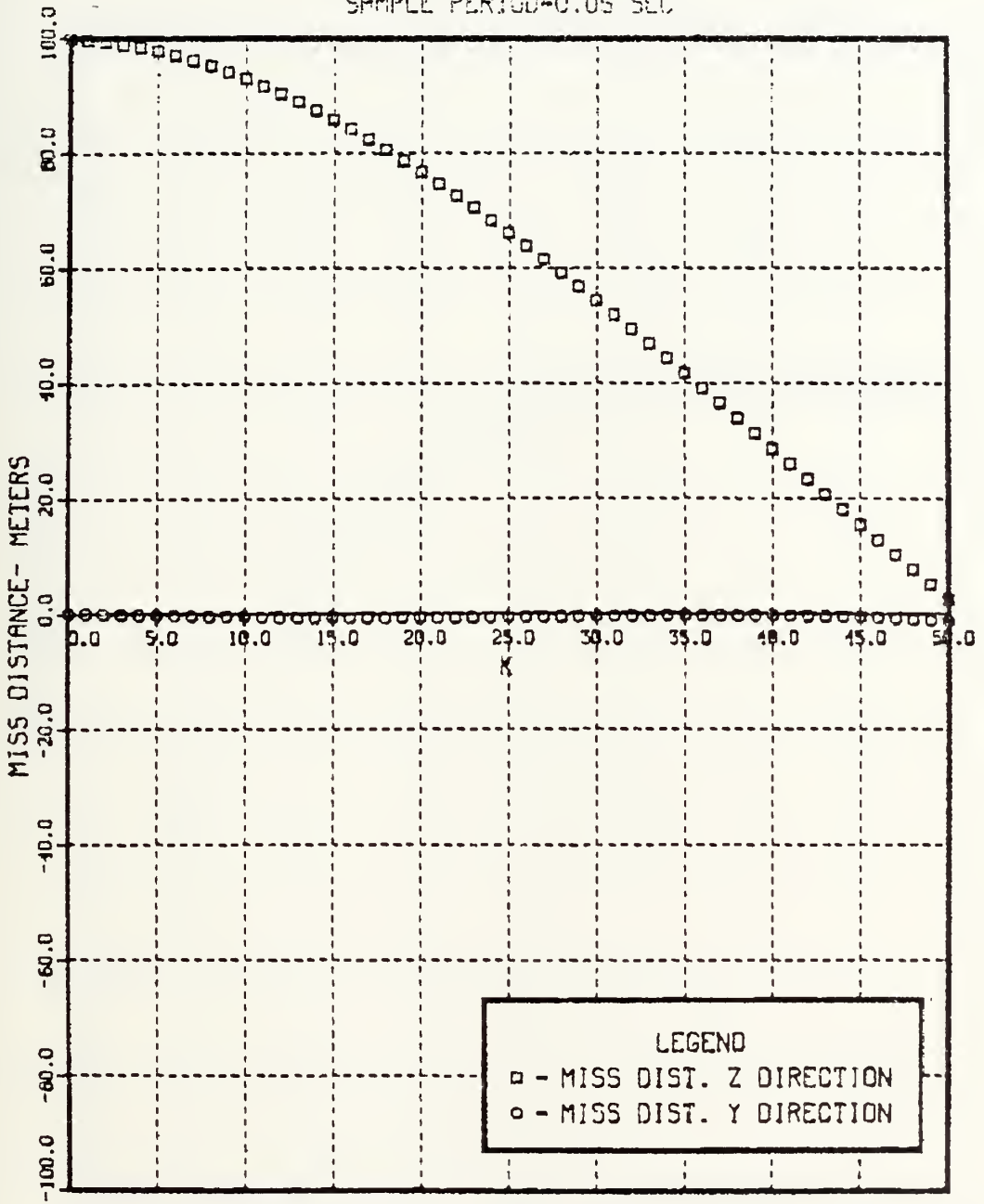


Figure 4.31 Miss Distance-Case 11.

11ST CASE
INITIAL TARGET ACCELERATION- -1. G
INITIAL TARGET POSITION-100 M
SAMPLE PERIOD-0.05 SEC

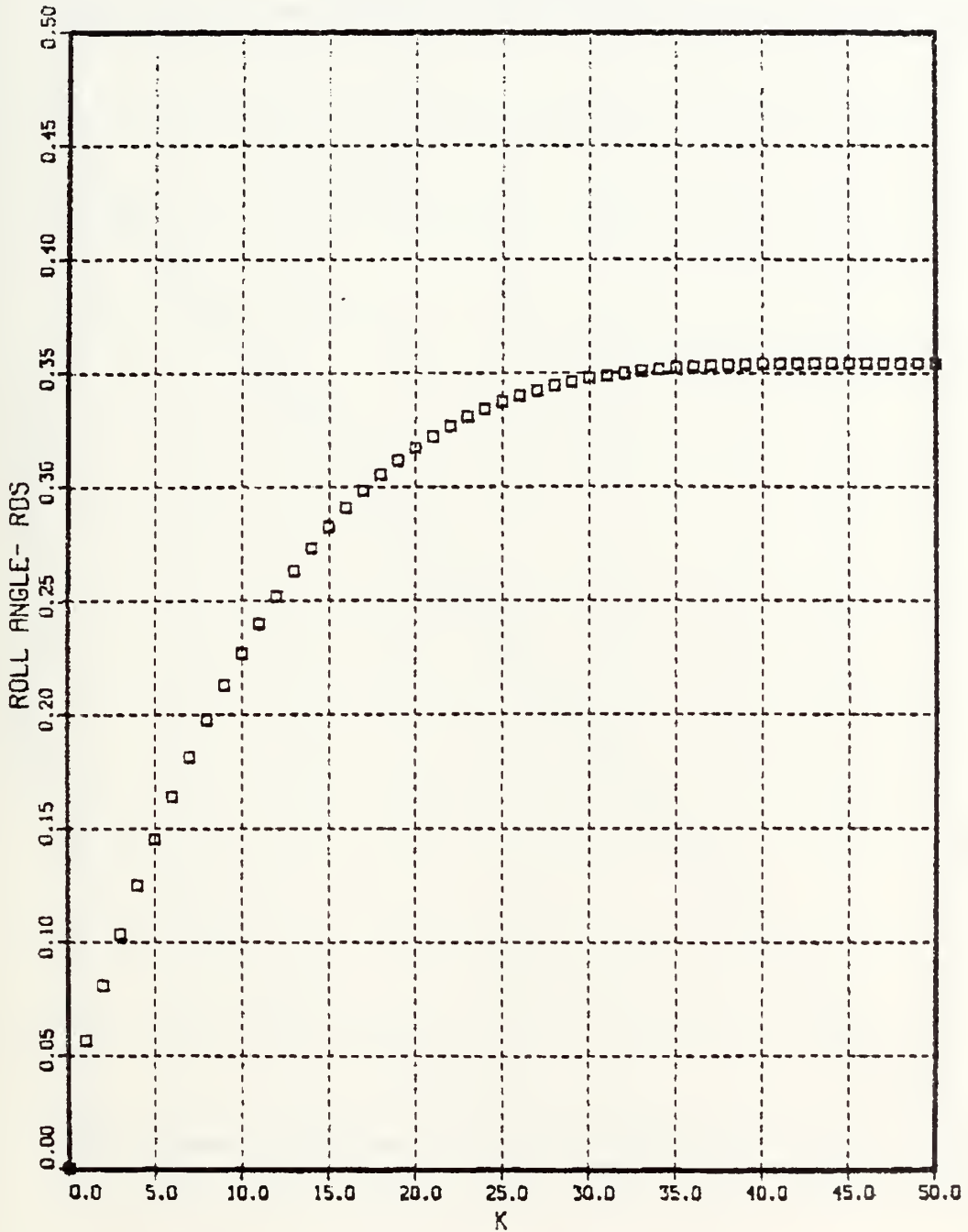


Figure 4.32 Roll Angle-Case 11.

12TH CASE
INITIAL TARGET ACCELERATION- -1. G
INITIAL TARGET POSITION-200 M
SAMPLE PERIOD-0.05 SEC

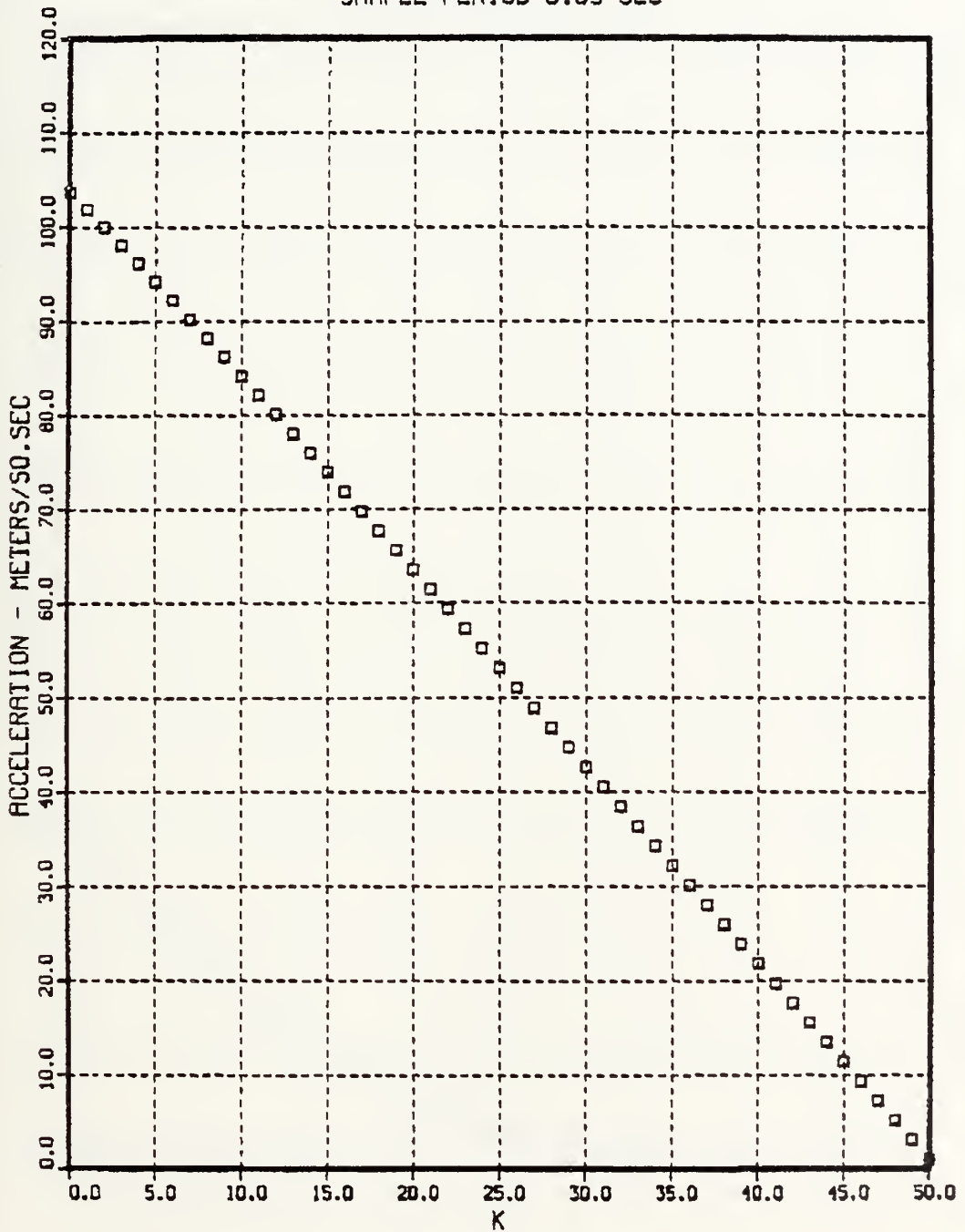


Figure 4.33 Commanded Acceleration-Case 12.

12TH CASE
INITIAL TARGET ACCELERATION- -1. G
INITIAL TARGET POSITION-200 M
SAMPLE PERIOD-0.05 SEC

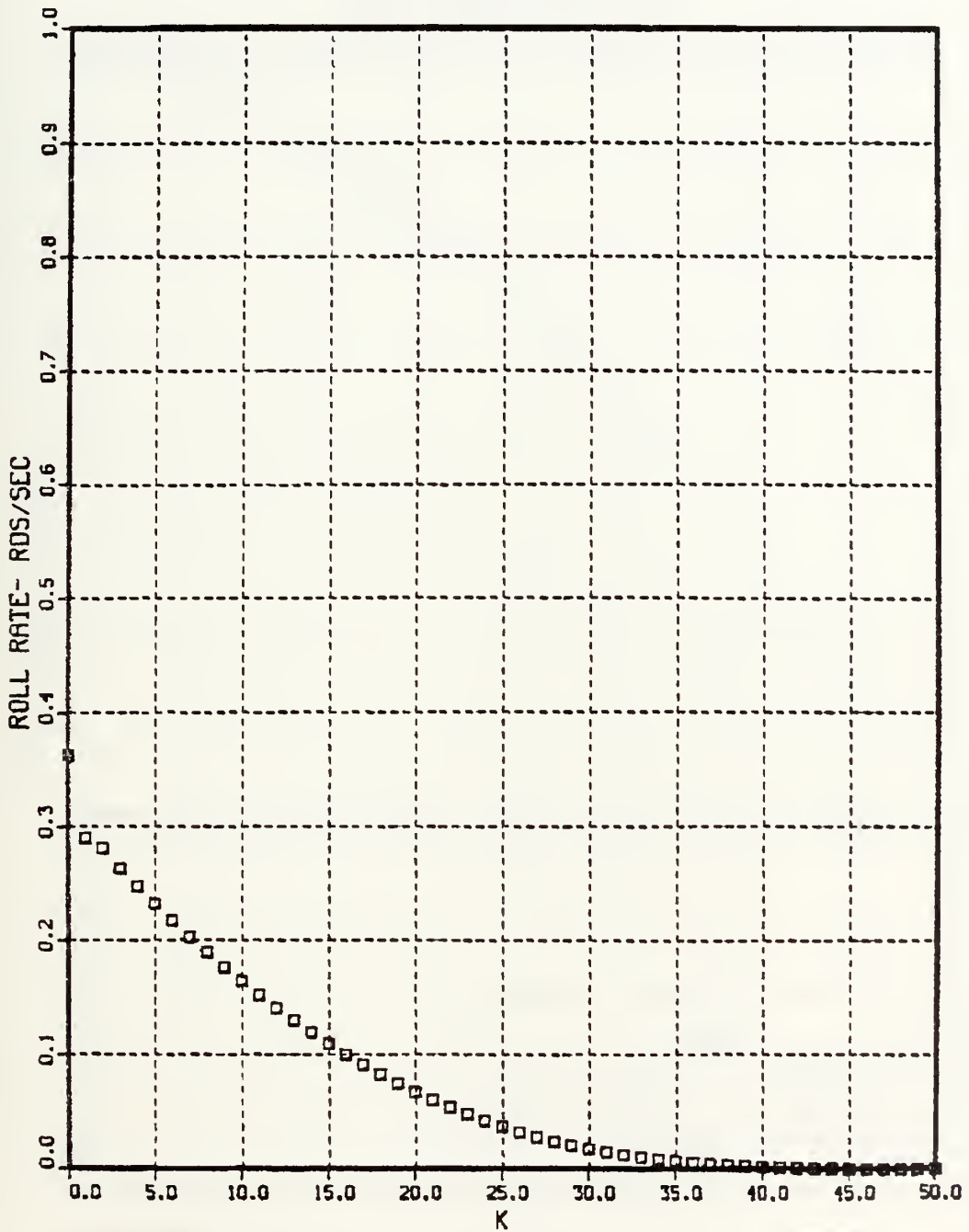


Figure 4.34 Commanded Roll Rate-Case 12.

12TH CASE
INITIAL TARGET ACCELERATION- -1. G
INITIAL TARGET POSITION-200 M
SAMPLE PERIOD-0.05 SEC

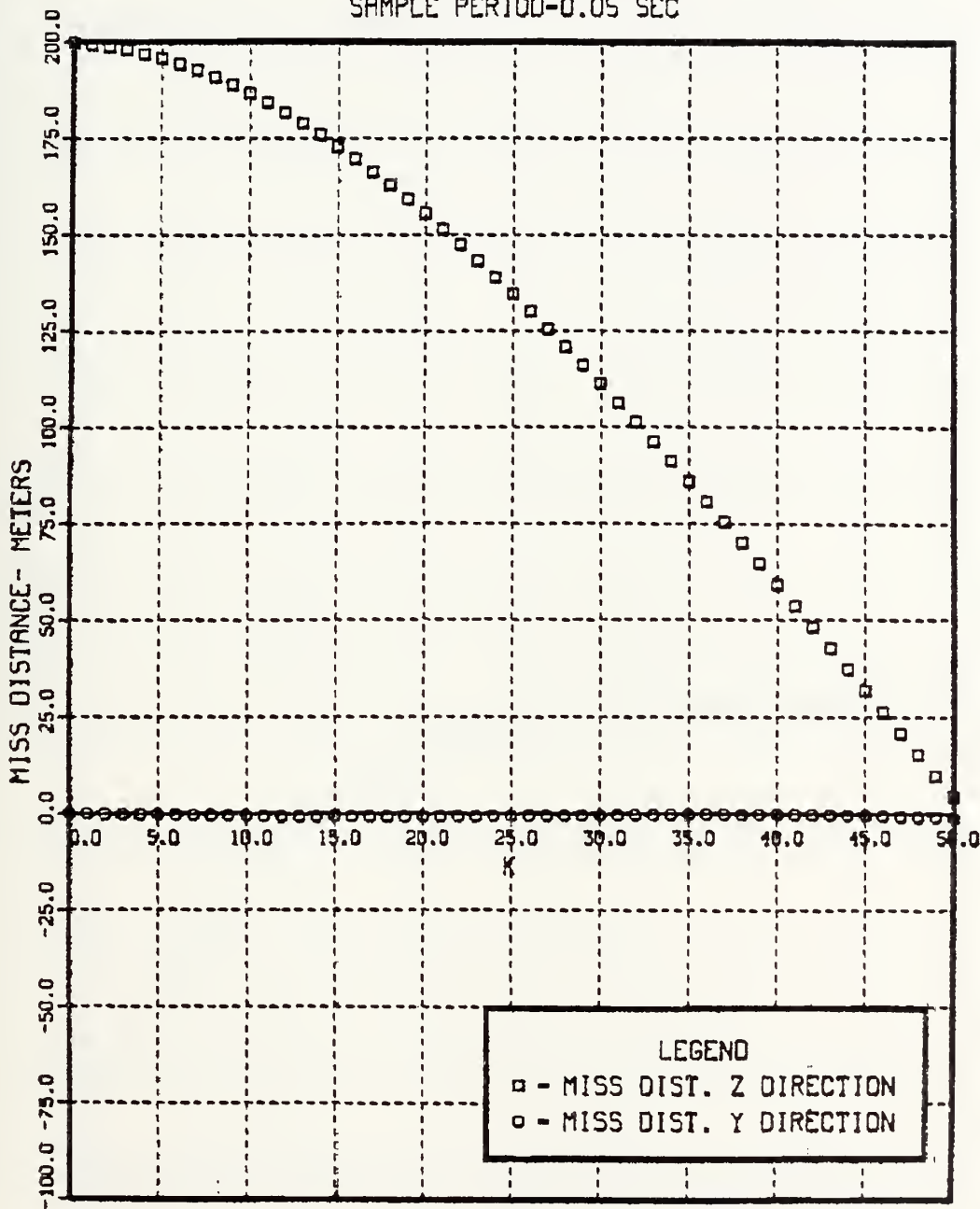


Figure 4.35 Miss Distance-Case 12.

12TH CASE
INITIAL TARGET ACCELERATION- -1. G
INITIAL TARGET POSITION-200 M
SAMPLE PERIOD-0.05 SEC

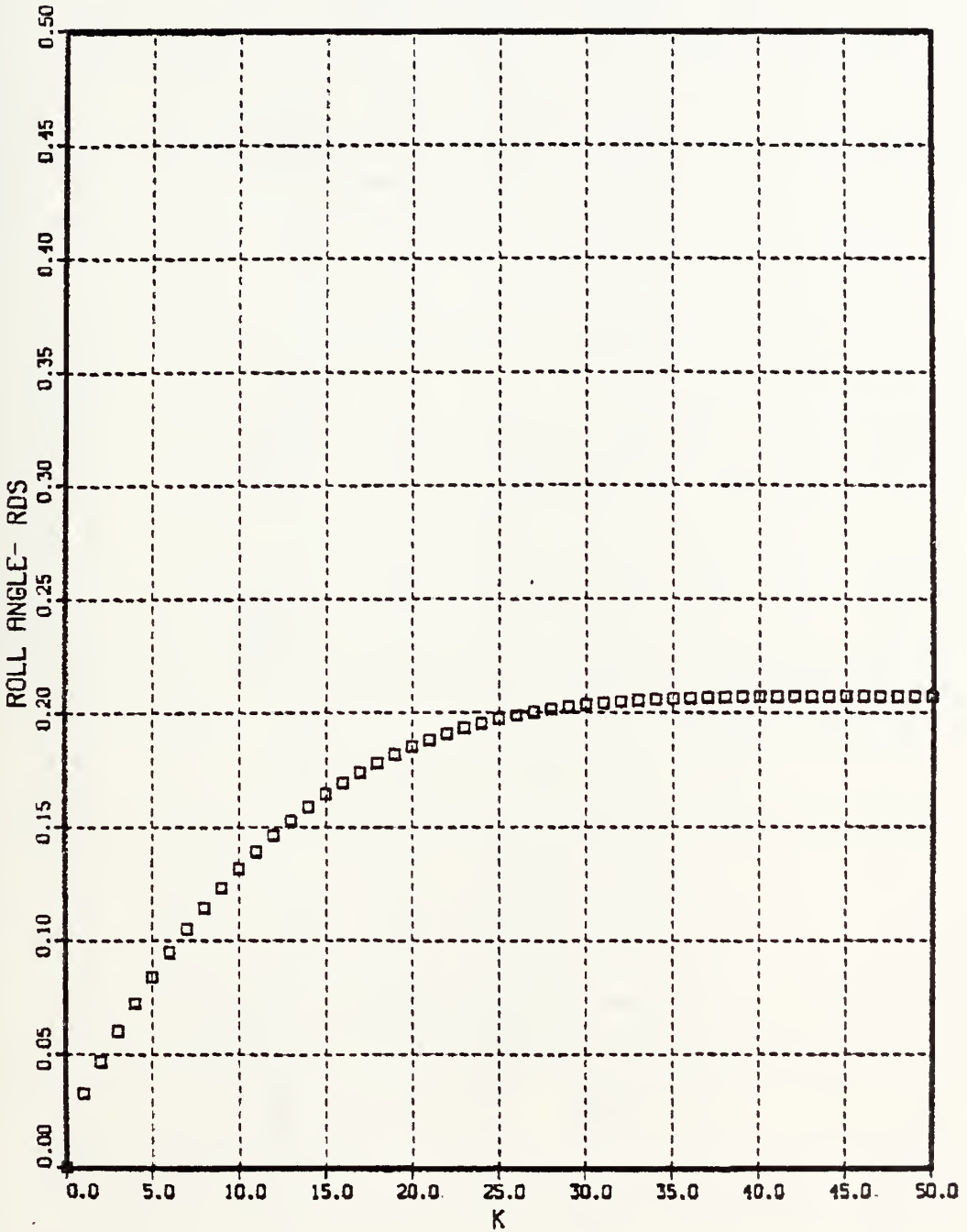


Figure 4.36 Roll Angle-Case 12.

TABLE V
Effect of Time to Intercept

Case	t	AC (m/sec)	PC (rad/sec)	miss distance y direction (m)	miss distance z direction (m)	(rad)	CG-to-CG miss distance (m)
11	0	59.01	.627	0.0	100.	0.0	100.
	11	.608	0.0	-1.31	2.53	.354	2.85
12	0	103.78	.363	0.0	200.	0.0	200.
	11	1.04	0.0	-1.01	4.69	.207	4.82

V. FINAL CONCLUSIONS AND COMMENTS

The scope of the present work was the development of an optimal digital control to be applied on a bank-to turn missile.

A two dimensional model, as suggested in reference 1, was adopted. After the digitalization of the continuous model it was necessary to solve a modified Ricatti equation since in the state equation there was a third term representing the gravity's effect. The approach that has been adopted is new, and although good results were obtained for the scenarios considered in this work, it is necessary that the algorithm be further tested and evaluated in similar problems due to its novelty.

The optimal was solved with an initial restriction to small angles. This condition was later relaxed so that large roll angles could be analyzed.

It is difficult to compare the present work with previous results since Stallard has indicated a mistake in his original paper, and further works in this area was not found.

However some comparison with Stallard work is possible. The commanded acceleration of the missile are such as to correct the ZEM at each point, this agrees with that reference. There is a proportional relationship between the commanded roll rate and the commanded acceleration, and the commanded roll rate is proportional to the defined ϕ_{ideal} at each point, which again agrees with reference 1.

The algorithm developed in this work requires extensive computation at each step, and is clear that some software optimization will be needed. The motivation for considering the constant steady-state gain due to gravity was to decrease this computational burden. This approach however resulted in unacceptable miss distance.

Another point of investigation that could reflect on the period available to the computer to perform its calculations was a change in the sample rate. Two different sample rates were investigated, both lead to larger errors than the nominal period of .05 seconds. A detailed study on this issue is left as suggestion for future works, since some optimal value of the sampling rate is clearly indicated.

It is important to keep in mind that the model adopted is two dimensional, while the actual problem is three dimensional, thus some brief studies were conducted in order to check the region of validity of the 2-D.

In the analysis of the pitch angle, one can see that is necessary to have small variations in pitch in order to approximate it as a constant. However, at the moment that this angle is different from zero, as explained in chapter 4, it is possible to have in the flight path reference frame a target maneuver in the Z direction that will lead to large acceleration commands, leading the missile to large miss distances, when considering a movable target. When the present system was tested against fixed targets, the results were quite good, this suggests the application of the model in air-to-surface missiles.

Further investigation were made on the effect of time-to-go. As expected, decreased time to go, results in increased miss distance. A detailed analysis of more complex scenarios is needed in order to properly define the effect of time to go.

Also, it would be interesting to extend the model to three dimensions and include the effects of lags on the system in future works. Finally, in appendix A, the computer model used in this work is enclosed. Some improvements in this program can be done, mainly in the data introduction, and in some optimization of the running time.

APPENDIX A
FORTRAN PROGRAM

These appendix provides a listing of the computer program used in the present study.

Since the routines used are non-IMSL, and a small change to double-precision was necessary, they are also being provided.

TESO0970
 TESO0980
 TESO0990
 TESO1000
 TESO1010
 TESO1020
 TESO1030
 TESO1040
 TESO1050
 TESO1060
 TESO1070
 TESO1080
 TESO1090
 TESO1100
 TESO1110
 TESO1120
 TESO1130
 TESO1140
 TESO1150
 TESO1160
 TESO1170
 TESO1180
 TESO1190
 TESO1200
 TESO1210
 TESO1220
 TESO1230
 TESO1240
 TESO1250
 TESO1260
 TESO1270
 TESO1280
 TESO1290
 TESO1300
 TESO1310
 TESO1320
 TESO1330
 TESO1340
 TESO1350
 TESO1360
 TESO1370
 TESO1380
 TESO1390
 TESO1400
 TESO1410
 TESO1420
 TESO1430
 TESO1440

```

C COSTET=1.0
C DELPHO=C.0
C INITIALIZATION OF STATE VECTOR X(K)
C X(1,1)=Y0
C X(2,1)=VY0
C X(3,1)=ATY0
C X(4,1)=ZC
C X(5,1)=VZO
C X(6,1)=ATZO
C X(7,1)=DELPHO
C
C *****
C DC 6 I=1,7
C X(I,1)=X(I,1)
C CCNT INUE
C
C DC 7 I=1,7
C X(I,1)=XS(I,1,K)
C CCNT INUE
C
C PHIO=PHI
C L=101
C CCOUNT=CCOUNT+1
C
C DO 19 N=K,L
C K1=N-1
C
C DC 9 I=1,7
C DU 8 J=1,7
C A(I,J)=0.
C CONTINUE
C CCNT INUE
C TAU=20.5C
C DELT=.05C
C E=2.718
C ACO=26.7
C TI=5.0-K1*T
C COSTET=1.0
C A(1,1)=1.
C A(1,2)=DELT
C A(2,2)=1.
C A(4,4)=1.
C A(5,5)=1.

```


TES01450
 TES01460
 TES01470
 TES01480
 TES01490
 TES01500
 TES01510
 TES01520
 TES01530
 TES01540
 TES01550
 TES01560
 TES01570
 TES01580
 TES01590
 TES01600
 TES01610
 TES01620
 TES01630
 TES01640
 TES01650
 TES01660
 TES01670
 TES01680
 TES01690
 TES01700
 TES01710
 TES01720
 TES01730
 TES01740
 TES01750
 TES01760
 TES01770
 TES01780
 TES01790
 TES01800
 TES01810
 TES01820
 TES01830
 TES01840
 TES01850
 TES01860
 TES01870
 TES01880
 TES01890
 TES01900
 TES01910
 TES01920

```

A(7,7)=1.
A(3,3)=DEXP(-1.*DELT/TAU)
A(6,6)=DEXP(-1.*DELT/TAU)
A(4,5)=DELT
A(1,3)=TAU*DELT-TAU**2*(1.-DEXP(-DELT/TAU))
A(4,6)=A(1,3)
A(2,3)=TAU*(1.-DEXP(-DELT/TAU))
A(5,6)=A(2,3)
A(1,7)=ACO*DCOS(PHIO)*(DELT**2-((2*K1+1.)/(2*TI))*DELT)*DELT*
A(2,7)=ACO*DCOS(PHIO)*(DELT-((2*K1+1.)/(2*TI))*DELT)**2)
A(4,7)=ACO*DSIN(PHIO)*(DELT**2-((2*K1+1.)/(2*TI))*DELT*
A(5,7)=ACO*DSIN(PHIO)*(DELT-((2*K1+1.)/(2*TI))*DELT)**2)
DO 11 I=1,7
DO 10 J=1,7
A3(I,J,N)=A(I,J)
CONTINUE
1C
11 CONTINUE
CALL GMTRA(A,A,T,7,7)
INITIALIZE MATRIX B
B12V=DELT**3/2.-((2.*K1+1.)/(4.*TI))*DELT**4
B22V=DELT**2/2.-((K1*DELT+DELT)**3/(3.*TI))
1+((K1*DELT+DELT)**2)*K1*DELT/(2.*TI)-((K1*DELT)**3)/(6.*TI)
B(1,1)=DSIN(PHIO)*DELT**2/2;
B(1,2)=ACO*DCOS(PHIO)*(B12V)
B(2,1)=DELT*DSIN(PHIO)
B(2,2)=ACO*DCOS(PHIO)*(B22V)
B(3,1)=0.
B(3,2)=C.
B(4,1)=-CCOS(PHIO)*DELT**2/2.
B(4,2)=ACO*DSIN(PHIO)*(B12V)
B(5,1)=-DELT*DCOS(PHIO)
B(5,2)=ACO*DSIN(PHIO)*(B22V)
B(6,1)=C.
B(6,2)=C.
B(7,1)=C.
B(7,2)=DELT
DO 13 I=1,7
DO 12 J=1,2
B3(I,J,N)=B(I,J)
CONTINUE
1C
12 CONTINUE
  
```


TESO1930
 TESO1940
 TESO1950
 TESO1960
 TESO1970
 TESO1980
 TESO1990
 TESO2000
 TESO2010
 TESO2020
 TESO2030
 TESO2040
 TESO2050
 TESO2060
 TESO2070
 TESO2080
 TESO2090
 TESO2100
 TESO2110
 TESO2120
 TESO2130
 TESO2140
 TESO2150
 TESO2160
 TESO2170
 TESO2180
 TESO2190
 TESO2200
 TESO2210
 TESO2220
 TESO2230
 TESO2240
 TESO2250
 TESO2260
 TESO2270
 TESO2280
 TESO2290
 TESO2300
 TESO2310
 TESO2320
 TESO2330
 TESO2340
 TESO2350
 TESO2360
 TESO2370
 TESO2380
 TESO2390
 TESO2400

```

12 CONTINUE
   CALL GMTRA(B,BT,7,2)
   DO 15 I=1,7
     DO 14 J=1,7
       AT3(I,J,N)=AT(I,J)
     CONTINUE
   CONTINUE
14 CONTINUE
15 CONTINUE
   DO 17 I=1,2
     DO 16 J=1,7
       BT3(I,J,N)=BT(I,J)
     CONTINUE
   CONTINUE
16 CONTINUE
17 INITIALIZE MATRIX E
   C
   C
   DO 18 I=1,7
     EI(I,1)=0.
   CONTINUE
   EI(4,1)=-DELT*2/2.*COSTET
   EI(5,1)=-DELT*COSTET
   CONTINUE
18 CONTINUE
19 INITIALIZE MATRIX Q
   C
   C
   Q(1,1)=.C0578
   Q(1,2)=C.
   Q(2,1)=C.
   Q(2,2)=5.
   C
   C
   C INITIALIZE MATRIX P
   C
   C
   DC 21 I=1,7
   DO 20 J=1,7
     P(I,J)=0.
   CONTINUE
20 CONTINUE
21 CONTINUE
   C
   C
   C *****
   C SCLUTION OF RICATTI EQUATION *
   C *****
   C *****
   M=101
   DC 22 IF(M.LT.1.)GO TO 31
   DO 24 I=1,7
     DO 23 J=1,7
       A(I,J)=A3(I,J,M)
       AT(I,J)=AT3(I,J,M)
     CONTINUE
   CONTINUE
23 CONTINUE
24 CCNTINUE
  
```



```

DO 26 I=1,7
DO 25 J=1,2
      B(I,J)=B3(I,J,M)
25 CONTINUE
26 CCNTINUE
DO 28 I=1,2
DO 27 J=1,7
      BT(I,J)=BT3(I,J,M)
27 CONTINUE
28 CCNTINUE
      CALL GMADD(P,S,PS,7,7)
      CALL GMPRD(BT,PS,BT,PS,2,7,7)
      CALL GMPRD(BT,PS,B,BT,PSB,2,7,2)
      CALL GMPRD(BT,PS,EI,BTSE,2,7,1)
      CALL GMPRD(BT,SG,BTSG,2,7,1)
      CALL GMALD(BT,SE,BTSEG,2,1)
      CALL GMALD(Q,BT,PSB,R,2,2)
      CALL GAUSS3(2,EPS,R,RINV,KER,2)
C
      CALL GMPRD(BT,PS,A,BT,PSA,2,7,7)
      CALL GMPRD(RINV,BT,PSA,F,2,2,7)
C
      CALL GMPRD(RINV,BTSEG,FG,2,2,1)
DO 30 I=1,2
DO 29 J=1,7
      F3(I,J,M)=F(I,J)
29 CONTINUE
30 CCNTINUE
C *****
C *****
      CALL GMFFD(B,F,BF,7,2,7)
      CALL GMSSUB(A,BF,ABF,7,7)
      CALL GMPRD(AT,PS,AT,PS,7,7,7)
C *****
      CALL GMPRD(B,FG,BFG,7,2,1)
      CALL GMSSUB(EI,BFG,EBFG,7,1)
      CALL GMPRD(AT,PS,EBFG,GS,7,7,1)
      CALL GMPRD(AT,SG,ATSG,7,7,1)
      CALL GMALD(GS,ATSG,SG,7,1)
C
      CALL GMPRD(AT,PS,ABF,S,7,7,7)
      WRITE(6,81)COUNT
      M=M-1
      GC TO 22
      31 CCNTINUE
C
      DEFINITION OF THE MATRIX G

```

```

TESO2410
TESO2420
TESO2430
TESO2440
TESO2450
TESO2460
TESO2470
TESO2480
TESO2490
TESO2500
TESO2510
TESO2520
TESO2530
TESO2540
TESO2550
TESO2560
TESO2570
TESO2580
TESO2590
TESO2600
TESO2610
TESO2620
TESO2630
TESO2640
TESO2650
TESO2660
TESO2670
TESO2680
TESO2690
TESO2700
TESO2710
TESO2720
TESO2730
TESO2740
TESO2750
TESO2760
TESO2770
TESO2780
TESO2790
TESO2800
TESO2810
TESO2820
TESO2830
TESO2840
TESO2850
TESO2860
TESO2870
TESO2880

```



```

C      G(1,1)=-9.8
C
C      X(K+1)=(A-EF)X(K)+EG(K)
C
C      K=CCOUNT+1
C      KP(K)=K-1
C      KN=K-1
C      32 IF(KN.EQ.K)GO TO 42
C
C      CC 34 I=1,2
C      FG(I,1)=FG3(I,1,KN+1)
C      DO 33 J=1,7
C      F(I,J)=F3(I,J,KN+1)
C      33 CONTINUE
C      34 CONTINUE
C *****
C      CALL GMPRC(F,X,UN,2,7,1)
C      CALL GMPRC(FG,G,UGN,2,1,1)
C      DO 35 I=1,2
C      U1(I,1)=-1.*UN(I,1)
C      UG(I,1)=-1.*UGN(I,1)
C      35 CONTINUE
C      UG(1,1)=14.70
C      UG(2,1)=0.0
C      35 CONTINUE
C      CALL GMADD(U1,UG,U,2,1)
C      DO 37 I=1,7
C      DO 26 J=1,7
C      AT(I,J)=AT3(I,J,KN+1)
C      A(I,J)=A3(I,J,KN+1)
C      36 CONTINUE
C      37 CONTINUE
C
C      DO 39 I=1,7
C      DO 28 J=1,2
C      B(I,J)=B3(I,J,KN+1)
C      38 CONTINUE
C      39 CONTINUE
C      DO 41 I=1,2
C      FG(I,I)=FG3(I,1,KN+1)
C      DO 40 J=1,7
C      BT(I,J)=BT3(I,J,KN+1)
C      F(I,J)=F3(I,J,KN+1)
C      40 CONTINUE
C      41 CONTINUE

```


TESO3850
 TESO3860
 TESO3870
 TESO3880
 TESO3890
 TESO3900
 TESO3910
 TESO3920
 TESO3930
 TESO3940
 TESO3950
 TESO3960
 TESO3970
 TESO3980
 TESO3990
 TESO4000
 TESO4010
 TESO4020
 TESO4030
 TESO4040
 TESO4050
 TESO4060
 TESO4070
 TESO4080
 TESO4090
 TESO4100
 TESO4110
 TESO4120
 TESO4130
 TESO4140
 TESO4150
 TESO4160
 TESO4170
 TESO4180
 TESO4190
 TESO4200
 TESO4210
 TESO4220
 TESO4230
 TESO4240
 TESO4250
 TESO4260
 TESO4270
 TESO4280
 TESO4290
 TESO4300
 TESO4310
 TESO4320

```

A(4,5)=CELT
A(1,3)=TAU*DELT-TAU**2*(1.-DEXP(-DELT/TAU))
A(4,6)=A(1,3)
A(2,3)=TAU*(1.-DEXP(-DELT/TAU))
A(5,6)=A(2,3)
A(1,7)=ACOS(DCOS(PHIO))*DELT**2/2.
A(2,7)=ACOS(DCOS(PHIO))*DELT
A(4,7)=ACOS(DSIN(PHIO))*DELT**2/2.
A(5,7)=ACOS(DSIN(PHIO))*DELT
CONTINUE
INITIALIZE MATRIX B
B(1,1)=DSIN(PHIO)*DELT**2/2.
B(1,2)=ACOS(DCOS(PHIO))*DELT**3/6.
B(1,2)=C.0
B(2,1)=DELT*DSIN(PHIO)
B(2,2)=ACOS(DCOS(PHIO))*DELT**2/2.
B(3,1)=C.
B(3,2)=C.
B(4,1)=-CCOS(PHIO)*DELT**2/2.
B(4,2)=ACOS(DSIN(PHIO))*DELT**3/6.
B(4,2)=C.0
B(5,1)=-DELT*DCOS(PHIO)
B(5,2)=ACOS(DSIN(PHIO))*DELT**2/2.
B(6,1)=C.
B(6,2)=C.
B(7,1)=C.
B(7,2)=CELT
IF(K.EQ.1.)GO TO 46
GO TO 47
CONTINUE
PH(K)=PHIO
YS(K)=X(1,1)
ZS(K)=X(4,1)
CONTINUE
CALL GMPRD(A,X,AX,7,7,1)
CALL GMPRD(B,U,BU,7,2,1)
CALL GMPRD(EI,G1,EIG,7,1,1)
CALL GMADD(AX,BU,AXBU,7,1)
CALL GMADD(AXBL,EIG,AX,7,1)
PHIO=PHIC+X(7,1)
DO 48 I=1,7
  XS(I,1,K+1)=X(I,1)
CONTINUE
46
47
48
  
```



```

IF(K.GT.1.)GO TO 49
GO TO 50
CONTINUE
PH(K)=PHIO
YS(K)=X(1,1)
ZS(K)=X(4,1)
CONTINUE
ACC(K)=U(1,1)
PCD(K)=U(2,1)

C
C
C
COUNT=CCLNT+1
GO TO 1
CONTINUE
DO 3 K=1,101
AC(K)=SNGL(ACD(K))
PC(K)=SNGL(PCD(K))
YM(K)=SNGL(YM(K))
ZM(K)=SNGL(ZS(K))
KPS(K)=SNGL(KP(K))
DPH(K)=SNGL(PH(K))
CGS(K)=SNGL(YM(K)**2+ZM(K)**2)
CONTINUE

WRITE(6,25)
WRITE(6,30)
WRITE(6,31)
WRITE(6,31)
WRITE(6,31)
WRITE(6,35)
WRITE(6,35)
*****
C INVOKE DISSPLA PACKAGE
*****
CALL HWKOT('MOVIE')
CALL AREA2C(7.0,9.0)
CALL XNAME('K$',100)
CALL YNAME('MISS DISTANCE- METERS$',100)
CALL HEADIN('4TH CASE$',100,1.,4)
CALL HEADIN('INITIAL TARGET ACCELERATION=-4. G$',100,1.,4)
CALL HEADIN('INITIAL TARGET POSITION=-600 M$',100,1.,4)
CALL HEADIN('SAMPLE PERIOD=0.05 SEC$',100,1.,4)
CALL CROSS
CALL GRAF(C.,SCALE,100.,-600.,SCALE,100.)
CALL CURVE(KPS,ZM,101,-1)
CALL FRAME

```

```

TESO4330
TESO4340
TESO4350
TESO4360
TESO4370
TESO4380
TESO4390
TESO4400
TESO4410
TESO4420
TESO4430
TESO4440
TESO4450
TESO4460
TESO4470
TESO4480
TESO4490
TESO4500
TESO4510
TESO4520
TESO4530
TESO4540
TESO4550
TESO4560
TESO4570
TESO4580
TESO4590
TESO4600
TESO4610
TESO4620
TESO4630
TESO4640
TESO4650
TESO4660
TESO4670
TESO4680
TESO4690
TESO4700
TESO4710
TESO4720
TESO4730
TESO4740
TESO4750
TESO4760
TESO4770
TESO4780
TESO4790
TESO4800

```



```

CALL CURVE (KPS, YM, 101, -1)
CALL LINESP (2, 0)
CALL LINES (MISS, CIST, Z DIRECTION$, IPAK, 1)
CALL LINES (MISS, DIST, Y DIRECTION$, IPAK, 2)
CALL LEGEND (IPAK, 2, 3, 5, 0.5)
CALL BLREC (3, 3, 0, 3, 3, 5, 1, 2, 0, 3)
CALL DASH (1, 1)
CALL GRID (1, 1, DASH)
CALL RESET (C)
CALL ENDPL (C)
CALL HWRGT (MOVIE)
CALL AREA2D (7, 0, 9, 0)
CALL XNAME (K$, 1, CO)
CALL YNAME (ACCELERATION - METERS/SQ.SEC$, 100)
CALL HEADIN (4TH CASE$, 100, 1, 4)
CALL HEADIN (INITIAL TARGET ACCELERATION= -4. G$, 100, 1, 4)
CALL HEADIN (INITIAL TARGET POSITION=-600 M$, 100, 1, 4)
CALL HEADIN (INITIAL TARGET PERIOD= 0.05 SEC$, 100, 1, 4)
CALL CROSS
CALL GRAF (C, SCALE, 100, -25, SCALE, 110)
CALL CURVE (KPS, AC, 101, -1)
CALL FRAME
CALL DASH (1, 1)
CALL GRID (1, 1, DASH)
CALL RESET (C)
CALL ENDPL (C)
CALL HWRGT (MOVIE)
CALL AREA2D (7, 0, 9, 0)
CALL XNAME (K$, 1, CO)
CALL YNAME (ROLL RATE - RDS/SEC$, 100)
CALL HEADIN (4TH CASE$, 100, 1, 4)
CALL HEADIN (INITIAL TARGET ACCELERATION= -4. G$, 100, 1, 4)
CALL HEADIN (INITIAL TARGET POSITION=-600 M$, 100, 1, 4)
CALL HEADIN (INITIAL TARGET PERIOD= 0.05 SEC$, 100, 1, 4)
CALL CROSS
CALL GRAF (C, SCALE, 100, 0, SCALE, 8)
CALL CURVE (KPS, PC, 101, -1)
CALL FRAME
CALL DASH (1, 1)
CALL GRID (1, 1, DASH)
CALL RESET (C)
CALL ENDPL (C)
CALL HWRGT (MOVIE)
CALL AREA2D (7, 0, 9, 0)
CALL XNAME (K$, 1, CO)
CALL YNAME (ROLL ANGLE - RDS$, 100)
CALL HEADIN (4TH CASE$, 100, 1, 4)
CALL HEADIN (INITIAL TARGET ACCELERATION= -4. G$, 100, 1, 4)

```

```

TES04810
TES04820
TES04830
TES04840
TES04850
TES04860
TES04870
TES04880
TES04890
TES04900
TES04910
TES04920
TES04930
TES04940
TES04950
TES04960
TES04970
TES04980
TES04990
TES05000
TES05010
TES05020
TES05030
TES05040
TES05050
TES05060
TES05070
TES05080
TES05090
TES05100
TES05110
TES05120
TES05130
TES05140
TES05150
TES05160
TES05170
TES05180
TES05190
TES05200
TES05210
TES05220
TES05230
TES05240
TES05250
TES05260
TES05270
TES05280

```



```

CALL HEADIN('INITIAL TARGET POSITION=-600 M$,100,1.,4)
CALL HEADIN('SAMPLE PERIOD=0.05 SEC$,100,1.,4)
CALL CROSS
CALL FRAME
CALL GRAF(C., 'SCALE',100.,0., 'SCALE',4.)
CALL DASH
CALL GRID(1,1)
CALL RESET ('DASH')
CALL CURVE(KPS,DPH,101,-1)
CALL ENDPL(C)
CALL DCNEPL
C *****
  25  FORMAT('1,')
  30  FCRMAT(1X/,5X,4X,'AC',9X,'PC',9X,'YM',9X,'ZM',9X,'DPH'
  1,12X,CGS,}
  31  FORMAT(1X/,5X,6(F9.4,3X)///)
  35  FORMAT(1X,//////,TYPE C
C *****
C SUBROUTINE GMTR A
SUBROUTINE GMTR(A,R,N,M)
DIMENSION A(1),R(1)
DCDOUBLE PRECISION A,R
IR=0
DC 10 I=1,N
IJ=I-N
DC 10 J=1,M
IJ=IJ+N
IR=IR+1
10 R(IR)=A(IJ)
RETURN
END
C *****
SUBROUTINE GMPRD
PURPOSE
MULTIPLY TWO GENERAL MATRICES TO FORM A RESULTANT GE
MATRIX
USAGE
CALL GMPRD(A,B,R,N,M,L)
DESCRIPTION OF PARAMETERS
A - NAME OF FIRST INPUT MATRIX
C *****
TESO5250
TESO5300
TESO5310
TESO5320
TESO5330
TESO5340
TESO5350
TESO5360
TESO5370
TESO5380
TESO5390
TESO5400
TESO5410
TESO5420
TESO5430
TESO5440
TESO5450
TESO5460
TESO5470
TESO5480
TESO5490
TESO5500
TESO5510
TESO5520
TESO5530
TESO5540
TESO5550
TESO5560
TESO5570
TESO5580
TESO5590
TESO5600
TESO5610
TESO5620
TESO5630
TESO5640
TESO5650
TESO5660
TESO5670
TESO5680
TESO5690
TESO5700
TESO5710
TESO5720
TESO5730
TESO5740
TESO5750
TESO5760

```



```

C .....
C SEARCH FCR LARGEST ELEMENT .....
C
C=1.0D0
NK=-N      K=1,N
DC 80      NK=NK+N
L(K)=K
M(K)=K
KK=NK+K
BIGA=A(KK)
DC 20      J=K,N
IZ=N*(J-1)
DC 20      I=K,N
IJ=IZ+I
1Q IF(DABS(BIGA)-DABS(A(IJ))) 15,20,20
15 BIGA=A(IJ)
L(K)=I
M(K)=J
2C CONTINUE

C INTERCHANGE ROWS
C
C
25 J=L(K)
   IF(J-K) 35,35,25
   KI=K-N
   KI=KI+N
   HCLD=-A(KI)
   I=KI-K+J
   A(KI)=A(JI)
3C A(JI)=HOLC

C INTERCHANGE COLUMNS
C
C
35 I=M(K)
38 IF(I-K) 45,45,38
   JP=N*(I-1)
   DC 40      J=I,N
   JK=NK+J
   JI=JP+J
   HOLD=-A(JK)
   A(JK)=A(JI)
4C A(JI)=HOLE

C DIVIDE CCLUMN BY MINUS PIVOT (VALUE OF PIVOT ELEMENT IS
C CONTAINED IN BIGA)
C

```

```

TES08170
TES08180
TES08190
TES08200
TES08210
TES08220
TES08230
TES08240
TES08250
TES08260
TES08270
TES08280
TES08290
TES08300
TES08310
TES08320
TES08330
TES08340
TES08350
TES08360
TES08370
TES08380
TES08390
TES08400
TES08410
TES08420
TES08430
TES08440
TES08450
TES08460
TES08470
TES08480
TES08490
TES08500
TES08510
TES08520
TES08530
TES08540
TES08550
TES08560
TES08570
TES08580
TES08590
TES08600
TES08610
TES08620
TES08630
TES08640

```



```

108 IF(I-K) 12C,120,1C8
    JC=N*(K-I)
    JR=N*(I-I)
    CO 110 J=1,N
    JK=JQ+J
    HCLD=A(JK)
    JI=JR+J
110 A(JK)=-A(JI)
120 J=M(K) =HOLD
125 IF(J-K) 10C,100,125
    KI=K-N
    DC 130 I=1,N
    KI=KI+N
    HCLD=A(KI)
    JI=KI-K+J
130 A(KI)=-A(JI)
150 GC TO 100
    RETURN
    END
CENTFY

```

```

TES09130
TES09140
TES09150
TES09160
TES09170
TES09180
TES09190
TES09200
TES09210
TES09220
TES09230
TES09240
TES09250
TES09260
TES09270
TES09280
TES09290
TES09300
TES09310
TES09320
TES09330
TES09340

```


LIST OF REFERENCES

1. Stallard, D. V., "An Approach to Optimal Guidance for a Bank-to-Turn Missile," Proceedings of AIAA Guidance and Control Conference, Danvers, Mass., August 1980.
2. Kwakernaak, H. and Sivan, R. Linear Optimal Control Systems, Wiley-Interscience, 1972.
3. Bryson, A. E. and Ho, Y. C. Applied Optimal Control, Halsted Press, 1975.

INITIAL DISTRIBUTION LIST

		No. Copies
1.	Defense Technical Information Center Cameron Station Alexandria, Virginia 22314	2
2.	Library, Code 0142 Naval Postgraduate School Monterey, California 93943	2
3.	Department Chairman, Code 67 Department of Aeronautical Engineering Naval Postgraduate School Monterey, California 93943	1
4.	Professor D.J. Collins, Code 67Co Department of Aeronautical Engineering Naval Postgraduate School Monterey, California 93943	3
5.	Professor H. A. Titus, Code 62Fs Department of Electrical Engineering Naval Postgraduate School Monterey, California 93943	1
6.	Office of The Air Attache Brazilian Embassy 3006 Massachusetts Av NW Washington DC 20008	3
7.	Centro Tecnico Aeroespacial Rua Paraibuna S/N 12200 Sao Jose dos Campos - SP Sao Paulo, BRAZIL	1
8.	Centro Tecnico Aeroespacial Instituto de Atividades Espaciais Rua Paraibuna S/N 12200 Sao Jose dos Campos - SP Sao Paulo, BRAZIL	2
9.	Centro Tecnico Aeroespacial Instituto de Atividades Espaciais Divisao de Sistemas Belicos Rua Paraibuna S/N 12200 Sao Jose dos Campos - SP Sao Paulo, BRAZIL	2
10.	MAJ Carlos A. L. Velloso Centro Tecnico Aeroespacial Instituto de Atividades Espaciais Rua Paraibuna S/N 12200 Sao Jose dos Campos - SP Sao Paulo, BRAZIL	3

207793

Thesis
V36282
c.1

Velloso

Optimal digital control of a bank-to-turn missile.

OCT 10 85
6 FEB 86

33038

207793

Thesis
V36282
c.1

Velloso

Optimal digital control of a bank-to-turn missile.



thesV36282

Optimal digital control of a bank-to-tur



3 2768 002 05419 9

DUDLEY KNOX LIBRARY